Properties of Composites Containing Spherical Inclusions Surrounded by an Inhomogeneous Interphase Region

by

Nick Lombardo

B.App.Sc (Hons) (RMIT University)

Dissertation submitted in total fulfilment of the requirements for the Degree of Doctor of Philosophy

School of Mathematical and Geospatial Sciences

RMIT University

Melbourne

Australia

June 22, 2007

DECLARATION

The candidate hereby declares that the work in this thesis, presented for the award of the Degree of Doctor of Philosophy and submitted in the School of Mathematical and Geospatial Sciences, RMIT University:

- **has been done by the candidate alone and has not been submitted previously, in whole or in part, in respect of any other academic award and has not been published in any form by any other person except where due reference is given, and**
- **has been carried out under the supervision of Dr. John A. Gear and Dr. Yan Ding.**

.....

Nick Lombardo

Certification

This is to certify that the above statements made by the candidate are correct to the best of our knowledge.

.....

Dr. John A. Gear

Senior Supervisor

.....

Dr. Yan Ding

Supervisor

Acknowledgements

I welcome this opportunity to firstly acknowledge my supervisors, Dr John A. Gear and Dr Yan Ding who I am mostly indebted to. Their ongoing support, encouragement and many valuable discussions regarding the research undertaken, made this possible for me. The help they have given me shall not be forgotten.

Thanks are also due to Assoc. Prof. John Shepherd for introducing me to the chemistry team lead by Prof. David Mainwaring and for being largely responsible for organising the alliance between all the parties involved in this research.

I would also like to thank Prof. David Mainwaring, Dr Pandiyan Murugaraj and PhD student Nelson Huertas for discussions regarding the nature of the composites that were studied and for providing insight into the experimental work that was carried out in the chemistry laboratory.

I would also like to acknowledge all the postgraduate students and staff in the school who have taken an interest in my research and who have provided a positive work environment in which to study.

I would like to thank my parents and parents in law for their continual support and finally my wife for her encouragement, support and for the perseverance in her new nurturing role as a mother to our daughter Rosemary who I dedicate this thesis to.

Contents

List of Figures

List of Tables

Summary

The properties of composite materials in which spherical inclusions are embedded in a matrix of some kind, have been studied for many decades and many analytical models have been developed which measure these properties. There has been a steady progression in the complexity of models over the years, providing greater insight into the nature of these materials and improving the accuracy in the measurement of their properties. Some of the properties with which this thesis is concerned are, the elastic, thermal and electrical properties of such composites.

The size of the spherical inclusion which acts as the reinforcing phase, has a major effect on the overall properties of composite materials. Once an inclusion is embedded into a matrix, a third region of different properties between the inclusion and matrix is known to develop which is called the interphase. It is well known in the composite community that the smaller the inclusion is, the larger the interphase region which develops around it. Therefore, with the introduction of nanoparticles as the preferred reinforcing phase for some composites, the interphase has a major effect on its properties.

It is the aim of this thesis to consider the role of the interphase on the properties of composites by modeling it as an inhomogeneous region. There is much scientific evidence to support the fact that the interphase has an inhomogeneous nature and many papers throughout the thesis are cited which highlight this. By modeling the inhomogeneous properties by arbitrary mathematical functions, results are obtained for the various properties in terms of these general functions. Some specific profiles for the inhomogeneous region are considered for each property in order to demonstrate and test the models against some established results.

Chapter 1

Introduction

This thesis is concerned with the study of composites which are materials made up of two or more different materials. Composites for example, may consist of layers or sheets of different materials sandwiched together, or of a matrix phase in which are embedded inclusions or otherwise known as fillers, of any arbitrary shape. There are many advantages of such materials over traditional materials, thereby making them more suitable for certain applications. Concrete is an example of a composite material which comprises a cement paste which is equivalent to the matrix phase and embedded small stones of arbitrary shape. In the case of reinforced concrete, steel rods are also embedded. The effect of combining two or more materials together is to produce a resultant material with different properties. Some of the properties that may be of interest to a materials scientist include such things as the mechanical, thermal and electrical properties of composite materials. The scientist may wish to enhance or influence a combination of these properties in order to produce a desired effect. Composites are particularly being used in such areas as the automotive, aerospace, maritime, building and microelectronics industry.

The type of composites that are studied in this thesis include those in which inclusions of a spherical shape are embedded in a matrix of some kind. A material, such as a polymer for example, that has some sort of reinforcing filler (or inclusion) embedded within it is known as a polymer composite. Fillers are added to the polymer with the aim of either improving the mechanical, thermal or electrical properties of the polymer or of improving a combination of these properties. The resulting composite material has many advantages

over the original polymer and is therefore more suitable for particular applications than other more traditional materials. For example, some polymer composites have a good strength to weight ratio and in certain cases, may be used to replace the more traditional materials used in the manufacturing of aircraft, space technology, cars, ships, or may be used for other potential applications where the ratio of strength to weight is an important factor. Depending on the application, the thermal and electrical properties may also be important factors which need to be considered when designing polymer composites.

In modeling the type of composite materials that this thesis is concerned with, some basic concepts or definitions need to be understood such as phase, interphase and interface. Generally, the matrix and inclusion is each known as a phase because they are each a material with a distinct chemical structure. The interphase is a three dimensional region immediately surrounding the inclusion that results from the bonding between the inclusion and matrix. The interface is a two dimensional region which borders any two distinct phases , such as the inclusion and interphase, or the interphase and matrix, or inclusion and matrix if the interphase is assumed to not exist.

The interphase is an important concept in composite materials science because the bonding between the matrix and inclusion occurs across this region. Therefore, the interphase is responsible for transferring load from matrix to inclusion or for transferring electrical and thermal effects from one phase to the other. Initial modeling of the properties of composites began by ignoring this region although the importance of the interphase to such properties has long been recognised [27]. It is known that the interphase is a region of finite size and that it has a different chemical structure than either of the two main phases [27].

Two broad approaches exist in modeling the interphase/interface zone. One is referred to as the *spring layer* model by Jayaraman et al. [28] which considers a very thin interfacial zone in which there is a discontinuity in the displacements or in the temperature or electrical potential across the interface. An example of a spring layer model is given by Hashin [18]. The other approach is referred to as the *interphase layer* model by Jayaraman et al. [28] which treats the interphase as a finite three dimensional distinct phase. Numerous interphase models exist of this second type. The models that are

discussed and presented in this thesis will be of this second type. In all such models it is assumed that perfect bonding exists between the inclusion, interphase and matrix. From a mechanical perspective, perfect bonding means there is a continuity of stresses and displacements across the interface between inclusion and interphase and between interphase and matrix. The modeling of 2-phase composites began with the simplifying assumption that perfect bonding existed across the inclusion/matrix interface. The three dimensional interphase represents a region of imperfect bonding which can be modeled by changing the thickness and properties of this region in order to represent the degree of debonding between the inclusion and matrix. It is also assumed throughout this thesis that the matrix and inclusions are isotropic materials. An isotropic material is a material whose properties are the same in all directions.

Several models exist in which the interphase is assumed to have uniform or constant properties. These models range from numerical models such as finite element models to more analytical micromechanics models [14, 12, 5]. Many researchers since then have gone on to consider a step-like graded interphase region in which the interphase is split into concentric layers whose properties are uniform within each layer [20, 21, 51]. Other researchers have considered an interphase whose properties vary as some continuous function. Such interphases are called functionally gradient or inhomogeneous. Many papers which model the interphase as inhomogeneous will be referenced throughout this thesis. Modeling the properties of the interphase as uniform presents the problem of choosing what single value to assign to this property. When using a step-like graded or an inhomogeneous interphase, it becomes important to choose the right function for the interphase, that is, one that best represents the physical reality of its properties. Some authors believe that the lack of knowledge of the interphase properties is *the Achilles heel* of composite science [32].

According to Theocaris [67], the presence of the interphase is due to the fact that each of the phases do not have smooth surfaces. For example, given a small enough scale, an inclusion may contain small cavities, bumps, sharp corners, edges, irregular curves, etc., along its surface thereby causing an interphase region to form in the immediate surrounding area, whose properties differ from those of the two main phases. The nature of

the interphase is also known to differ for different types of composites [32]. For example, in polymer matrix composites, ceramic matrix composites and metal matrix composites, the bonding mechanisms in each of these composites differ, that is, the factors that influence the adhesion between matrix and filler are different and therefore cause an interphase region to develop whose structure is also different. According to Reifsnider [54], the interphase region may be a diffusion zone, a nucleation zone, a chemical reaction zone, or any combination of these. The type and size of the inclusion is also known to effect the structure and size of the interphase.

The reinforcing filler may assume a variety of shapes such as long needle like fibres, round spheres, thin disks, round platelets, etc. Numerous studies suggest that the size of the filler and its shape has a major influence on the overall properties of the composite. Much research has focused recently on fillers with one or more dimensions in the nanometer length range [13, 4, 50]. Such composites are known as nanocomposites because they contain fillers that have one or more dimensions of the order of nanometers ($1nm = 10^{-9}m$). Modeling of the properties of these materials is still in a rather premature phase since the size of the fillers make it a rather hard object of study. Such fillers bond to the matrix much differently to the more conventional fillers of larger dimension. This is due to the fact that for such nano-sized fillers, the matter out of which they are composed is discrete as opposed to continuous. For example, a typical nanoparticle might look like a caged ball with much of the empty space taken up by electrons which exist between the bonds of distant atoms. The bonding that occurs between the filler and matrix in these nanocomposites is typically very strong and for this reason they have received much recent attention amongst the composite community. The interphase region that forms in nanocomposites is also much larger relative to the size of the filler. Such fillers are becoming increasingly popular as reinforcing agents due to the much improved overall properties of the composite at relatively low volume fractions of filler. Carbon nanotubes which were discovered by Iijima [24] in 1991 have received much attention within the last decade. Their remarkable mechanical, thermal and electrical properties make them ideal as reinforcing agents in some polymers. The superior properties of these composites make them well suited for the structural components of spacecraft. Carbon

nanotubes are long cylindrical tubes with diameter of the order of 1 nm and typical lengths ranging from nanometers to micrometers. They consist of a hexagonal array of carbon atoms rolled into a thin tube with end caps consisting of pentagonal rings. The properties of the nanotubes change depending on the angle they are rolled. The atomic structure of other types of fillers with one or more dimensions in the nanometer range appear to be less known. Other fillers include spherical like particles such as Carbon Black nanoparticles, Aluminium, Silica and Titanium Oxides with diameter ranging from 30-300 nm. Conducting nanoparticles such as Carbon Black are often used for designing polymer composites for applications such as strain sensors, electromagnetic shielding and electrostatic discharge (see [58] and references therein). An important factor in designing composites for such applications is the factor of percolation. The percolation threshold is said to have been reached when the composite changes almost instantaneously from being an insulator to being a conductor. Nanocomposites reinforced by platelet shaped fillers have also received much attention [13, 4]. These platelet shaped fillers have a thickness of the order of 1 nm and naturally occur in stacks. The platelets occurring in these stacks need to be exfoliated and dispersed within the polymer. The properties of the resulting composite depend on the degree of exfoliation and dispersion.

Due to the *small* dimensions associated with these types of fillers, modeling of the mechanical properties of these nanocomposites appears to be a more difficult task than other more traditional fillers of larger dimension. At these length scales, any analysis based only on continuum assumptions may be inadequate as assumed by some authors [50, 49]. This is due to the fact that the filler and the polymer near the filler no longer form a continuum and therefore the underlying assumption in such an approach may not be appropriate. Although some have discussed the applicability of the continuum approach in tackling such problems [35], it is strictly advised that caution be used since the continuum assumptions may break down in certain cases. It is the focus of this thesis to model the properties of a composite consisting of a polymer with spherically shaped nanoparticles embedded within it. The analysis has been carried out based on the assumption that each of the phases is continuous, therefore it is not known exactly how applicable these results are to such composites. It is felt however that the results obtained are useful for

the more traditional composites consisting of larger spherically shaped fillers.

Composites consisting of the more traditional fillers of larger dimension have been widely studied for many years. Such research has focused on the determination of mechanical, electrical and thermal properties in particular. An excellent review article is given by Hashin [15].

The composites that are researched in this thesis consist of a matrix phase with inclusions of spherical shape embedded within it, and the properties that are discussed include the mechanical, thermal and electrical properties. In this thesis, the spherical inclusion and surrounding interphase is modeled as a new effective spherical particle extending out to the outer boundary of the interphase. The interphase we assume to terminate at a finite distance away from the inclusion, as supported by Jayaraman et al. [27]. We also take the interphase to be inhomogeneous, that is, we describe its properties using continuous mathematical functions.

In chapters 2 and 3 we model the bulk and shear modulus respectively, in chapter 4 we model the thermal expansion coefficient which utilises results obtained from the derivation of the bulk modulus in chapter 2 and in chapter 5 we model the electrical properties, or more specifically, the dielectric properties. The model that is used in this thesis has as its foundation, results obtained already from the modeling of 2-phase composites. It is shown how these 2-phase results may be adapted to account for an inhomogenoeus interphase, surrounding each inclusion.

The results for the bulk modulus given in chapter 2 are exact since the 2-phase results that are used in the model are exact for the bulk modulus. Determination of the shear modulus however, is a harder problem even for two phases. An exact solution to the 2-phase problem for the shear modulus was derived by Christensen et al. [8] and an approximation has also been derived using the Mori-Tanaka method [2, 46, 77]. Hashin [15] has given bounds on the shear modulus using the composite spheres assemblage model. The bounds for the shear modulus do not coincide as they do for the bulk modulus using this model. The model for the shear modulus that is presented in this thesis is based on the approximation obtained using the Mori-Tanaka method. Consequently, our model for the shear modulus is not exact, however, a technique is employed which also utilises

results from the bulk modulus case in order to improve on our estimation.

The 2-phase results used for the thermal expansion coefficient in chapter 4 is exact and has been derived by several authors [33, 55, 59], therefore, our results for the inhomogeneous interphase are also exact for this case.

For the dielectric properties our model is based on the 2-phase Maxwell-Garnett mixing rule [43] which has also been derived by Hashin [16] using the composite spheres assemblage model. This mixing rule however does not account for percolation effects as some other models do such as the Bruggeman model [80] or certain percolation models. For percolation models, an excellent review article is given by McLachlan et al. [44]. Percolation occurs when a critical volume fraction of the conducting inclusion phase is reached whereby the composite changes almost instantaneously from being an insulator to a conductor. Other models for the electrical properties of composites are based on quantum mechanical tunneling between the conducting inclusions [83, 66]. Due to the insulating matrix material between each inclusion, electrons are confronted by some barrier on their motion from one filler particle to the next. If this potential energy barrier has a certain height, then classical Newtonian mechanics predicts that the electron can only get through this barrier if it has kinetic energy which is greater than the potential energy height of the barrier. In quantum mechanics however, even if the electron does not have enough kinetic energy to surmount the potential barrier, there is still some probability for it to emerge on the other side. Such a penetration of a barrier is called tunneling. It is generally thought that this tunneling phenomenon plays an important part in the conductivity of composite materials. No papers to my knowledge have been written which take into account the effects of a surrounding interphase on the tunneling that occurs between conducting inclusions and so there seems to be much scope for future work in this area.

Chapter 2

The Bulk Modulus of a Composite with Inhomogeneous Interphase

2.1 Introduction

Of particular importance on the overall mechanical properties of a composite is the interphase which is a 3-dimensional region immediately surrounding the inclusion. The interphase plays an important role in this respect due to the fact that forces are transferred across this region from the matrix to the inclusion. The bonding between the matrix and the inclusion occurs across this region and the stiffness properties of this region differ from that of the matrix and the inclusion. As described by Theocaris [67], the interphase (or mesophase as described by Theocaris) is due to the fact that in reality the surfaces of each of the phases are not perfectly smooth thereby creating voids or stress singularities in the nearby region where they join together. The inclusion in particular is usually comprised of a material which has infinitesimal cracks, sharp edges, irregular curves along its surface thus creating a layer around its surface having non uniform properties. Composite materials may also be engineered by coating the surface of the inclusion with some material prior to placing them within the matrix, thereby creating a deliberate interphase in order to produce better adhesion between the matrix and the inclusion.

The earlier work done in modeling the mechanical properties of composites began by ignoring the effect of the interphase region. In a paper written by Hashin [15], the author

constructs bounds for the elastic moduli of 2-phase composite materials using variational theorems of the theory of elasticity. For the case where the inclusions are spherical particles, (Composite Spheres Assemblage model), the bounds for the bulk modulus were found to coincide thus providing a solution while the bounds for the shear modulus were fairly close together but not coincident. The same solution for the bulk modulus was also derived by Weng [77] using the concepts of *average stress in a matrix* developed by Mori and Tanaka [46] and Eshelby's solutions of an ellipsoidal inclusion [11]. Using this method, Weng was also able to derive an expression for the shear modulus. These results were found under certain conditions to be related to more generalised bounds obtained by Hashin and Shtrikman [19] using variational principles. Solutions for the bulk and shear moduli of a 2-phase composite consisting of spherical inclusions have also been derived using the Generalised Self Consistent method which was fully developed by Christensen and Lo [8]. The solution obtained for the bulk modulus using this method [7] was the same as that obtained by the Composite Spheres Assemblage model and the Mori-Tanaka method while the shear modulus obtained was different to that obtained by the Mori-Tanaka method.

Naturally, the more recent work has gone on to consider the effects of an interphase although the existence of the interphase was also known to the earlier workers in the field. In a paper written by Qiu and Weng [52], the authors use a method known as the replacement method to derive the elastic moduli of composites containing coated particles or fibres. Existing formulas for the moduli that were previously derived in the field of composite technology, were used to determine the moduli of a coated particle/fibre which together, (i.e. the particle/fibre and its coating) is then modeled as a new effective particle/fibre. The formulas are then re-used to determine the elastic moduli of a composite containing these effective particles/fibres embedded in a matrix of some third material. This same replacement method has also been proposed by Hashin [17] to account for an interphase of different mechanical properties. In this thesis we adopt the same principle as used in the replacement method to determine the effective modulus of an inclusion together with its interphase. The moduli of the interphase region however will be assumed to vary as continuous functions rather than just being constant.

Modeling the variation in properties of the interphase region seems to have been the focus of many material scientists particularly over the recent decade. There are too many papers to discuss all of them so we shall restrict our discussion to a few of the more important earlier ones. The mechanical properties of the interphase region are usually taken to be isotropic and are described by functions which vary only with respect to the radial direction from the centre of the inclusion. Theocaris [67] derived a nonlinear variation in the Young's modulus of the interphase region of a fibre reinforced composite which he used to calculate the mechanical properties of the composite using concepts of thermodynamics and glass transition temperature. It was assumed in his model that the properties of the interphase matched the fibre and matrix at their respective boundaries. Jayaraman and Reifsnider [26] solved a differential equation for the displacement in the interphase region for a fibre reinforced composite subject to a uniform temperature change. They considered Power, Reciprocal and Cubic variations in the Young's modulus and assumed a constant Poisson's ratio and constant thermal expansion coefficient of the interphase region. Jasiuk and Kouider [25] considered a power variation in the Young's modulus with constant Poisson's ratio and a linear variation in both the Young's modulus and Poisson's ratio of the interphase region of a fibre reinforced composite. From their solutions for the displacement they were able to derive the bulk and shear modulus of the composite. In a model used by Lutz and Zimmerman [41], they assumed that the moduli of the interphase zone varied continuosly outside of the (spherical) inclusion and that the interphase region did not terminate but extended outward infinitely. For a power law variation in the moduli they were able to solve a differential equation for the radially symmetric deformation of the interphase region and inclusion when subjected to hydrostatic loading. The result for the single inclusion was used to estimate the overall bulk modulus by subjecting the inhomogeneous body consisting of a dispersion of such inclusions, to hydrostatic loading and equating the strain energy stored in this body to that stored in an identically shaped homogeneous body.

In this chapter we use the principle of the replacement method, as described by Qiu and Weng [52] and Hashin [17], to establish a model that we can use to determine the bulk modulus of a composite containing spherical inclusions with an interphase region of

varying properties. First we shall generalise the results for any given profile for the bulk and shear modulus describing the interphase by deriving a coupled pair of first order linear differential equations with non-constant coefficients. We then use these results to derive a closed form expression for the bulk modulus of a composite using a specific profile for the interphase region given by a power law variation, as described in the work of Vörös and Pukánszky [72, 73].

2.2 The Model

2.2.1 Foundation and Assumptions

The bulk modulus of a 2-phase composite, consisting of isotropic spherical inclusions of identical size surrounded by an isotropic matrix, as given by the Mori-Tanaka method [77], the Composite Spheres Assemblage model [15] and the Generalised self Consistent Method [7] is,

$$\kappa = \kappa_m + \frac{c}{\frac{1}{\kappa_p - \kappa_m} + \frac{3(1-c)}{3\kappa_m + 4\mu_m}} \tag{2.1}$$

where κ_p is the bulk modulus of the inclusions, κ_m and μ_m are respectively the bulk and shear modulus of the matrix and c is the volume fraction of the inclusions. We shall refer to (2.1) simply as the Mori-Tanaka solution for convenience.

To account for the presence of the interphase region consider Figure 2.1 representing a small portion of a 3-phase composite consisting of spherical particles all of radius a, surrounded by an annular interphase region of radius b, embedded in a surrounding matrix.

To introduce the model, we shall firstly assume that the bulk and shear modulus of the interphase region are constant throughout and are given respectively by κ_g and μ_g and that κ_p, κ_m and μ_m are as defined above. We then model the inclusion and interphase together as forming a new, effective spherical particle of radius b, with moduli intermediate between the moduli of the inclusion and of the interphase. It shall be assumed throughout this work that the inclusions are well spaced apart and that the interphase regions don't overlap. It shall also be assumed in our model that the interphase region is of finite size

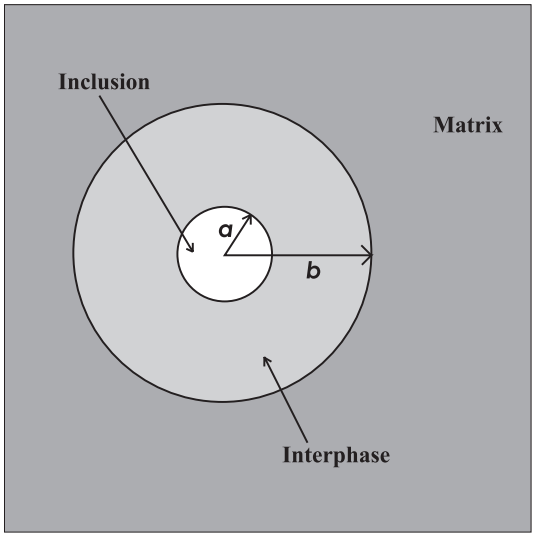

Figure 2.1: A small portion of a composite.

unlike the model of Lutz and Zimmerman [41].

Using (2.1), the bulk modulus, κ_E, of the effective particle consisting of interphase and inclusion is given by,

$$\kappa_E = \kappa_g + \frac{d}{\frac{1}{\kappa_p - \kappa_g} + \frac{3(1-d)}{3\kappa_g + 4\mu_g}} \tag{2.2}$$

where $d = \frac{a^3}{b^3}$ is the volume fraction of the inclusion relative to the interphase.

Therefore, putting this back into (2.1) gives the bulk modulus of the 3-phase composite as,

$$\kappa = \kappa_m + \frac{c}{\frac{1}{\kappa_E - \kappa_m} + \frac{3(1-c)}{3\kappa_m + 4\mu_m}} \tag{2.3}$$

where c is the volume fraction of the effective particles of radius b each consisting of an inclusion and surrounding interphase region. In terms of the known parameters,

$$c = d_0 \frac{b^3}{a^3} \tag{2.4}$$

where d_0 is the volume fraction of inclusions relative to all phases.

Suppose now that the interphase consists of 3 regions or layers around the inclusion as in Figure 2.2, and that the properties of these three regions are each different from one

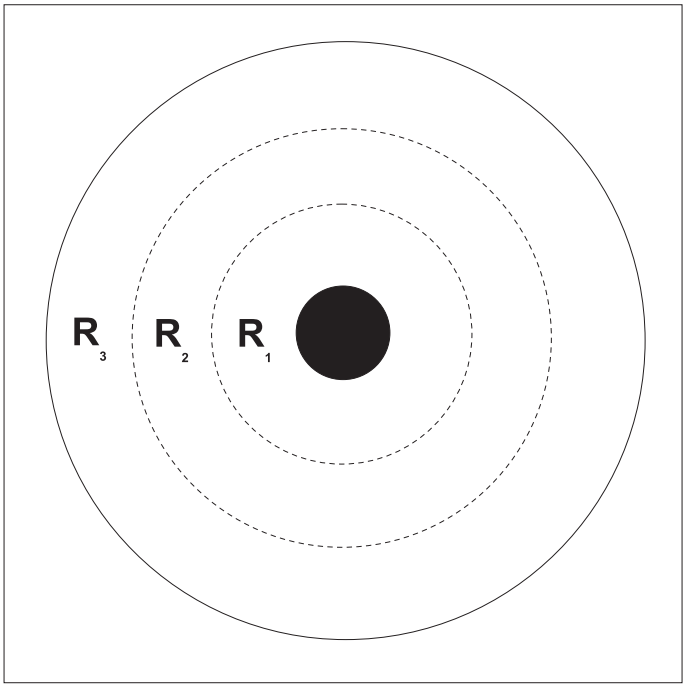

Figure 2.2: Interphase consisting of 3 regions.

another and from the matrix and inclusion.

Using the model described above, it would be possible to find the effective modulus of the particle and the first layer of interphase and to model this as a new particle with radius extending out to the outer boundary of R_1. Repeating the process for the region R_2 and so on for R_3, we would eventually be able to determine what the effective modulus of the particle consisting of the inclusion and the whole interphase region would be. Once the effective modulus of this particle has been found, it is then a simple process to determine the bulk modulus of the composite. A difficulty that is encountered in modeling the problem in this way however, is that once the number of layers becomes large, the calculations involved become rather large also.

It is the aim of this paper to show that by letting the number of layers in the interphase approach infinity, it is possible to derive a coupled pair of first order linear differential equations with non-constant coefficients, where the bulk and shear moduli of the interphase region are described by two continuously varying functions.

2.2.2 Formulation of the Problem

Mathematical Basis

We shall now suppose that the properties of the interphase vary as continuous functions of x, where x represents the radial distance from the centre of the inclusion as shown in Figure 2.3. That is, the bulk and shear moduli of the interphase region are described by $\kappa(x)$ and $\mu(x)$ respectively, where $x \in [a, b]$. We shall also assume that $\kappa(x)$ and $\mu(x)$ are smooth, bounded and continuous functions.

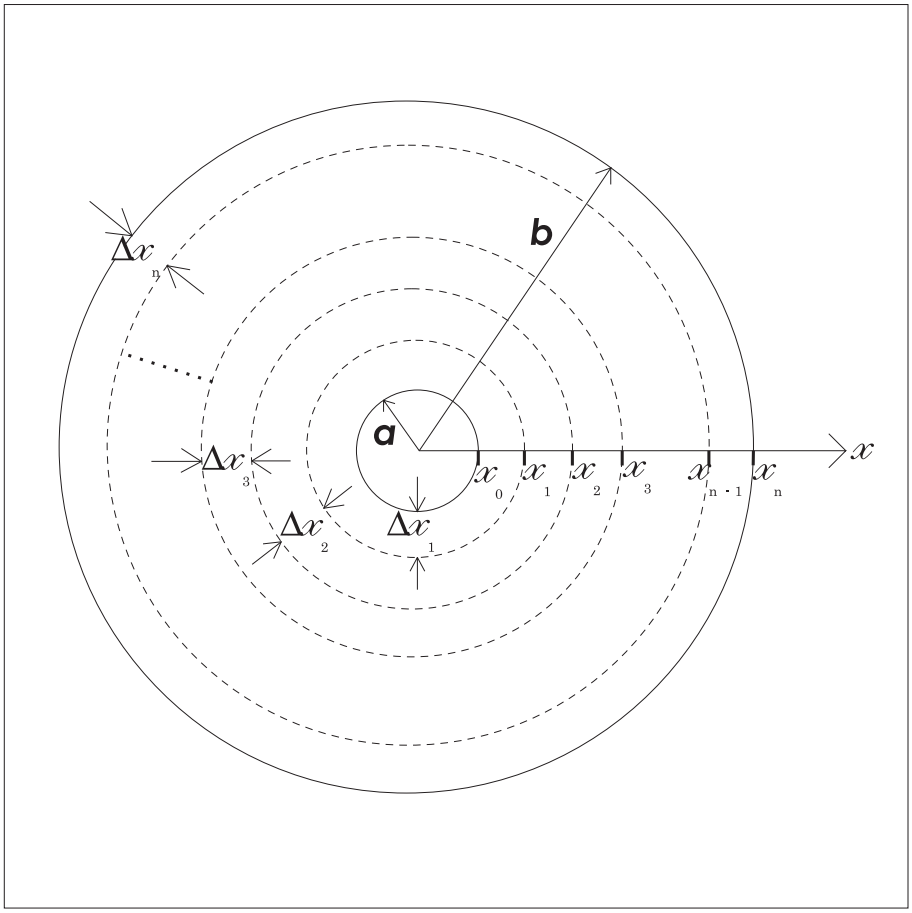

Figure 2.3: Interphase consisting of n regions or layers.

Consider a partition $\mathcal{P}$ of $[a, b]$ into n subintervals defined by,

$$a = x_0 < x_1 < x_2 < \cdots < x_{i-1} < x_i < \cdots < x_{n-1} < x_n = b.$$

The lengths Δx_1, Δx_2, Δx_3, $\ldots$, Δx_n of the subintervals $[x_0, x_1]$, $[x_1, x_2]$, $[x_2, x_3]$, $\ldots$, $[x_{n-1}, x_n]$ associated with the partition $\mathcal{P}$, presently need not be the same. In each subinterval $[x_{i-1}, x_i]$, choose any point ξ_i; that is $\xi_i \in [x_{i-1}, x_i]$.

The effective bulk modulus κ_1 of the inclusion and the 1st layer is approximated by,

$$\kappa_1 = \kappa(\xi_1) + \frac{d_1}{\frac{1}{\kappa_0 - \kappa(\xi_1)} + \frac{3(1-d_1)}{3\kappa(\xi_1)+4\mu(\xi_1)}}$$

where $d_1 = (\frac{x_0}{x_1})^3$ and $\kappa_0 = \kappa_p$.

The effective bulk modulus κ_2 of the inclusion up to the 2nd layer is approximated by,

$$\kappa_2 = \kappa(\xi_2) + \frac{d_2}{\frac{1}{\kappa_1 - \kappa(\xi_2)} + \frac{3(1-d_2)}{3\kappa(\xi_2)+4\mu(\xi_2)}}$$

where $d_2 = (\frac{x_1}{x_2})^3$. Note that κ_1 is an approximation to the bulk modulus of the *inner composite sphere* as described by Hashin [17], consisting of the inclusion and the first layer.

Continuing in this way, we have, as an approximation for the effective bulk modulus κ_i of the inclusion up to the i-th layer,

$$\kappa_i = \kappa(\xi_i) + \frac{d_i}{\frac{1}{\kappa_{i-1} - \kappa(\xi_i)} + \frac{3(1-d_i)}{3\kappa(\xi_i)+4\mu(\xi_i)}} \tag{2.5}$$

where $d_i = \left(\frac{x_{i-1}}{x_i}\right)^3$, $i \in \{\mathbb{N} : 1 \leq i \leq n\}$ and κ_{i-1} is an approximation to the bulk modulus of the *inner composite sphere* that is calculated from the previous step.

Our aim is to find the effective bulk modulus, κ_E, of the inclusion and whole interphase region which would be given by,

$$\kappa_E = \lim_{n\to\infty} \kappa_n$$

where κ_n is found by solving the recurrence relation (2.5).

Conversion of Reccurence Relation to Simultaneous Difference Equations

We may rewrite (2.5) as,

$$\kappa_i = \frac{A_i \kappa_{i-1} + B_i}{C_i \kappa_{i-1} + D_i} \tag{2.6}$$

where,

$$A_i = f_i d_i \kappa(\xi_i) + d_i, \qquad B_i = \kappa(\xi_i) - f_i d_i \kappa(\xi_i)^2 - d_i \kappa(\xi_i),$$
$$C_i = f_i d_i, \qquad D_i = 1 - f_i d_i \kappa(\xi_i),$$

and,

$$f_i = \frac{3(1-d_i)}{d_i(3\kappa(\xi_i) + 4\mu(\xi_i))}.$$

By evaluating the first few terms of the recurrence relation (2.6), a pattern can be seen as emerging which enables us to suitably estimate κ_i as,

$$\kappa_i = \frac{S_i(A_1\kappa_0 + B_1) + T_i(C_1\kappa_0 + D_1)}{U_i(A_1\kappa_0 + B_1) + V_i(C_1\kappa_0 + D_1)} \tag{2.7}$$

where,

$$S_i = A_i S_{i-1} + B_i U_{i-1} \tag{2.8}$$
$$U_i = C_i S_{i-1} + D_i U_{i-1} \tag{2.9}$$

which together form a pair of simultaneous first order linear difference equations with non-constant coefficients and initial conditions, $S_1 = 1$, $U_1 = 0$. Also we have, $i \in \{\mathbb{N} : 2 \leq i \leq n\}$.

We also have for T_i and V_i,

$$T_i = A_i T_{i-1} + B_i V_{i-1} \tag{2.10}$$
$$V_i = C_i T_{i-1} + D_i V_{i-1} \tag{2.11}$$

which are a pair of simultaneous equations identical to (2.8) and (2.9), but with initial conditions, $T_1 = 0$ and $V_1 = 1$. Also we have, $i \in \{\mathbb{N} : 2 \leq i \leq n\}$.

Verification of the Representation of κ_i as given by (2.7)

Using mathematical induction, it can be shown that κ_i as represented by (2.7) along with (2.8)-(2.11), is identical to the representation given by (2.6).

It is easily verified that both statements for κ_i are equal to one another for $i = 1$ and $i = 2$. It remains to be shown that the truth of Q_j implies the truth of Q_{j+1} for all $j \geq 3$ where,

$$Q_j : \qquad \frac{A_j\kappa_{j-1} + B_j}{C_j\kappa_{j-1} + D_j} = \frac{S_j(A_1\kappa_0 + B_1) + T_j(C_1\kappa_0 + D_1)}{U_j(A_1\kappa_0 + B_1) + V_j(C_1\kappa_0 + D_1)}$$

and,

$$Q_{j+1} : \qquad \frac{A_{j+1}\kappa_j + B_{j+1}}{C_{j+1}\kappa_j + D_{j+1}} = \frac{S_{j+1}(A_1\kappa_0 + B_1) + T_{j+1}(C_1\kappa_0 + D_1)}{U_{j+1}(A_1\kappa_0 + B_1) + V_{j+1}(C_1\kappa_0 + D_1)}$$

The right hand side ($R.H.S.$) of Q_{j+1} is given by,

$$\begin{aligned} R.H.S. &= \frac{(A_{j+1}S_j + B_{j+1}U_j)(A_1\kappa_0 + B_1) + (A_{j+1}T_j + B_{j+1}V_j)(C_1\kappa_0 + D_1)}{(C_{j+1}S_j + D_{j+1}U_j)(A_1\kappa_0 + B_1) + (C_{j+1}T_j + D_{j+1}V_j)(C_1\kappa_0 + D_1)} \\ &= \frac{A_{j+1}(S_j(A_1\kappa_0 + B_1) + T_j(C_1\kappa_0 + D_1)) + B_{j+1}(U_j(A_1\kappa_0 + B_1) + V_j(C_1\kappa_0 + D_1))}{C_{j+1}(S_j(A_1\kappa_0 + B_1) + T_j(C_1\kappa_0 + D_1)) + D_{j+1}(U_j(A_1\kappa_0 + B_1) + V_j(C_1\kappa_0 + D_1))} \\ &= \frac{A_{j+1}\kappa_j + B_{j+1}}{C_{j+1}\kappa_j + D_{j+1}} \end{aligned}$$

on dividing newmerator and denominator by, $(U_j(A_1\kappa_0 + B_1) + V_j(C_1\kappa_0 + D_1))$. Therefore, Q_j is true for all $j \geq 3$.

2.2.3 The Governing Differential Equations

We may rewrite (2.8) and (2.9) as,

$$S_{i+1} = A_{i+1}S_i + B_{i+1}U_i \tag{2.12}$$

$$U_{i+1} = C_{i+1}S_i + D_{i+1}U_i \tag{2.13}$$

where $S_1 = 1$, $U_1 = 0$ and $i \in \{\mathbb{N} : 1 \leq i \leq (n-1)\}$.

We have from before,

$$A_i = f_i d_i \kappa(\xi_i) + d_i, \qquad B_i = \kappa(\xi_i) - f_i d_i \kappa(\xi_i)^2 - d_i \kappa(\xi_i),$$
$$C_i = f_i d_i, \qquad D_i = 1 - f_i d_i \kappa(\xi_i),$$

where,

$$f_i = \frac{3(1-d_i)}{d_i(3\kappa(\xi_i) + 4\mu(\xi_i))} \qquad \text{and} \qquad d_i = \left(\frac{x_{i-1}}{x_i}\right)^3.$$

For each subinterval $[x_{i-1}, x_i]$ of the partition $\mathcal{P}$ let each Δx_i have the same width Δx and choose ξ_i to be the right hand end point, that is, we shall take $\xi_i = x_i$. Then we have,

$$(1 - d_i) = \Delta x g_i \qquad \text{where} \qquad g_i = \frac{x_i^2 + x_i x_{i-1} + x_{i-1}^2}{x_i^3}.$$

For notational convenience, A_i, B_i, C_i, and D_i may be re-written as,

$$A_i = \Delta x \alpha_i + d_i \qquad \text{where} \qquad \alpha_i = \frac{3 g_i \kappa(x_i)}{3\kappa(x_i) + 4\mu(x_i)},$$

$$B_i = \Delta x \beta_i \qquad \text{where} \qquad \beta_i = \frac{4 g_i \kappa(x_i)\mu(x_i)}{3\kappa(x_i) + 4\mu(x_i)},$$

$$C_i = \Delta x \gamma_i \qquad \text{where} \qquad \gamma_i = \frac{3 g_i}{3\kappa(x_i) + 4\mu(x_i)},$$

and $D_i = 1 - \Delta x \alpha_i$.

Let $A_2, A_3, A_4, \ldots, A_n$ be discrete values of a function $A(x)$ at the discrete points x_i where $i = 2, 3, 4, \ldots, n$. For example, A_i is the value of $A(x)$ at the discrete point x_i, i.e.

$A_i = A(x_i)$. Also we have $A_{i+1} = A(x_i + \Delta x)$. Similarly for B_i, C_i, and D_i we have the functions $B(x)$, $C(x)$ and $D(x)$. Also, let S_i and U_i be values of the functions $S(x)$ and $U(x)$ at the discrete points x_i. Then, (2.12) and (2.13) may be re-written as,

$$S(x_i + \Delta x) = A(x_i + \Delta x)S(x_i) + B(x_i + \Delta x)U(x_i) \tag{2.14}$$

$$U(x_i + \Delta x) = C(x_i + \Delta x)S(x_i) + D(x_i + \Delta x)U(x_i) \tag{2.15}$$

where $S(x_1) = 1$, $U(x_1) = 0$ and $i \in \{\mathbb{N} : 1 \leq i \leq (n-1)\}$.

After re-arranging equation (2.14) and taking the limit of both sides as $\Delta x \to 0$, we get,

$$\begin{aligned} S'(x_i) =& A'(x_i)S(x_i) + S(x_i) \lim_{\Delta x \to 0} \left(\frac{A(x_i) - 1}{\Delta x} \right) \\ &+ B'(x_i)U(x_i) + U(x_i) \lim_{\Delta x \to 0} \left(\frac{B(x_i)}{\Delta x} \right) \end{aligned}$$

where,

$$\lim_{\Delta x \to 0} \left(\frac{A(x_i) - 1}{\Delta x} \right) = -\frac{3}{x_i} \left(\frac{4\mu(x_i)}{3\kappa(x_i) + 4\mu(x_i)} \right)$$

and

$$\lim_{\Delta x \to 0} \left(\frac{B(x_i)}{\Delta x} \right) = \frac{3}{x_i} \left(\frac{4\kappa(x_i)\mu(x_i)}{3\kappa(x_i) + 4\mu(x_i)} \right).$$

It can also be shown that,

$$A'(x_i) = \alpha'(x_i) \lim_{\Delta x \to 0} (\Delta x) + \lim_{\Delta x \to 0} \left(\frac{\left(\frac{x_i}{x_{i+1}} \right)^3 - \left(\frac{x_{i-1}}{x_i} \right)^3}{\Delta x} \right)$$

and

$$B'(x_i) = \beta'(x_i) \lim_{\Delta x \to 0} (\Delta x).$$

It is easily shown that the second term in the expression for $A'(x_i)$ is equal to zero. Due to the conditions imposed earlier on the nature of the functions $\kappa(x)$ and $\mu(x)$, $\alpha(x)$ and

$\beta(x)$ will also be smooth, bounded and continuous functions in the interval $[a, b]$ and hence $\alpha'(x_i)$ and $\beta'(x_i)$ will be finite for all $x_i \in [a, b]$. Therefore, we have $A'(x_i) = 0$ and $B'(x_i) = 0$ at all points $x_i \in [a, b]$.

Re-arranging equation (2.15) and taking the limit of both sides as $\Delta x \to 0$ gives,

$$\begin{aligned} U'(x_i) =& C'(x_i)S(x_i) + S(x_i) \lim_{\Delta x \to 0} \left(\frac{C(x_i)}{\Delta x} \right) \\ &+ D'(x_i)U(x_i) + U(x_i) \lim_{\Delta x \to 0} \left(\frac{D(x_i) - 1}{\Delta x} \right) \end{aligned}$$

where,

$$\lim_{\Delta x \to 0} \left(\frac{C(x_i)}{\Delta x} \right) = \frac{3}{x_i} \left(\frac{3}{3\kappa(x_i) + 4\mu(x_i)} \right)$$

and

$$\lim_{\Delta x \to 0} \left(\frac{D(x_i) - 1}{\Delta x} \right) = -\frac{3}{x_i} \left(\frac{3\kappa(x_i)}{3\kappa(x_i) + 4\mu(x_i)} \right).$$

Also, we have,

$$C'(x_i) = \gamma'(x_i) \lim_{\Delta x \to 0} (\Delta x)$$

and

$$D'(x_i) = -\alpha'(x_i) \lim_{\Delta x \to 0} (\Delta x).$$

It has been shown that $\alpha'(x_i)$ is finite and similarly $\gamma'(x_i)$ will be finite for all $x_i \in [a, b]$. Hence, $C'(x_i) = 0$ and $D'(x_i) = 0$ at all points $x_i \in [a, b]$.

The initial conditions are $S(x_1) = 1$ and $U(x_1) = 0$. In the limit as $n \to \infty$ or $\Delta x \to 0$ we have, $S(a) = 1$ and $U(a) = 0$.

Therefore, the two simultaneous difference equations have been converted into a pair of simultaneous differential equations given by,

$$S'(x) = -\frac{3}{x}\left(\frac{4\mu(x)}{3\kappa(x)+4\mu(x)}\right)S(x) + \frac{3}{x}\left(\frac{4\kappa(x)\mu(x)}{3\kappa(x)+4\mu(x)}\right)U(x) \tag{2.16}$$

$$U'(x) = \frac{3}{x}\left(\frac{3}{3\kappa(x)+4\mu(x)}\right)S(x) - \frac{3}{x}\left(\frac{3\kappa(x)}{3\kappa(x)+4\mu(x)}\right)U(x) \tag{2.17}$$

where $S(a) = 1$ and $U(a) = 0$ and $x \in [a, b]$.

Similarly, the simultaneous difference equations given by (2.10) and (2.11), may be converted into an identical pair of simultaneous differential equations given by,

$$T'(x) = -\frac{3}{x}\left(\frac{4\mu(x)}{3\kappa(x)+4\mu(x)}\right)T(x) + \frac{3}{x}\left(\frac{4\kappa(x)\mu(x)}{3\kappa(x)+4\mu(x)}\right)V(x) \tag{2.18}$$

$$V'(x) = \frac{3}{x}\left(\frac{3}{3\kappa(x)+4\mu(x)}\right)T(x) - \frac{3}{x}\left(\frac{3\kappa(x)}{3\kappa(x)+4\mu(x)}\right)V(x) \tag{2.19}$$

where $T(a) = 0$ and $V(a) = 1$ and $x \in [a, b]$.

Note that the pair of equations given by (2.18) and (2.19) differ to the pair of equations given by (2.16) and (2.17) only in the boundary conditions. Therefore, only one pair of equations need to be solved with appropriate care taken when accounting for the boundary conditions.

2.2.4 The General Solution for the Bulk Modulus

The effective bulk modulus of the inclusion and interphase is given by,

$$\kappa_E = \lim_{n\to\infty} \kappa_n$$

where from (2.7),

$$\kappa_n = \frac{S_n(A_1\kappa_0 + B_1) + T_n(C_1\kappa_0 + D_1)}{U_n(A_1\kappa_0 + B_1) + V_n(C_1\kappa_0 + D_1)}.$$

As $n \to \infty$ we have $A_1 \to 1$, $B_1 \to 0$, $C_1 \to 0$ and $D_1 \to 1$. Also we have,

$$\lim_{n\to\infty} S_n = S(b), \qquad \lim_{n\to\infty} U_n = U(b),$$

$$\lim_{n\to\infty} T_n = T(b), \qquad \text{and} \qquad \lim_{n\to\infty} V_n = V(b).$$

Therefore, the effective bulk modulus of the particle and interphase is,

$$\kappa_E = \frac{\kappa_0 S(b) + T(b)}{\kappa_0 U(b) + V(b)}. \tag{2.20}$$

The bulk modulus of the composite can then easily be found by using (2.3) and (2.4).

2.3 A Specific Profile for the Bulk and Shear Moduli of the Interphase Region

We model the changing properties of the interphase region by a power law function that was described in the work of Vörös and Pukánszky [72, 73]. Such a function has also been considered by others and is assumed to be an adequate representation of some interphase regions while at the same time retaining the simplicity required to obtain analytical solutions.

Consider the two functions describing the properties of the interphase region given by,

$$\lambda(x) = \lambda_m f(x) \qquad \text{and} \qquad \mu(x) = \mu_m f(x)$$

where

$$f(x) = J\left(\frac{a}{x}\right)^P.$$

$\lambda(x)$ and $\mu(x)$ are the Lamé coefficients describing the mechanical properties of the interphase region which is assumed to be isotropic and dependent only on x which represents the radial distance from the centre of the inclusion.

The constants λ_m and μ_m represent the Lamé coefficients of the matrix which is assumed to be a homogeneous and isotropic material. Also, for such a representation, the Poisson's ratio of the interphase will be a constant ν_m, equal to the Poisson's ratio of the matrix.

The constant J represents the modulus at the surface of the inclusion relative to the modulus of the matrix, while the constant P represents the rate at which the modulus of the interphase changes with respect to x. It will be assumed that at the boundary between interphase and matrix, that the moduli of the interphase match those of the matrix. In such a case we have, $b = aJ^{1/P}$. In using this representation, it is however not necessary that the moduli of the interphase region at either boundary match the inclusion or matrix, although such conditions may be imposed if one wishes to model the interphase in such a way.

The constants λ_m, μ_m and J are positive by definition while the constant P may be either positive or negative.

The bulk modulus of the interphase region is given by,

$$\kappa(x) = \left(\lambda_m + \frac{2}{3}\mu_m\right) f(x)$$

while the shear modulus is given by $\mu(x)$ above.

Letting $c_1 = \left(\lambda_m + \frac{2}{3}\mu_m\right) J$ and $c_2 = \mu_m J$ and substituting the two functions for $\kappa(x)$ and $\mu(x)$ into (2.16) and (2.17) gives,

$$S'(x) = \frac{m_1}{x} S(x) + m_2 \left(\frac{1}{x}\right)^{1+P} U(x) \tag{2.21}$$

$$U'(x) = m_3 \left(\frac{1}{x}\right)^{1-P} S(x) + \frac{m_4}{x} U(x) \tag{2.22}$$

where $S(a) = 1$, $U(a) = 0$ and m_1, m_2, m_3, and m_4 are constants defined by,

$$m_1 = \frac{-12c_2}{3c_1 + 4c_2}, \qquad m_2 = \left(\frac{12c_1c_2}{3c_1 + 4c_2}\right) a^P,$$
$$m_3 = \left(\frac{9}{3c_1 + 4c_2}\right) a^{-P}, \qquad m_4 = \frac{-9c_1}{3c_1 + 4c_2}.$$

Equations (2.21) and (2.22) may be converted into a second-order differential equation given by,

$$S''(x) + \frac{w_1}{x} S'(x) + \frac{w_2}{x^2} S(x) = 0 \tag{2.23}$$

where

$$S(a) = 1, \qquad S'(a) = \frac{m_1}{a} \tag{2.24}$$

and w_1 and w_2 are constants defined by,

$$w_1 = 4 + P, \qquad w_2 = -m_1 P.$$

Note that $U(x)$ is given by,

$$U(x) = \frac{x^{1+P}}{m_2} S'(x) - \frac{m_1}{m_2} x^P S(x). \tag{2.25}$$

The problem therefore reduces down to (2.23) which is a second-order linear homogeneous Euler differential equation. Therefore, an exact closed form solution for the bulk modulus of the composite exists for this particular profile.

The solution to this differential equation depends on the roots of the characteristic equation given by,

$$\lambda^2 + (w_1 - 1)\lambda + w_2 = 0.$$

The constants, λ_m, μ_m and J are always positive and therefore c_1 and c_2 are always positive, while the constant P may be both positive and negative. The form of the solution depends on whether the roots are real and distinct, real and equal, or complex. It can be shown that the roots of the characteristic equation are always real and distinct for all allowable values of the parameters by analysing the discriminant of the characteristic equation. That is, if we suppose that,

$$(w_1 - 1)^2 - 4w_2 > 0$$

for all allowable values of the parameters, then one ends up with the inequality,

$$3c_1(P + 3)^2 + 4c_2(P - 3)^2 > 0.$$

The above inequality holds for all $c_1, c_2 > 0$ and for all P. Therefore, the roots of the characteristic equation are always real and distinct since the discriminant is always positive.

The general solution of the differential equation (2.23) is given by,

$$S(x) = r_1 x^{\lambda_1} + r_2 x^{\lambda_2} \tag{2.26}$$

where r_1 and r_2 are constants to be determined from the boundary conditions and λ_1 and λ_2 are roots of the characteristic equation given by,

$$\lambda_1 = \frac{1 - w_1 + q}{2}, \qquad \lambda_2 = \frac{1 - w_1 - q}{2}$$

where

$$q = \sqrt{(w_1 - 1)^2 - 4w_2}.$$

Substitution of the boundary conditions (2.24) into (2.26) enables us to find the constants r_1 and r_2 which are given by,

$$r_1 = \left(\frac{1}{2} - \frac{1}{2q}(1 - w_1 - 2m_1)\right) a^{-\lambda_1}, \qquad r_2 = \left(\frac{1}{2} + \frac{1}{2q}(1 - w_1 - 2m_1)\right) a^{-\lambda_2}.$$

Substituting r_1 and r_2 into (2.26) gives the solution for $S(x)$ which after some rearranging is,

$$S(x) = \frac{1}{2}\left(\frac{a}{x}\right)^{-\lambda_2} \left\{ \left(1 + \left(\frac{a}{x}\right)^{-q}\right) + \frac{(1 - w_1 - 2m_1)}{q}\left(1 - \left(\frac{a}{x}\right)^{-q}\right)\right\} \tag{2.27}$$

Use of (2.25) enables us to find the solution for $U(x)$ which after some rearranging is,

$$U(x) = \frac{x^P}{m_2}\frac{1}{2}\left(\frac{a}{x}\right)^{-\lambda_2} \left(\frac{(1 - w_1 - 2m_1)^2}{2q} - \frac{q}{2}\right)\left(1 - \left(\frac{a}{x}\right)^{-q}\right). \tag{2.28}$$

Substitution of $\kappa(x)$ and $\mu(x)$ into (2.18) and (2.19) gives the same second-order differential equation but with slightly different boundary conditions. That is, we have,

$$T''(x) + \frac{w_1}{x}T'(x) + \frac{w_2}{x^2}T(x) = 0$$

where

$$T(a) = 0, \qquad T'(a) = \frac{m_2}{a^{1+P}} \tag{2.29}$$

and

$$V(x) = \frac{x^{1+P}}{m_2}T'(x) - \frac{m_1}{m_2}x^P T(x).$$

The general solution is the same as before and is given by,

$$T(x) = t_1 x^{\lambda_1} + t_2 x^{\lambda_2}$$

where t_1 and t_2 are constants that are determined from the boundary conditions (2.29) as,

$$t_1 = \frac{m_2}{qa^P} a^{-\lambda_1}, \qquad t_2 = -\frac{m_2}{qa^P} a^{-\lambda_2}.$$

Therefore, the solution for $T(x)$ and $V(x)$ are given by,

$$T(x) = \frac{m_2}{qa^P} \left(\frac{a}{x}\right)^{-\lambda_2} \left(\left(\frac{a}{x}\right)^{-q} - 1\right) \tag{2.30}$$

and

$$V(x) = \frac{1}{2q} \left(\frac{a}{x}\right)^{-\lambda_2 - P} (1 - w_1 - 2m_1) \left(\left(\frac{a}{x}\right)^{-q} - 1\right) + \frac{1}{2} \left(\frac{a}{x}\right)^{-\lambda_2 - P} \left(\left(\frac{a}{x}\right)^{-q} + 1\right). \tag{2.31}$$

The solutions (2.27), (2.28), (2.30) and (2.31) enable us to calculate the effective bulk modulus κ_E of the inclusion and interphase which is given by (2.20). The bulk modulus of the composite can then be found from (2.3) and (2.4).

2.4 Results

2.4.1 Fixed Interphase Thickness

It is assumed that at the boundary between matrix and interphase, i.e. at $x = b$, that $\kappa(b) = \kappa_m$ and $\mu(b) = \mu_m$. For such a condition we must have $b = aJ^{1/P}$. At $x = a$ we have, $\frac{\kappa(a)}{\kappa_m} = J$. It will be assumed in the discussion that follows that the inclusion is harder than the pure matrix. Thus, if we allow $\kappa(a)$ to vary between 0 and κ_p, i.e. $0 < \kappa(a) \leq \kappa_p$, then we have,

$$0 < J \leq \frac{\kappa_p}{\kappa_m}.$$

$J < 1$ corresponds to an interphase region which is softer than the matrix, while $J > 1$ corresponds to an interphase region which is harder than the matrix.

P may be chosen so that the interphase thickness is a certain percentage of the inclusion radius a. Example, if the interphase is assumed to have a thickness which is 30% of the radius of inclusion, then set $P = \frac{\ln(J)}{\ln(1.3)}$.

Figure 2.4 shows the relative bulk modulus of a composite as a function of inclusion concentration for various values of the parameter J. The mechanical properties for the matrix and inclusion that were used are given by $\kappa_m = 14$, $\mu_m = 3$ and $\kappa_p = 22$. The interphase region was assumed to have a thickness of 25% of the radius of inclusion. The curve corresponding to $J = 1$ and hence $P = 0$ coincides with the Mori-Tanaka solution for a 2-phase composite in the absence of an interphase region. The curves for $J = 1.3$ and $J = 1.15$ which lie above the Mori-Tanaka solution, correspond to an interphase region which is harder than the pure matrix. The curves for $J = 0.9$ and $J = 0.8$ which lie below the Mori-Tanaka solution, correspond to an interphase region which is softer than the pure matrix.

The results for this particular profile show a fairly strong dependence of the overall bulk modulus of the composite on the properties of the interphase. From Figure 2.4 we can see that the higher the volume fraction of the inclusion phase, the greater the effect of the interphase region on the bulk modulus of the composite. This result seems consistent with what is expected since the volume fraction of the interphase is directly proportional

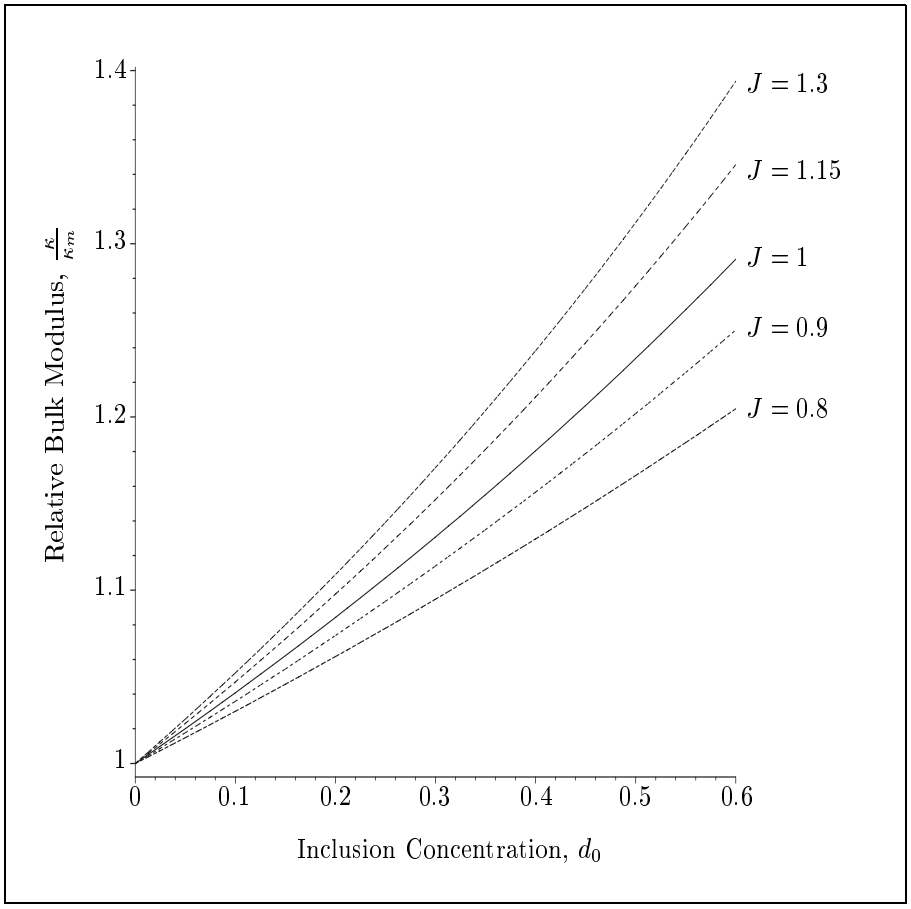

Figure 2.4: The Relative Bulk Modulus of a composite as a function of inclusion concentration for various values of J using $\kappa_m = 14$, $\mu_m = 3$ and $\kappa_p = 22$. The interphase region was assumed to have a thickness of 25% of the radius of inclusion. The above results remain the same if the radius of inclusion is allowed to vary.

to the volume fraction of the inclusions.

Therefore, the results seem to suggest that it is important to know what the properties of the interphase region are if an accurate theoretical measurement of the overall bulk modulus is to be made, particularly if the volume fraction of the inclusion phase is high. In the absence of such information, experimental results that are plotted against the Mori-Tanaka solution for a 2-phase composite may give us some insight into the nature of the interphase region that is forming in such composites. For example, if the experimental results lie below the Mori-Tanaka curve, then this may suggest the presence of an interphase region that is softer than the pure matrix. This conclusion will have greater force if perfect bonding is assumed to exist between the phases. On the other hand, if the experimental results lie above the Mori-Tanaka curve, then it seems that this would strongly suggest the presence of an interphase region that is harder than the pure matrix since the effect of imperfect bonding between the phases will only make the composite weaker.

If the radius of the inclusion is varied, then the relative bulk modulus as a function of volume fraction (for all values of J) will remain the same provided that the relative size of the interphase region does not change. For example, if the inclusion has radius a and the size of the interphase region remains 25% of a, then the calculations yield the same results for all values of a. This result seems to agree intuitively with what is expected from the model since the inclusion and interphase region would be expected to form an effective particle with the same properties, if the ratio of their volume fractions remains the same.

Therefore the results indicate that changing the radius of the inclusion will not effect the bulk modulus if the volume fraction remains the same. This result does not seem to be consistent with what is expected of nanocomposites which seem to offer better reinforcement at relatively low volume fractions of the inclusion phase (see [36, 65] and references therein). To explain this inconsistency we must conclude that either the present model is inadequate in modelling such composites or that we are not right to concede that the interphase region remains the same relative size as the radius of inclusion is varied, or that both these explanations are true. It is however generally thought that as the size of

the inclusion decreases, the relative size of the interphase region becomes larger. This is due to the fact that as the size of the inclusion decreases the surface area to volume ratio increases, that is, the surface area of the spherical inclusion increases relative to its volume. It is believed that the more surface area that is in contact with the surrounding matrix, the larger the relative size of the interphase region. Therefore, in the case of nanocomposites, the interphase would have a greater effect on their mechanical properties.

2.4.2 Variable Interphase Thickness

Composite materials are often designed by coating the filler with a third material before placing them within the matrix in order to produce better adhesion between the phases. For such applications it may be useful to know how the properties of the composite vary as a function of the thickness of this coating. If the interphase region has a variable thickness that is described by allowing the parameter b to vary, then the effective bulk modulus of a particle of radius b would be given by,

$$\kappa_E(b) = \frac{\kappa_0 S(b) + T(b)}{\kappa_0 U(b) + V(b)}. \tag{2.32}$$

In order to ensure the condition $b = aJ^{1/P}$, we must have

$$P = \frac{\ln(J)}{\ln(\frac{b}{a})}, \tag{2.33}$$

that is, P will vary as a function of b. Note that the solutions (2.27), (2.28), (2.30) and (2.31) still hold for the given profile since P will be fixed for a specific b.

Using the same mechanical properties as before for the inclusion and matrix, Figure 2.5 shows a plot of the effective bulk modulus of the inclusion and interphase for various values of the parameter J. The case for 2-phase composites, i.e. $J = 1$, which neglects the interphase is also plotted for comparison. The spherical inclusion was assumed to have a radius of $a = 1$. We can see from the graph that the harder the interphase, the greater the bulk modulus of the effective particle. The graph shows a decrease in the effective bulk modulus with respect to b which is what would be expected since the inclusion is assumed to be harder than the interphase. The graph also shows that for relatively small values of the parameter b, the effective bulk modulus changes rapidly.

Figure 2.6 shows a plot of the relative bulk modulus of a composite as a function of interphase thickness at a fixed volume fraction of inclusions given by, $d_0 = 0.1$. The case where $J = 1$ and hence $P = 0$ is plotted for comparison and is shown to be constant with respect to b. The graph shows that if the interphase is harder than the matrix, then the bulk modulus of the composite increases as b increases. The graph also shows that if the interphase is softer than the matrix, then the bulk modulus of the composite decreases

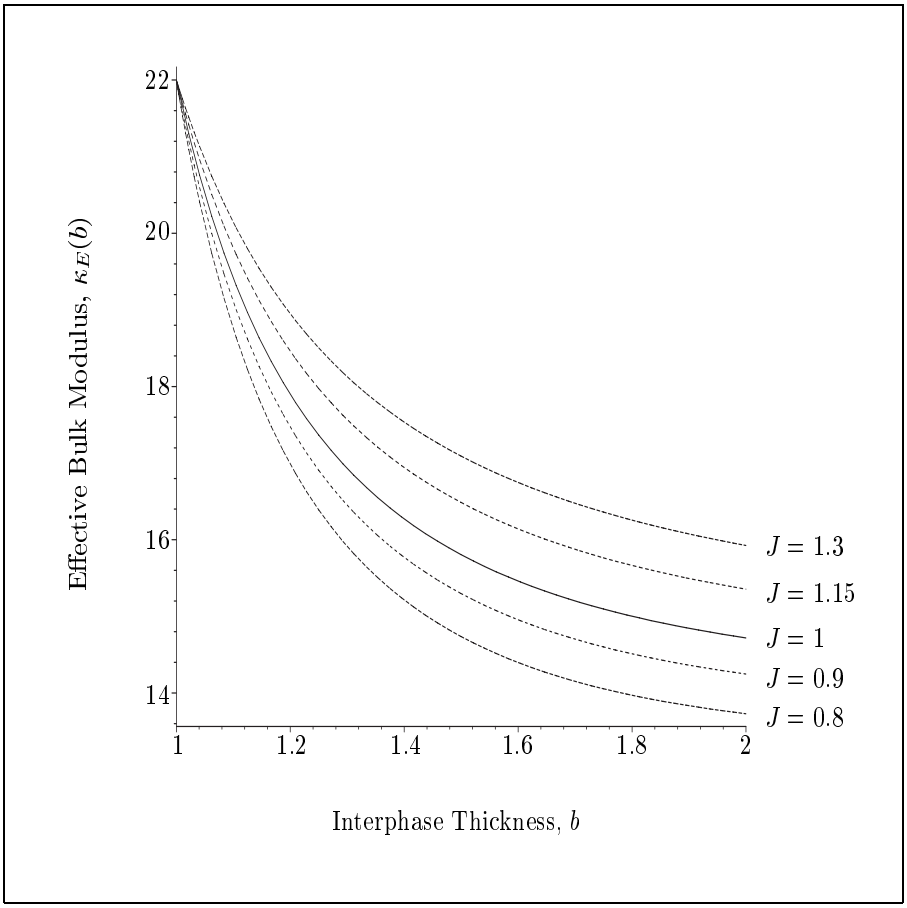

Figure 2.5: The Effective Bulk Modulus of the inclusion and interphase as a function of the interphase thickness using $\kappa_m = 14$, $\mu_m = 3$ and $\kappa_p = 22$. The radius of the inclusion is given by $a = 1$.

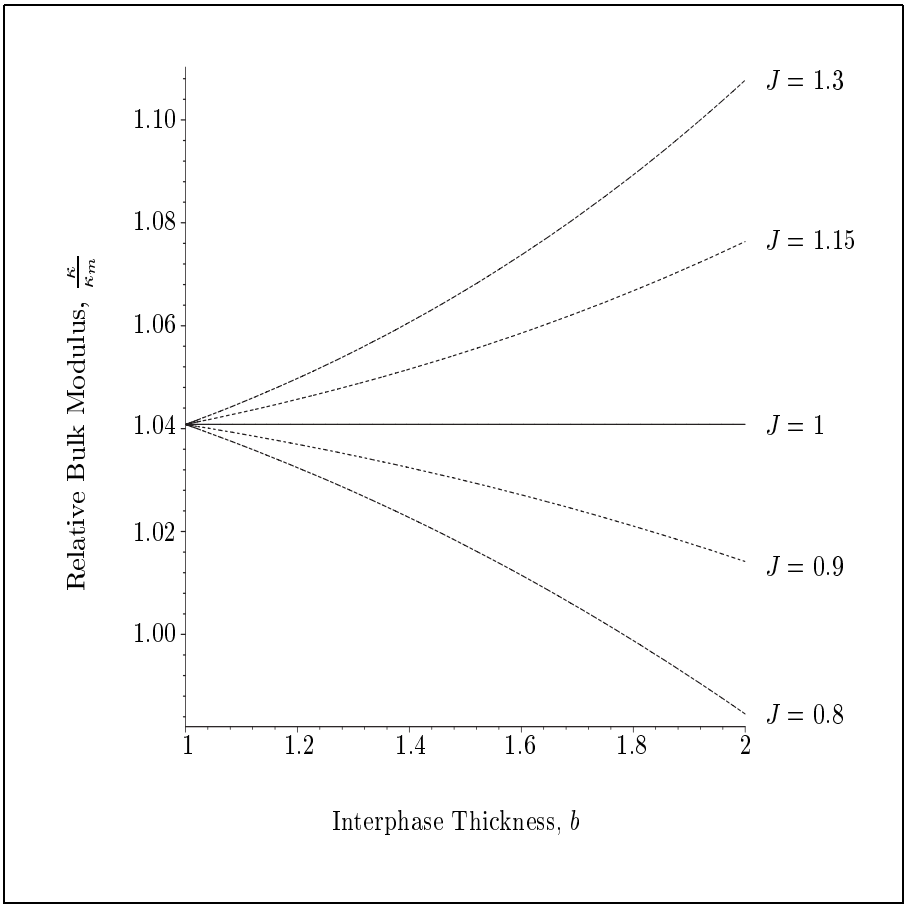

Figure 2.6: The Relative Bulk Modulus of a composite as a function of the interphase thickness. The above reults were computed using $\kappa_m = 14$, $\mu_m = 3$ and $\kappa_p = 22$. The inclusion concentration is fixed at a volume fraction of $d_0 = 0.1$. The radius of the inclusion is given by $a = 1$.

as b increases. This result agrees intuitively with what is expected since if the interphase is harder than the matrix, then the thicker the interphase the greater the bulk modulus of the composite. Also, if the interphase is softer than the matrix, then the thicker the interphase, the smaller the bulk modulus of the composite.

Note that if the radius of the inclusion is given by $a = 2$ and the graphs in Figures 2.5 and 2.6 are plotted for $2 \leq b \leq 4$, then the shape of the curves will be the same for the values of J that are indicated in the figures.

2.5 Conclusion

By using a replacement method we have been able to use a well established formula for the bulk modulus of a 2-phase composite containing spherical inclusions to account for an interphase region of varying properties. We were able to do this by splitting the interphase region into n concentric layers and converting a recurrence relation to a pair of coupled differential equations as $n \to \infty$. Therefore, by assuming that the properties of the interphase region vary as continuous functions of the radial distance from the center of the inclusion, the bulk modulus of the composite may be found whose solution is dependent on the solution of these differential equations. The differential equations hold assuming that the functions for the bulk and shear moduli which describe the mechanical properties of the interphase region are smooth, bounded and continuous. The model also assumes that the interphase region terminates at some specified point away from the inclusion, that the regions do not overlap and that the inclusions are homogeneously dispersed.

A closed form solution for the bulk modulus was found for a power law variation in the moduli as described in the work of Vörös and Pukánszky [72, 73]. Such a variation in the moduli results in a constant Poisson's ratio for the interphase which reduces considerably the complexity of the differential equations. Results were plotted as a function of inclusion concentration for various values of the parameters and showed how the properties of the interphase effect the relative bulk modulus compared to the well established solution for a 2-phase composite, which neglects the effect of the interphase. The results seem to be consistent with what one would expect by implementing such a model. For example, if the interphase is assumed to be softer than the matrix and inclusion, then the resulting composite would appear to be weaker if the interphase is taken into account. The effect of the interphase thickness was also examined and showed how varying the size of this region effects the effective bulk modulus of the inclusion and interphase and consequently the bulk modulus of the composite.

It is believed that it would also be possible to conduct a similar approach to find the shear modulus of a composite containing spherical inclusions surrounded by an inhomoge-

neous interphase provided that the solution for a 2-phase composite is of the appropriate form. The solution for the shear modulus provided by Weng [77] using the Mori-Tanaka method is of such a form and will be used in chapter 3 to account for an inhomogeneous interphase. An exact closed form expression for the shear modulus will also be derived for the same power law profile given above.

Regarding the initial problem which was to determine the mechanical properties of a composite containing spherical nanoparticles, it is not known how valid the model would be since continuum assumptions may break down at these scales. It is felt by some that traditional micromechanics models are no longer adequate for modeling nanocomposites but not altogether useless and therefore new research has recently focused on finding some middle ground between these models and a molecular dynamics approach [50, 49]. Although the need is felt for new models to be created in order to account for the discrete nature of matter at these length scales, some have modeled the mechanical behaviour of nanocomposites using only the continuum approach. In a paper written by Liu and Chen [35], a continuum mechanics approach using the Boundary Element Method is used to model the mechanical properties of composites reinforced with carbon nanotubes. The paper discusses the relevance of applying a continuum analysis on the nanometer scale mentioning the fact that continuum mechanics has been successful in modeling mechanical properties of carbon nanotubes to a certain extent. The paper also discusses the inferiority of a molecular dynamics approach highlighting the fact that the simulations involved can only deal with very *small* length and time scales and consequently may not be appropriate for certain studies, the continuum approach believed to be superior by the authors in certain cases. The authors research suggests that the continuum approach works when the dimensions are a few hundred nanometers and larger but that the continuum models are probably not suitable for length scales less than that due to the discrete nature of matter at that level. However, if we assume that the model is valid and that the size of the nanoparticle is large enough such that a continuum analysis may be employed, we are still confronted with the problem of knowing what the variation in the mechanical properties of the interphase would be for such composites and the size of this region. Therefore, implementing the current model in the case of nanocomposites would seem to

depend on new research being made available as to the the size of the interphase region and the distribution of its mechanical properties.

Chapter 3

A Two-way Particle Mapping for Calculation of the Shear Modulus of a Spherical Inclusion Composite with Inhomogeneous Interphase

3.1 Introduction

The shear modulus of a 2-phase composite consisting of isotropic spherical inclusions surrounded by an isotropic matrix has been derived by Weng [77] using the Mori-Tanaka method [46] and a different expression has also been derived by Christensen and Lo [8] using the Generalised Self Consistent Scheme. Hashin [15] was able to derive bounds for the shear modulus of such composites using variational theorems of the theory of elasticity. These bounds were found to be fairly close together but were not coincident as was the case for the bulk modulus. The model used by Hashin is known as the Composite Spheres Assemblage (CSA) model.

Hashin and Shritkman [19] have also used variational principles in the theory of elasticity to derive more generalised bounds for the elastic moduli of multiphase composites with inclusions of arbitrary shape. The lower and upper bounds for the bulk and shear moduli of a 2-phase composite where the inclusions have arbitrary shape were specifically

stated. These are given here for reference as,

$$\kappa^{(+)} = \kappa_2 + \frac{c_1}{\frac{1}{\kappa_1-\kappa_2} + \frac{3c_2}{3\kappa_2+4\mu_2}}$$
$$\kappa^{(-)} = \kappa_1 + \frac{c_2}{\frac{1}{\kappa_2-\kappa_1} + \frac{3c_1}{3\kappa_1+4\mu_1}}$$
$$\mu^{(+)} = \mu_2 + \frac{c_1}{\frac{1}{\mu_1-\mu_2} + \frac{6(\kappa_2+2\mu_2)c_2}{5\mu_2(3\kappa_2+4\mu_2)}}$$
$$\mu^{(-)} = \mu_1 + \frac{c_2}{\frac{1}{\mu_2-\mu_1} + \frac{6(\kappa_1+2\mu_1)c_1}{5\mu_1(3\kappa_1+4\mu_1)}}$$

where the subscripts 1 and 2 refer to the phases, κ and μ represent the bulk and shear modulus respectively and the negative $(-)$ and positive $(+)$ supercripts refer respectively to the lower and upper bound. Also, we have, $\kappa_2 > \kappa_1$ and $\mu_2 > \mu_1$.

It was found that the bulk modulus of a composite consisting of spherical inclusions as derived by Hashin [15] using the CSA model, was found to coincide with the lower Hashin-Shritkman (H-S) bound for the bulk modulus given above. When the spherical inclusions are softer than the matrix, this same expression for the bulk modulus was found to coincide with the H-S upper bound. This suggests that when the inclusion is stiffer than the matrix, spheres offer the poorest reinforcement. It also suggests that when the inclusion is softer than the matrix, spheres offer the best reinforcement. Note that the bulk modulus of a 2-phase composite containing spherical inclusions with both phases isotropic derived using the CSA model, is the same as that derived using the Mori-Tanaka method and the Generalised Self Consistent Scheme.

As has been stated, Weng [77] has been able to derive an exact expression for the shear modulus using the Mori-Tanaka method. At first he uses the method to generalise solutions for the elastic moduli of anisotropic multiphase composites containing arbitrarily orientated anisotropic inclusions. The results obtained for the bulk and shear modulus of 2-phase composites containing spherical inclusions were found to be related to the H-S bounds given above. It was found that when the matrix is the softest phase, both moduli coincide with the H-S lower bounds and when it is the harder phase, they coincide with their upper bounds.

It is worthwhile to briefly discuss some of the aspects of the micromechanics models mentioned thus far in order to gain some insight into their underlying principles. We begin with the composites spheres assemblage model of Hashin [15]. This is a 2-phase model which examines the change in the strain energy of a material that is subject to a uniform boundary traction as spherical composite spheres are added to what is initially a purely homogeneous material consisting entirely of the matrix phase. The composite spheres consist of an inclusion surrounded by a concentric spherical shell which is allowed to vary in size and has the property of the matrix. The composite is constructed by filling the homogeneous material with these composite spheres such that the space between the spheres in the limit vanishes. The strain energy of the composite is then found by summing the strain energies stored in all the composite spheres.

We leave our discussion of the Mori-Tanaka method till the next section where we give a more detailed description since its results are specifically used in our model for the shear modulus.

We now move on to the Generalised Self Consistent method which is a model that was fully developed by Christensen and Lo [8]. In this model, a composite sphere or cylinder consisting of the inclusion and a concentric shell with the property of the matrix, is embedded in a surrounding material which has the unknown properties of the composite material. For the case where both the inclusion and matrix phase are isotropic, the bulk modulus obtained coincides with the Composite Spheres Assemblage model and with the Mori-Tanaka method. The result for the shear modulus however, is the solution of a quadratic equation whose coefficients are functions of the phase properties and the volume fraction of inclusions. We give here the solution for the shear modulus according to this method which may be utilized in our model that takes into account the inhomogeneity of the interphase region. According to the Generalised Self Consistent Method, the shear modulus μ of a 2-phase composite containing spherical inclusions is given by Christensen and Lo [8] as the solution of the quadratic equation,

$$A\left(\frac{\mu}{\mu_m}\right)^2 + B\left(\frac{\mu}{\mu_m}\right) + C = 0 \tag{3.1}$$

where

$$
\begin{aligned}
A =& 8\left(\frac{\mu_p}{\mu_m}-1\right)(4-5\nu_m)\eta_1 c^{10/3} - 2\left[63\left(\frac{\mu_p}{\mu_m}-1\right)\eta_2 + 2\eta_1\eta_3\right]c^{7/3} \\
&+ 252\left(\frac{\mu_p}{\mu_m}-1\right)\eta_2 c^{5/3} - 25\left(\frac{\mu_p}{\mu_m}-1\right)(7-12\nu_m+8\nu_m^2)\eta_2 c + 4(7-10\nu_m)\eta_2\eta_3,
\end{aligned}
$$

$$
\begin{aligned}
B =& -4\left(\frac{\mu_p}{\mu_m}-1\right)(1-5\nu_m)\eta_1 c^{10/3} + 4\left[63\left(\frac{\mu_p}{\mu_m}-1\right)\eta_2 + 2\eta_1\eta_3\right]c^{7/3} \\
&- 504\left(\frac{\mu_p}{\mu_m}-1\right)\eta_2 c^{5/3} + 150\left(\frac{\mu_p}{\mu_m}-1\right)(3-\nu_m)\nu_m\eta_2 c + 3(15\nu_m-7)\eta_2\eta_3,
\end{aligned}
$$

$$
\begin{aligned}
C =& 4\left(\frac{\mu_p}{\mu_m}-1\right)(5\nu_m-7)\eta_1 c^{10/3} - 2\left[63\left(\frac{\mu_p}{\mu_m}-1\right)\eta_2 + 2\eta_1\eta_3\right]c^{7/3} \\
&+ 252\left(\frac{\mu_p}{\mu_m}-1\right)\eta_2 c^{5/3} + 25\left(\frac{\mu_p}{\mu_m}-1\right)(\nu_m^2-7)\eta_2 c - (7+5\nu_m)\eta_2\eta_3,
\end{aligned}
$$

with

$$
\eta_1 = \left(\frac{\mu_p}{\mu_m}-1\right)(7-10\nu_m)(7+5\nu_p) + 105(\nu_p-\nu_m),
$$

$$
\eta_2 = \left(\frac{\mu_p}{\mu_m}-1\right)(7+5\nu_p) + 35(1-\nu_p),
$$

$$
\eta_3 = \left(\frac{\mu_p}{\mu_m}-1\right)(8-10\nu_m) + 15(1-\nu_m),
$$

where the subscripts p and m again refer to the inclusion and matrix phases respectively and c denotes the volume fraction of inclusions. Also, the symbol ν refers to the Poisson's ratio.

In this work we use the shear modulus for a 2-phase composite containing spherical inclusions as derived by Weng [77] and Benveniste [2] using the Mori-Tanaka method, to account for an inhomogeneous interphase region surrounding each inclusion. A replacement method is used as we did for the bulk modulus case in Chapter 2 and in [40]. We generalise the results for any profile of the interphase region by deriving a coupled pair

of first order differential equations. The differential equations are then solved exactly for the same power law profile given in [40], giving a closed form solution for the shear modulus. The results are then presented to illustrate the effect of various parameters on the shear modulus of a composite. Since the differential equations that are derived are based on the Mori-Tanaka solution for the shear modulus which is only an approximation, we propose an improved model based on the generalised self consistent method incorporating a homogeneous interphase. The results for the improved model are close to the present method except for certain special cases which shall be discussed later.

3.2 The Mori-Tanaka Method

Using Mori-Tanaka theory [46] as well as concepts proposed by Eshelby [11], we shall attempt to derive the bulk and shear moduli of a 2-phase composite containing isotropic spherical inclusions surrounded by an isotropic matrix. This method has come to be generally known throughout the composite community as the Mori-Tanaka method although contributions from both Mori-Tanaka and Eshelby were necessary in its initial development. A more recent and simplified derivation of the Mori-Tanaka method has been given by Benveniste [2] which involves using a *direct approach* that ignores the concepts of Eshelby.

3.2.1 General Results for a 2-phase Composite

We begin with a more general derivation where we suppose that the inclusions are of arbitrary shape and that both phases may be anisotropic. The derivation used here follows the work of Weng [77] who considered the more general case of a multiphase anisotropic composite.

In our derivation we shall denote the matrix phase by a subscript m and the inclusion phase by a subscript i. The symbols σ and ϵ shall respectively denote stress and strain tensors which are by definition tensors of rank 2, while bold capital letters shall denote tensors of rank 4. Also, a bar on any lower case Greek letter such as $\bar{\sigma}$ or $\bar{\epsilon}$ shall denote a uniform or constant value. The inner product of two tensors is written such that $\mathbf{L}\epsilon = L_{ijkl}\epsilon_{kl}$, and $\mathbf{LA} = L_{ijkl}A_{klmn}$.

Consider a composite material which we shall refer to using the suffix 1 and an identically shaped comparison material with the property of the matrix. Both materials are subjected to the same boundary displacement causing a uniform strain $\bar{\epsilon}$ in both materials.

The boundary displacement would be given by, $u_i(S) = \epsilon^0_{ij}x_j$ where $u_i(S)$ represents the displacement vector at the surface S, ϵ^0_{ij} represents the constant strain tensor and x_j represents the position vector. Alternatively, a traction boundary condition could be used given by $T_i(S) = \sigma^0_{ij}n_j$ where $T_i(S)$ is the traction at S, σ^0_{ij} is the constant stress tensor and n_j represents the outward normal to the surface. Such boundary conditions

are referred to as homogeneous boundary conditions and are used for composite materials because they produce statistically homogeneous stress and strain fields. These homogeneous fields are necessary for composite materials in order to ensure that the inclusions remain homogeneously dispersed after the applied constraint.

The average stresses produced in each material as a result of this uniform strain are given by the constitutive equations,

$$\bar{\sigma} = \mathbf{L}_1 \bar{\epsilon} \qquad \text{and} \qquad \bar{\sigma}_m = \mathbf{L}_m \bar{\epsilon} \tag{3.2}$$

where $\mathbf{L}$ is generally referred to as the elastic stiffness tensor or elastic moduli tensor whose inverse is referred to as the compliance tensor. Our aim is to determine the elastic stiffness tensor $\mathbf{L}_1$ of the composite. Note that if we use the homogeneous boundary traction condition, the constitutive equations would be expressed in terms of the compliance tensor.

Mori-Tanaka's concept of *average stress* states that the average stress in the matrix phase of a composite is uniform or constant. This average stress which we denote by $\bar{\sigma}_m^1$ is caused by an average strain in the matrix phase of the composite given by $\bar{\epsilon}_m^1$.

Define an average perturbed stress $\tilde{\sigma}$ in the matrix phase of the composite as,

$$\tilde{\sigma} = \bar{\sigma}_m^1 - \bar{\sigma}_m. \tag{3.3}$$

That is, we define the average perturbed stress of the matrix phase as the difference between the actual average stress of the matrix in the composite material and the stress in the homogeneous comparison material since one is different to the other due to the presence of inclusions. This average perturbed stress would be caused by an average perturbed strain in the matrix phase which would therefore be defined as,

$$\tilde{\epsilon} = \bar{\epsilon}_m^1 - \bar{\epsilon}. \tag{3.4}$$

Using (3.3) and (3.4) we then have,

$$\bar{\sigma}_m + \tilde{\sigma} = \mathbf{L}_m(\bar{\epsilon} + \tilde{\epsilon}).$$

Likewise, we define an average perturbed stress σ^{pt} in the inclusion phase to be the difference between the actual average stress within an inclusion and the actual average stress in the matrix phase. That is,

$$\sigma^{pt} = \bar{\sigma}_i^1 - \bar{\sigma}_m^1. \tag{3.5}$$

This average perturbed stress is caused by an average perturbed strain which would therefore be defined as,

$$\epsilon^{pt} = \bar{\epsilon}_i^1 - \bar{\epsilon}_m^1. \tag{3.6}$$

Using, (3.3), (3.4), (3.5) and (3.6), the stress and strain in an inclusion are given by,

$$\bar{\sigma}_i^1 = \bar{\sigma}_m + \tilde{\sigma} + \sigma^{pt} \tag{3.7}$$

$$\bar{\epsilon}_i^1 = \bar{\epsilon} + \tilde{\epsilon} + \epsilon^{pt}. \tag{3.8}$$

Therefore, we have,

$$\bar{\sigma}_m + \tilde{\sigma} + \sigma^{pt} = \mathbf{L}_i(\bar{\epsilon} + \tilde{\epsilon} + \epsilon^{pt}). \tag{3.9}$$

We may rewrite the relationship (3.9) in terms of the matrix elastic moduli tensor $\mathbf{L}_m$ by using Eshelby's [11] idea of *stress-free* strain also referred to as eigenstrain by Mura [47]. The equivalent stress-free strain is according to Eshelby, the strain that the inclusion would undergo if it were to be imaginarily cut out of the composite material and allowed to transform freely under the applied constraint. Denoting the stress-free strain by ϵ^*, it is related to the average perturbed strain in the inclusion by the relation,

$$\epsilon^{pt} = \mathbf{S}\epsilon^* \tag{3.10}$$

where $\mathbf{S}$ is known as Eshelby's tensor whose elements are a function of the shape of the inclusion and the property of the matrix. Components of the Eshelby tensor for different inclusion shapes are given in Mura [47]. Using this proposed concept, (3.9) may be rewritten as,

$$\bar{\sigma}_i^1 = \bar{\sigma}_m + \tilde{\sigma} + \sigma^{pt} = \mathbf{L}_m(\bar{\epsilon} + \tilde{\epsilon} + \epsilon^{pt} - \epsilon^*). \tag{3.11}$$

The total average strain in the composite can be expressed in terms of the average strain of each of the phases and their respective volume fractions as,

$$\bar{\epsilon} = c\bar{\epsilon}_i^1 + (1-c)\bar{\epsilon}_m^1$$

where c is the volume fraction of inclusions. Using (3.4), (3.6) and (3.10) this leads to a relationship between the perturbed strain in the matrix and the stress-free strain given by,

$$\tilde{\epsilon} = -c\mathbf{S}\epsilon^*. \tag{3.12}$$

Use of (3.8) and (3.11) leads to the following relationship between the average strain in an inclusion and the stress-free strain,

$$\mathbf{L}_i\bar{\epsilon}_i^1 = \mathbf{L}_m(\bar{\epsilon} + \tilde{\epsilon} + \epsilon^{pt} - \epsilon^*) = \mathbf{L}_m(\bar{\epsilon}_i^1 - \epsilon^*)$$

$$\Rightarrow \bar{\epsilon}_i^1 = -(\mathbf{L}_i - \mathbf{L}_m)^{-1}\mathbf{L}_m\epsilon^*. \tag{3.13}$$

where $(\cdot)^{-1}$ denotes the inverse of the indicated quantity.

Therefore, using (3.8), (3.12) and (3.13), we obtain a relationship between the average strain in the composite and the stress-free strain given by,

$$c\mathbf{S}\epsilon^* - \mathbf{S}\epsilon^* - (\mathbf{L}_i - \mathbf{L}_m)^{-1}\mathbf{L}_m\epsilon^* = \bar{\epsilon}. \tag{3.14}$$

Defining a fourth order tensor $\mathbf{A}$ through the relation,

$$\epsilon^* = \mathbf{A}\bar{\epsilon} \tag{3.15}$$

gives when substituting into (3.14),

$$c\mathbf{S}\mathbf{A} - [\mathbf{S} + (\mathbf{L}_i - \mathbf{L}_m)^{-1}\mathbf{L}_m]\mathbf{A} = \mathbf{I} \tag{3.16}$$

which is a relationship from which the tensor $\mathbf{A}$ can be found and where $\mathbf{I}$ is the fourth order identity tensor defined as $I_{ijkl} = \frac{1}{2}(\delta_{ik}\delta_{jl} + \delta_{il}\delta_{jk})$ and δ_{ij} is the Kronecker delta. The tensor $\mathbf{A}$ is referred to as the strain concentration tensor.

Using (3.8), (3.12) and (3.15) the average strain inside an inclusion can be expressed in terms of the total average strain in the composite as,

$$\bar{\epsilon}_i^1 = [\mathbf{I} - c\mathbf{SA} + \mathbf{SA}]\bar{\epsilon}.$$

Like the total average strain, the total average stress in the composite can be expressed in terms of the average stress in the inclusion and matrix and their respective volume fractions. That is,

$$\bar{\sigma} = c\bar{\sigma}_i^1 + (1-c)\bar{\sigma}_m^1.$$

Using (3.3) and (3.5), this leads to the following expression for the total average stress in the composite,

$$\bar{\sigma} = \bar{\sigma}_m + \tilde{\sigma} + c\sigma^{pt}$$

$$\Rightarrow \bar{\sigma} = \bar{\sigma}_m + \mathbf{L}_m\tilde{\epsilon} + c\mathbf{L}_i\epsilon^{pt}. \tag{3.17}$$

We may express $\mathbf{L}_i\epsilon^{pt}$ in terms of $\mathbf{L}_m$ and ϵ^* using Eshelby's principle, that is,

$$\mathbf{L}_i\epsilon^{pt} = \mathbf{L}_m(\epsilon^{pt} - \epsilon^*) = \mathbf{L}_m(\mathbf{S} - \mathbf{I})\epsilon^*. \tag{3.18}$$

Substituting (3.12) and (3.18) into (3.17) gives,

$$\bar{\sigma} = \bar{\sigma}_m - c\mathbf{L}_m\epsilon^*.$$

Using the constitutive equation for the comparison material given in (3.2), that is $\bar{\sigma}_m = \mathbf{L}_m\bar{\epsilon}$, along with (3.15), this leads to,

$$\bar{\sigma} = \mathbf{L}_m[\mathbf{I} - c\mathbf{A}]\bar{\epsilon}.$$

Therefore, using the constitutive equation for the composite material given in (3.2), that is $\bar{\sigma} = \mathbf{L}_1\bar{\epsilon}$, we have found the elastic stiffness tensor of a 2-phase composite which is given by,

$$\mathbf{L}_1 = \mathbf{L}_m[\mathbf{I} - c\mathbf{A}]. \tag{3.19}$$

Note that this expression for the elastic stiffness tensor is valid for all inclusion shapes such that the Eshelby tensor $\mathbf{S}$ is defined for. These shapes are referred to as ellipsoids and include such shapes as perfectly round spheres, long cylinders, thin disks, etc. Also, no assumptions regarding the properties of the phases have been used, that is both phases may be anisotropic.

3.2.2 Results For Isotropic Spherical Inclusions in an Isotropic Matrix

We now attempt to use expression (3.19) to derive the elastic moduli of a 2-phase composite containing isotropic spherical inclusions surrounded by an isotropic matrix.

For isotropic bodies, the stress and strain tensors using tensor notation are related through [31],

$$\sigma_{ij} = \kappa\delta_{ij}\epsilon_{kk} + 2\mu(\epsilon_{ij} - \frac{1}{3}\delta_{ij}\epsilon_{kk}) \tag{3.20}$$

where κ and μ are the bulk and shear moduli.

We may rewrite the stress and strain tensors in terms of hydrostatic and deviatoric parts as,

$$\epsilon_{ij} = \epsilon'_{ij} + \frac{1}{3}\delta_{ij}\epsilon_{kk}, \qquad \sigma_{ij} = \sigma'_{ij} + \frac{1}{3}\delta_{ij}\sigma_{kk},$$

where the deviatoric parts are given by,

$$\epsilon'_{ij} = \epsilon_{ij} - \frac{1}{3}\delta_{ij}\epsilon_{kk}, \qquad \sigma'_{ij} = \sigma_{ij} - \frac{1}{3}\delta_{ij}\sigma_{kk}.$$

Upon substitution into (3.20), this leads to,

$$\sigma_{kk} = 3\kappa\epsilon_{kk}, \qquad \sigma'_{ij} = 2\mu\epsilon'_{ij}.$$

Therefore, the hydrostatic and deviatoric parts of the elastic stiffness tensor $\mathbf{L}$ of an isotropic body are given respectively by, 3κ and 2μ.

According to Eshelby, for isotropic spheres embedded in an isotropic matrix, the hydrostatic and deviatoric parts of the $\mathbf{S}$ tensor are expressed through the following relations between the perturbed strain, ϵ^{pt}, and stress-free strain ϵ^*;

$$\epsilon^{pt}_{kk} = \alpha_m \epsilon^*_{kk}, \qquad \epsilon^{pt\prime}_{ij} = \beta_m \epsilon^{*\prime}_{ij}$$

where

$$\alpha_m = \frac{3\kappa_m}{3\kappa_m + 4\mu_m}, \qquad \beta_m = \frac{6}{5}\frac{\kappa_m + 2\mu_m}{3\kappa_m + 4\mu_m}.$$

Therefore, equating hydrostatic and deviatoric parts of (3.19) gives respectively the bulk and shear modulus of the composite as,

$$\kappa = \kappa_m + \frac{c}{\frac{1}{\kappa_i - \kappa_m} + \frac{3(1-c)}{3\kappa_m + 4\mu_m}},$$

$$\mu = \mu_m + \frac{c}{\frac{1}{\mu_i - \mu_m} + \frac{6}{5}\frac{(1-c)(\kappa_m + 2\mu_m)}{\mu_m(3\kappa_m + 4\mu_m)}}.$$

Further work on the Mori-Tanaka method where different inclusion shapes are considered has been given by Chen, Dvorak and Benveniste [6], which included the prediction of elastic moduli of multiphase composites reinforced by transversely isotropic fibres and platelets that are aligned and randomly orientated. Extensions to aligned orthotropic fibres were also considered. Two-phase composites reinforced by elliptical cylinders were analysed by Zhao and Weng [84]. Two cases were considered, (a) where the elliptical cylinders are aligned in the axial direction but randomly aligned in the transverse direction and (b) where they are aligned in both directions.

3.3 The Model

In this section we derive our model for the shear modulus of a composite with an inhomogeneous interphase. It is shown that the derivation for the shear modulus case is similar to the bulk modulus case and therefore the same symbols have been used here in order to show the parallels between the two cases. The reader however, is cautioned to keep in mind the differences in the definitions assigned to some of the variables.

3.3.1 Foundation and Assumptions

The shear modulus of a 2-phase composite containing isotropic spherical inclusions surrounded by an isotropic matrix, as given by the Mori-Tanaka method is,

$$\mu = \mu_m + \frac{c}{\frac{1}{\mu_p - \mu_m} + \frac{6}{5}\frac{(1-c)(\kappa_m + 2\mu_m)}{\mu_m(3\kappa_m + 4\mu_m)}} \tag{3.21}$$

where c is the volume fraction of the inclusions, μ_p is the shear modulus of the inclusion and κ_m, μ_m are respectively the bulk and shear modulus of the matrix.

Again we consider an interphase region of finite size surrounding each inclusion as in [40]. The properties of the interphase are assumed to vary as a function of the radial distance from the centre of the inclusion. These functions are again assumed to be smooth, bounded and continuous functions. The radius of the inclusion is assumed to have length a and the thickness of the interphase is given by $(b - a)$.

We model the inclusion and interphase together as forming a new, effective spherical particle of radius b. It shall also be assumed that the inclusions are well spaced apart and that the interphase regions don't overlap. Note also that for the composite with an inhomogeneous interphase, we denote the volume fraction of inclusions relative to all phases by d_0.

By splitting the interphase region into different layers or regions as in [40], we begin with the particle and first layer of interphase and model this as a new effective spherical particle. We then re-apply equation (3.21) using this new effective spherical particle as the inclusion phase and the next layer of interphase as being equivalent to the matrix phase. We continue to apply (3.21) by using the replacement method proposed by Qiu

and Weng [52] and also by Hashin [17] over and over until all the layers have been used up.

3.3.2 Formulation of the Problem

Expression (3.21) for the shear modulus is similar to the bulk modulus, so it seems that if we again assume that the properties of the interphase region vary as functions of x (that is, the radial distance from the centre of the inclusion), it would be possible to derive a pair of coupled differential equations as before which would enable us to calculate the shear modulus of the composite.

As before, we split the interphase region into n concentric layers as shown in [40], causing a partition $\mathcal{P}$ of $[a, b]$ into n subintervals. The lengths of these subintervals presently need not be the same and we choose any point within each subinterval given by $\xi_i \in [x_{i-1}, x_i]$. Then everything proceeds here analogously to the bulk modulus case [40].

The effective shear modulus μ_i of the particle up to the i-th layer is approximated by,

$$\mu_i = \mu(\xi_i) + \frac{d_i}{\frac{1}{\mu_{i-1}-\mu(\xi_i)} + \frac{6}{5}\frac{(1-d_i)(\kappa(\xi_i)+2\mu(\xi_i))}{\mu(\xi_i)(3\kappa(\xi_i)+4\mu(\xi_i))}} \tag{3.22}$$

where $d_i = \left(\frac{x_{i-1}}{x_i}\right)^3$, $i \in \{\mathbb{N} : 1 \leq i \leq n\}$, $\xi_i \in [x_{i-1}, x_i]$ and $\mu_p = \mu_0$. $\kappa(x)$ and $\mu(x)$ are functions describing the properties of the interphase region such that $x \in [a, b]$ and μ_{i-1} is an approximation to the shear modulus of the inner composite sphere.

Our aim now is to find the effective shear modulus, μ_E, of the inclusion and whole interphase region which would be given by,

$$\mu_E = \lim_{n\to\infty} \mu_n$$

where μ_n is found by solving the recurrence relation (3.22).

Conversion of Reccurence Relation to Simultaneous Difference Equations

We may rewrite (3.22) as,

$$\mu_i = \frac{A_i\mu_{i-1} + B_i}{C_i\mu_{i-1} + D_i} \tag{3.23}$$

where,

$$A_i = f_i d_i \mu(\xi_i) + d_i, \qquad B_i = \mu(\xi_i) - f_i d_i \mu(\xi_i)^2 - d_i \mu(\xi_i),$$
$$C_i = f_i d_i, \qquad D_i = 1 - f_i d_i \mu(\xi_i),$$

and,

$$f_i = \frac{6(1-d_i)(\kappa(\xi_i) + 2\mu(\xi_i))}{d_i 5\mu(\xi_i)(3\kappa(\xi_i) + 4\mu(\xi_i))}.$$

The recurrence relation (3.23) is the same as for the bulk modulus case so we may therefore immediately write down the alternative representation for μ_i given by,

$$\mu_i = \frac{S_i(A_1\mu_0 + B_1) + T_i(C_1\mu_0 + D_1)}{U_i(A_1\mu_0 + B_1) + V_i(C_1\mu_0 + D_1)} \tag{3.24}$$

where,

$$S_i = A_i S_{i-1} + B_i U_{i-1} \tag{3.25}$$
$$U_i = C_i S_{i-1} + D_i U_{i-1} \tag{3.26}$$

which together form a pair of simultaneous first order linear difference equations with non-constant coefficients and initial conditions, $S_1 = 1$, $U_1 = 0$. Also we have, $i \in \{\mathbb{N} : 2 \leq i \leq n\}$.

We also have for T_i and V_i,

$$T_i = A_i T_{i-1} + B_i V_{i-1} \tag{3.27}$$
$$V_i = C_i T_{i-1} + D_i V_{i-1} \tag{3.28}$$

which are a pair of simultaneous equations identical to (3.25) and (3.26), but with initial conditions, $T_1 = 0$ and $V_1 = 1$. Also we have, $i \in \{\mathbb{N} : 2 \leq i \leq n\}$.

3.3.3 The Governing Differential Equations

Again, we may rewrite (3.25) and (3.26) as,

$$S_{i+1} = A_{i+1}S_i + B_{i+1}U_i \tag{3.29}$$

$$U_{i+1} = C_{i+1}S_i + D_{i+1}U_i \tag{3.30}$$

where $S_1 = 1$, $U_1 = 0$ and $i \in \{\mathbb{N} : 1 \leq i \leq (n-1)\}$.

For each subinterval $[x_{i-1}, x_i]$ of the partition $\mathcal{P}$ let each Δx_i have the same width Δx and choose ξ_i to be the right hand end point, that is, we shall take $\xi_i = x_i$. Then we have,

$$(1 - d_i) = \Delta x g_i \qquad \text{where} \qquad g_i = \frac{x_i^2 + x_i x_{i-1} + x_{i-1}^2}{x_i^3}.$$

We re-write A_i, B_i, C_i, and D_i for notational convenience as,

$$A_i = \Delta x \alpha_i + d_i \qquad \text{where} \qquad \alpha_i = \frac{6g_i(\kappa(x_i) + 2\mu(x_i))}{5(3\kappa(x_i) + 4\mu(x_i))},$$

$$B_i = \Delta x \beta_i \qquad \text{where} \qquad \beta_i = g_i \mu(x_i) \left(1 - \frac{6(\kappa(x_i) + 2\mu(x_i))}{5(3\kappa(x_i) + 4\mu(x_i))}\right),$$

$$C_i = \Delta x \gamma_i \qquad \text{where} \qquad \gamma_i = \frac{6g_i(\kappa(x_i) + 2\mu(x_i))}{5\mu(x_i)(3\kappa(x_i) + 4\mu(x_i))},$$

and $D_i = 1 - \Delta x \alpha_i$.

As before we let $A_2, A_3, A_4, \ldots, A_n$ be discrete values of a function $A(x)$. Similarly we have the functions $B(x)$, $C(x)$ and $D(x)$. Also, let S_i and U_i be values of the functions $S(x)$ and $U(x)$. Then, (3.29) and (3.30) may be re-written as,

$$S(x_i + \Delta x) = A(x_i + \Delta x)S(x_i) + B(x_i + \Delta x)U(x_i) \tag{3.31}$$

$$U(x_i + \Delta x) = C(x_i + \Delta x)S(x_i) + D(x_i + \Delta x)U(x_i) \tag{3.32}$$

where $S(x_1) = 1$, $U(x_1) = 0$ and $i \in \{\mathbb{N} : 1 \leq i \leq (n-1)\}$.

After re-arranging equation (3.31) and taking the limit of both sides as $\Delta x \to 0$, we get,

$$S'(x_i) = A'(x_i)S(x_i) + S(x_i)\lim_{\Delta x\to 0}\left(\frac{A(x_i)-1}{\Delta x}\right) + B'(x_i)U(x_i) + U(x_i)\lim_{\Delta x\to 0}\left(\frac{B(x_i)}{\Delta x}\right)$$

where,

$$\lim_{\Delta x\to 0}\left(\frac{A(x_i)-1}{\Delta x}\right) = -\frac{3}{5x_i}\left(\frac{9\kappa(x_i)+8\mu(x_i)}{3\kappa(x_i)+4\mu(x_i)}\right)$$

and,

$$\lim_{\Delta x\to 0}\left(\frac{B(x_i)}{\Delta x}\right) = \frac{3\mu(x_i)}{5x_i}\left(\frac{9\kappa(x_i)+8\mu(x_i)}{3\kappa(x_i)+4\mu(x_i)}\right).$$

It can also be shown that,

$$A'(x_i) = \alpha'(x_i)\lim_{\Delta x\to 0}(\Delta x) + \lim_{\Delta x\to 0}\left(\frac{\left(\frac{x_i}{x_{i+1}}\right)^3 - \left(\frac{x_{i-1}}{x_i}\right)^3}{\Delta x}\right)$$

and

$$B'(x_i) = \beta'(x_i)\lim_{\Delta x\to 0}(\Delta x).$$

As in chapter 2, we have the second term in the expression for $A'(x_i)$ equal to zero. The properties of the interphase are such that the functions $\alpha(x)$ and $\beta(x)$ are smooth, bounded and continuous in the interval $[a,b]$ and hence $\alpha'(x_i)$ and $\beta'(x_i)$ will be finite for all $x_i \in [a,b]$. Therefore, we have $A'(x_i) = 0$ and $B'(x_i) = 0$ at all points $x_i \in [a,b]$.

Re-arranging equation (3.32) and taking the limit of both sides as $\Delta x \to 0$ gives,

$$U'(x_i) = C'(x_i)S(x_i) + S(x_i)\lim_{\Delta x\to 0}\left(\frac{C(x_i)}{\Delta x}\right) + D'(x_i)U(x_i) + U(x_i)\lim_{\Delta x\to 0}\left(\frac{D(x_i)-1}{\Delta x}\right)$$

where,

$$\lim_{\Delta x\to 0}\left(\frac{C(x_i)}{\Delta x}\right) = \frac{18}{5x_i\mu(x_i)}\left(\frac{\kappa(x_i)+2\mu(x_i)}{3\kappa(x_i)+4\mu(x_i)}\right)$$

and

$$\lim_{\Delta x \to 0} \left(\frac{D(x_i) - 1}{\Delta x} \right) = -\frac{18}{5x_i} \left(\frac{\kappa(x_i) + 2\mu(x_i)}{3\kappa(x_i) + 4\mu(x_i)} \right).$$

Also, we have,

$$C'(x_i) = \gamma'(x_i) \lim_{\Delta x \to 0} (\Delta x)$$

and

$$D'(x_i) = -\alpha'(x_i) \lim_{\Delta x \to 0} (\Delta x).$$

The imposed restrictions on the inhomogeneous properties of the interphase imply that both $\alpha'(x_i)$ and $\gamma'(x_i)$ are finite for all points $x_i \in [a, b]$. Consequently both $C'(x_i)$ and $D'(x_i)$ are equal to zero.

The initial conditions in the limit as $n \to \infty$ or $\Delta x \to 0$ become, $S(a) = 1$ and $U(a) = 0$.

Therefore, as was the case for the bulk modulus, the two simultaneous difference equations have been converted into a pair of simultaneous differential equations given by,

$$S'(x) = -\frac{3}{5x} \left(\frac{9\kappa(x) + 8\mu(x)}{3\kappa(x) + 4\mu(x)} \right) S(x) + \frac{3\mu(x)}{5x} \left(\frac{9\kappa(x) + 8\mu(x)}{3\kappa(x) + 4\mu(x)} \right) U(x) \tag{3.33}$$

$$U'(x) = \frac{18}{5x\mu(x)} \left(\frac{\kappa(x) + 2\mu(x)}{3\kappa(x) + 4\mu(x)} \right) S(x) - \frac{18}{5x} \left(\frac{\kappa(x) + 2\mu(x)}{3\kappa(x) + 4\mu(x)} \right) U(x) \tag{3.34}$$

where $S(a) = 1$, $U(a) = 0$ and $x \in [a, b]$.

Similarly, the simultaneous difference equations given by (3.27) and (3.28), may be converted into an identical pair of simultaneous differential equations given by,

$$T'(x) = -\frac{3}{5x} \left(\frac{9\kappa(x) + 8\mu(x)}{3\kappa(x) + 4\mu(x)} \right) T(x) + \frac{3\mu(x)}{5x} \left(\frac{9\kappa(x) + 8\mu(x)}{3\kappa(x) + 4\mu(x)} \right) V(x) \tag{3.35}$$

$$V'(x) = \frac{18}{5x\mu(x)} \left(\frac{\kappa(x) + 2\mu(x)}{3\kappa(x) + 4\mu(x)} \right) T(x) - \frac{18}{5x} \left(\frac{\kappa(x) + 2\mu(x)}{3\kappa(x) + 4\mu(x)} \right) V(x) \tag{3.36}$$

where $T(a) = 0$, $V(a) = 1$ and $x \in [a, b]$.

Note that these differential equations which govern the shear modulus behaviour of a composite with an inhomogeneous interphase are not the same equations which govern the bulk modulus behaviour. However, like the bulk modulus case, note again how the pair of equations given by (3.35) and (3.36) differ to the pair of equations given by (3.33) and (3.34) only in the boundary conditions. Therefore, only one pair of equations needs to be solved with appropriate care taken when accounting for the boundary conditions.

3.3.4 The General Solution for the Shear Modulus

The effective shear modulus of the inclusion and interphase is given by,

$$\mu_E = \lim_{n\to\infty} \mu_n$$

where from (3.24) we have,

$$\mu_n = \frac{S_n(A_1\mu_0 + B_1) + T_n(C_1\mu_0 + D_1)}{U_n(A_1\mu_0 + B_1) + V_n(C_1\mu_0 + D_1)}$$

As $n \to \infty$ we have $A_1 \to 1$, $B_1 \to 0$, $C_1 \to 0$ and $D_1 \to 1$. Also, like the bulk modulus case we have,

$$\lim_{n\to\infty} S_n = S(b), \qquad \lim_{n\to\infty} U_n = U(b),$$

$$\lim_{n\to\infty} T_n = T(b), \qquad \text{and} \qquad \lim_{n\to\infty} V_n = V(b).$$

Therefore, the effective shear modulus of the particle and interphase is given by,

$$\mu_E = \frac{\mu_0 S(b) + T(b)}{\mu_0 U(b) + V(b)}. \tag{3.37}$$

The shear modulus of the composite can then easily be found by substituting $\mu_p = \mu_E$ in equation (3.21) and letting $c = d_0\frac{b^3}{a^3}$. That is, the shear modulus is given by,

$$\mu = \mu_m + \frac{c}{\frac{1}{\mu_E - \mu_m} + \frac{6}{5}\frac{(1-c)(\kappa_m+2\mu_m)}{\mu_m(3\kappa_m+4\mu_m)}}$$

where

$$c = d_0\frac{b^3}{a^3}$$

and d_0 is the volume fraction of inclusions relative to all phases.

3.4 Improvement in the Accuracy of the Interphase Model

It is worthwhile to note that the essence of the model lay in finding the shear modulus of the effective particle consisting of inclusion and surrounding interphase region. This effective particle is then considered as the new inclusion with different size and properties to the original inclusion. Therefore, other micromechanics models which have an explicit solution for the shear modulus may be incorporated into the present results. For example, in the Generalised Self Consistent Scheme, the shear modulus is given by the solution of the quadratic equation (3.1). Therefore, if in this equation we allow $\mu_p = \mu_E$ and $c = d_0 \frac{b^3}{a^3}$, then the shear modulus may be obtained which takes into account the effects of an inhomogeneous interphase. Note that the Poisson's ratio of the effective particle consisting of inclusion and inhomogeneous interphase would be given by,

$$\nu_E = \frac{1}{2}\left(\frac{3\kappa_E - 2\mu_E}{3\kappa_E + \mu_E}\right)$$

where κ_E has been found in [40]. This result is useful in that it enables us to test the effect of the inhomogeneous region using other micromechanics models. This was the approach used recently by Shen and Li [60] who checked their results against finite element computations. It was found that their model was rather accurate when the properties of the interphase vary between those of particle/fibre and matrix but was unsatisfactory when the interphase was much harder than both particle/fibre and matrix. The present model is similar to the model proposed by Shen and Li [60] although the governing differential equations differ.

The GSC method of Christensen and Lo [8] gives the exact solution to the 2-phase shear problem whereas the Mori-Tanaka solution is only an approximation. Therefore, there is an error in the current method in that the shear modulus of the effective particle consisting of inclusion and interphase is found based on the Mori-Tanaka solution. The exact shear modulus of the effective particle will then be different to the value found by the current method which is given by (3.37). Note that the result for the bulk modulus however is exact.

Wang and Jasiuk [75] have solved the shear modulus problem exactly for the power law profile using the GSC method by solving a partial differential equation for the displacement of the material that is subjected to shear strain at infinity. Use of this approach for other profiles may however be problematic due to the complexity of the partial differential equation governing the displacement.

We propose an alternative approach where we use results of Theocaris [68] who derives the shear modulus of a particulate composite with homogeneous interphase using the GSC method of Christensen and Lo [8]. The interphase was assumed to have uniform properties and for such a case the shear modulus derived is exact. To account for an inhomogeneous interphase, Theocaris [68] employs an averaging technique whereby the average shear property of the interphase is estimated.

In order to estimate the shear property of the interphase we map the homogeneous properties of the effective particle consisting of inclusion and interphase onto a 2-phase composite as shown in Figure 3.1. Note that perfect bonding is assumed to exist between the phases. We can do this by solving the following two simultaneous equations for κ_i and μ_i, that is,

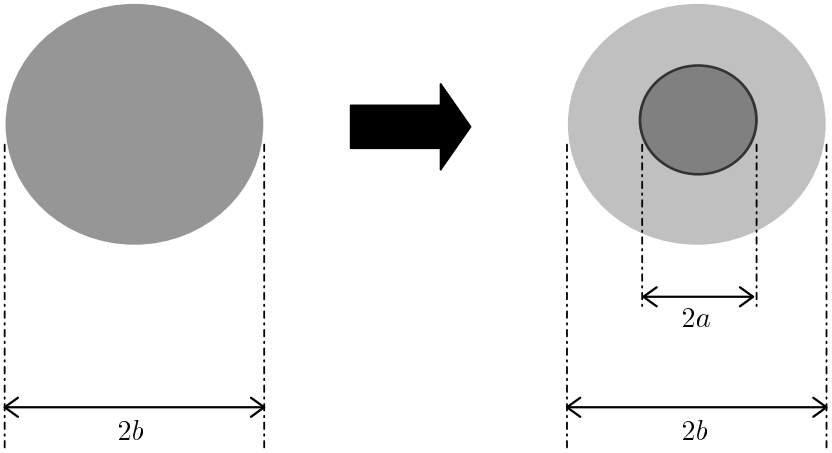

Figure 3.1: A mapping of a homogeneous particle consisting of inclusion and interphase onto a 2-phase composite.

$$\kappa_E = \kappa_i + \frac{\frac{a^3}{b^3}}{\frac{1}{\kappa_p - \kappa_i} + \frac{3(1-\frac{a^3}{b^3})}{3\kappa_i + 4\mu_i}}, \tag{3.38}$$

$$\mu_E = \mu_i + \frac{\frac{a^3}{b^3}}{\frac{1}{\mu_p - \mu_i} + \frac{6}{5}\frac{(1-\frac{a^3}{b^3})(\kappa_i + 2\mu_i)}{\mu_i(3\kappa_i + 4\mu_i)}}, \tag{3.39}$$

where the subscript i denotes the interphase. Note that κ_E is given in Chapter 2 or in [40] and μ_E is given by (3.37) or in [39].

Therefore, by utilizing the above values for κ_i and μ_i and then solving the shear problem with a homogeneous interphase using the GSC method, we should improve on the accuracy of our results.

Shen and Li [61] have extended one of their previous papers [60] which is a model based on the replacement method. In their previous model, the replacement method is used to compute the bulk and shear modulus of a fibre/sphere surrounded by an inhomogeneous interphase. They found a first order non-linear Riccati differential equation which models this. It can be shown that the two linear coupled differential equations which model the bulk or shear modulus that are presented in this thesis, can be converted to the differential equation found by Shen and Li [60]. This is not surprising since both models are based on the replacement method. Therefore, the present model serves as an alternative set of equations. It was concluded by Shen and Li [60] that their model was unsatisfactory for the case where the inhomogeneous properties of the interphase do not vary between the properties of inclusion and matrix. It is also mentioned by Shen and Li [61] that there are physically realistic grounds for this type of scenario and so they try to rectify this situation in their second paper [61]. To do this they map the inhomogeneous properties of the interphase onto a homogeneous interphase, that is, the inhomogeneous properties of the interphase are converted to an equivalent homogeneous interphase. The most effective way of doing this they describe by a mapping very similar to the mapping described above. There is however a slight difference in the procedure worth noting. The first part of the procedure is the same, that is, a differential equation based on the replacement method is solved in order to compute the homogeneous properties of an inclusion surrounded by an inhomogeneous interphase. This homogeneous sphere is then mapped onto a 2-phase

composite, in order to find the constant bulk and shear modulus of the interphase. To do this, Shen and Li [61] have used the average value for the Poisson's ratio of the interphase. Although it is shown by Shen and Li [61] that the variation in the Poisson's ratio of the interphase has a small effect, one does not have to use the average value for the Poisson's ratio in order to obtain these constants. The present method solves two coupled equations, that is, equations (3.38) and (3.39), giving several solutions, the correct one being that which is physically realistic, that is, both constants positive. Shen and Li [61] also describe a uniform interphase model, which is a simple averaging technique that can also be used to find these constants although there are some limitations posed by this model.

In order to determine the shear modulus of the composite, Shen and Li [61] determine the strain energy change of an infinite matrix due to the presence of a single inclusion surrounded by an inhomogeneous interphase using the GSC method. Thus, to determine the strain energy change, an 8×8 linear system of equations must be solved. The method presented in this thesis however, utilises the GSC scheme with the presence of a homogeneous interphase as developed by Theocaris [68] , which involves the solution of a 12×12 linear system. This method is presented in detail in the following section.

3.5 The Shear Modulus of a Particulate Composite with a Homogeneous Interphase Derived using the GSC Method

The exact shear modulus of a particulate composite with homogeneous interphase was derived by Theocaris [68]. We give a brief form of the derivation here. A summary of the GSC method is given in the introduction of this report. We now simply incorporate the interphase region. To begin with, we consider Figure 3.2.

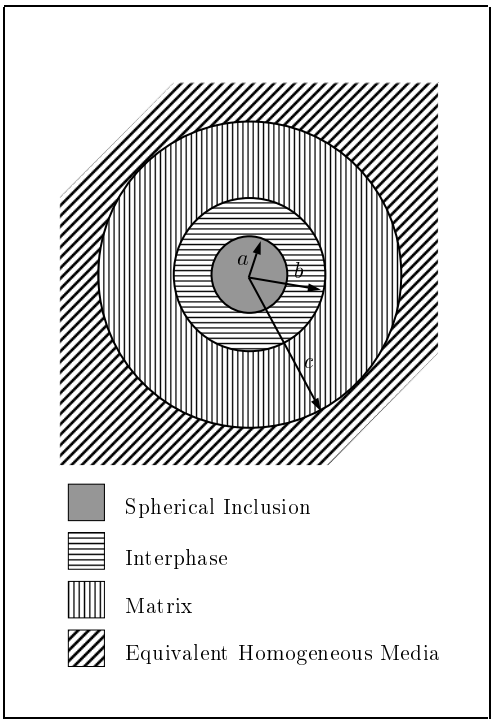

Figure 3.2: The GSC model incorporating a homogeneous interphase region.

According to Christensen and Lo [8], the displacement **u** in each of the phases is represented in spherical polar coordinates as,

$$u_r = U_r(r)\sin^2\theta\cos 2\phi,$$
$$u_\theta = U_\theta(r)\sin\theta\cos\theta\cos 2\phi,$$
$$u_\phi = U_\phi(r)\sin\theta\sin 2\phi,$$
$$U_\theta = -U_\phi.$$

Note that r represents the radial distance from the centre of the inclusion. In what follows, the Greek letters μ and ν shall denote the shear modulus and Poisson's ratio respectively. Also, a variable without a subscript shall denote the property of the composite.

The solutions of the equations of equilibrium in each of the homogeneous phases are given by Christensen and Lo [8] as,

(i) For the equivalent homogeneous medium, $r \geq c$, (denoted by a superscript e),

$$U_r^e = D_1 + \frac{3D_3}{r^4} + \frac{(5-4\nu)}{(1-2\nu)}\frac{D_4}{r^2}$$
$$U_\theta^e = D_1 r - \frac{2D_3}{r^4} + \frac{2D_4}{r^2}$$

(ii) In the matrix phase, $b \leq r \leq c$, (denoted by a subscript or superscript m),

$$U_r^m = C_1 r - \frac{6\nu_m}{(1-2\nu_m)}C_2 r^3 + \frac{3C_3}{r^4} + \frac{(5-4\nu_m)C_4}{(1-2\nu_m)r^2}$$
$$U_\theta^m = C_1 r - \frac{(7-4\nu_m}{(1-2\nu_m)}C_2 r^3 + \frac{2C_3}{r^4} + \frac{2C_4}{r^2}$$

(iii) In the interphase, $a \leq r \leq b$, (denoted by a subscript or superscript i),

$$U_r^i = B_1 r - \frac{6\nu_i}{(1-2\nu_i)}B_2 r^3 + \frac{3B_3}{r^4} + \frac{(5-4\nu_i)B_4}{(1-2\nu_i)r^2}$$
$$U_\theta^i = B_1 r - \frac{(7-4\nu_i}{(1-2\nu_i)}B_2 r^3 + \frac{2B_3}{r^4} + \frac{2B_4}{r^2}$$

(iv) In the particle inclusion phase, $0 \leq r \leq a$, (denoted by a subscript or superscript p),

$$U_r^p = A_1 r - \frac{6\nu_p}{(1-2\nu_p)} A_2 r^3$$
$$U_\theta^p = A_1 r - \frac{(7-4\nu_p}{(1-2\nu_p)} A_2 r^3$$

As $r \to \infty$ we have the following conditions of simple shear,

$$\begin{aligned}
u_r^0 &= D_1 r \sin^2\theta \cos 2\phi, \\
u_\theta^0 &= D_1 r \sin\theta \cos\theta \cos 2\phi, \\
u_\phi^0 &= -D_1 r \sin\theta \sin 2\phi, \\
\sigma_{rr}^0 &= 2\mu D_1 \sin^2\theta \cos 2\phi, \\
\tau_{r\theta}^0 &= 2\mu D_1 \sin\theta \cos\theta \cos 2\phi, \\
\tau_{r\phi}^0 &= -2\mu D_1 \sin\theta \sin 2\phi.
\end{aligned}$$

Therefore, D_1 is defined in terms of the shear loading condition at infinity. Theocaris [68] expresses D_1 as $D_1 = \frac{\tau_\infty}{2\mu}$, where τ_∞ is the shear stress at infinity.

The 12 unknown constants, A_1, A_2, B_1, B_2, B_3, B_4, C_1, C_2, C_3, C_4, D_3, D_4, are to be determined by the continuity conditions at the interfaces. This involves the continuity of the stresses, σ_{rr}, $\tau_{r\theta}$ and $\tau_{r\phi}$ and the displacements u_r, u_θ and u_ϕ. These conditions are,

$$\begin{array}{lllll}
u_r^p = u_r^i, & u_\theta^p = u_\theta^i, & \sigma_{rr}^p = \sigma_{rr}^i, & \tau_{r\theta}^p = \tau_{r\theta}^i & \text{at} \quad r = a, \\
u_r^i = u_r^m, & u_\theta^i = u_\theta^m, & \sigma_{rr}^i = \sigma_{rr}^m, & \tau_{r\theta}^i = \tau_{r\theta}^m & \text{at} \quad r = b, \\
u_r^m = u_r^e, & u_\theta^m = u_\theta^e, & \sigma_{rr}^m = \sigma_{rr}^e, & \tau_{r\theta}^m = \tau_{r\theta}^e & \text{at} \quad r = c.
\end{array} \tag{3.40}$$

The stress and strain components in each of the phases are given in Appendix A.

To find the shear modulus of the composite, Christensen and Lo [8] use the following result obtained by Eshelby, that is, for a homogeneous medium containing an inclusion, the strain energy U, under applied displacement conditions is given by,

$$U = U_0 - \frac{1}{2}\int_S (T_i^0 u_i^e - T_i^e u_i^0)\, dS \tag{3.41}$$

where S is the surface of the composite sphere defined by $r = c$, U_0 is the strain energy in the material when it contains no inclusion, T_i^0 and u_i^0 are the tractions and displacements in the material due to the applied loading when it contains no inclusion and T_i^e and u_i^e are the tractions and displacements due to the applied loading when it does contain the inclusion.

To find the shear modulus, an equivalent homogeneous comparison material is introduced such that under the same applied loading, the same energy U is stored in this homogeneous comparison material. Therefore, the energy of this equivalent homogeneous comparison material which we denote by U_{equiv}, is the same as the energy stored in our composite material if no inclusion is present which is given by Eshelby as U_0. Therefore, we have $U = U_{equiv}$ and $U_{equiv} = U_0$, which gives $U = U_0$. Hence, equation (3.41) becomes,

$$\int_S (T_i^0 u_i^e - T_i^e u_i^0)\, dS = 0$$

which in spherical polar coordinates is given by,

$$\int_S (\sigma_{rr}^0 u_r^e + \tau_{r\theta}^0 u_\theta^e + \tau_{r\phi}^0 u_\phi^e - \sigma_{rr}^e u_r^0 - \tau_{r\theta}^e u_\theta^0 - \tau_{r\phi}^e u_\phi^0)\, dS = 0$$

Substitution of the appropriate expressions for the stresses and displacements into this equation gives the result,

$$D_4 = 0.$$

Therefore, putting $D_4 = 0$ into the equations (3.40) enables us to solve for the shear modulus μ of the composite. With $D_4 = 0$, the 12×12 linear system may be written in matrix form as,

$$
\begin{bmatrix}
1 & \frac{-6\nu_p a^2}{(1-2\nu_p)} & -1 & \frac{6\nu_i a^2}{(1-2\nu_i)} & -\frac{3}{a^5} & -\frac{(5-4\nu_i)}{(1-2\nu_i)a^3} & 0 & 0 & 0 & 0 & 0 & 0 \\
1 & -\frac{(7-4\nu_p)a^2}{(1-2\nu_p)} & -1 & \frac{(7-4\nu_i)a^2}{(1-2\nu_i)} & \frac{2}{a^5} & -\frac{2}{a^3} & 0 & 0 & 0 & 0 & 0 & 0 \\
2\mu_p & \frac{6\nu_p\mu_p a^2}{(1-2\nu_p)} & -2\mu_i & \frac{-6\nu_i\mu_i a^2}{(1-2\nu_i)} & \frac{24\mu_i}{a^5} & -\frac{4(\nu_i-5)\mu_i}{(1-2\nu_i)a^3} & 0 & 0 & 0 & 0 & 0 & 0 \\
2\mu_p & -\frac{(14+4\nu_p)\mu_p a^2}{(1-2\nu_p)} & -2\mu_i & \frac{(14+4\nu_i)\mu_i a^2}{(1-2\nu_i)} & -\frac{16\mu_i}{a^5} & -\frac{4(1+\nu_i)\mu_i}{(1-2\nu_i)a^3} & 0 & 0 & 0 & 0 & 0 & 0 \\
0 & 0 & 1 & \frac{-6\nu_i b^2}{(1-2\nu_i)} & \frac{3}{b^5} & \frac{(5-4\nu_i)}{(1-2\nu_i)b^3} & -1 & \frac{6\nu_m b^2}{(1-2\nu_m)} & -\frac{3}{b^5} & -\frac{(5-4\nu_m)}{(1-2\nu_m)b^3} & 0 & 0 \\
0 & 0 & 1 & -\frac{(7-4\nu_i)b^2}{(1-2\nu_i)} & -\frac{2}{b^5} & \frac{2}{b^3} & -1 & \frac{(7-4\nu_m)b^2}{(1-2\nu_m)} & \frac{2}{b^5} & -\frac{2}{b^3} & 0 & 0 \\
0 & 0 & 2\mu_i & \frac{6\nu_i\mu_i b^2}{(1-2\nu_i)} & -\frac{24\mu_i}{b^5} & \frac{4(\nu_i-5)\mu_i}{(1-2\nu_i)b^3} & -2\mu_m & \frac{-6\nu_m\mu_m b^2}{(1-2\nu_m)} & \frac{24\mu_m}{b^5} & -\frac{4(\nu_m-5)\mu_m}{(1-2\nu_m)b^3} & 0 & 0 \\
0 & 0 & 2\mu_i & -\frac{(14+4\nu_i)\mu_i b^2}{(1-2\nu_i)} & \frac{16\mu_i}{b^5} & \frac{4(1+\nu_i)\mu_i}{(1-2\nu_i)b^3} & -2\mu_m & \frac{(14+4\nu_m)\mu_m b^2}{(1-2\nu_m)} & -\frac{16\mu_m}{b^5} & -\frac{4(1+\nu_m)\mu_m}{(1-2\nu_m)b^3} & 0 & 0 \\
0 & 0 & 0 & 0 & 0 & 0 & 1 & -\frac{6\nu_m c^2}{(1-2\nu_m)} & \frac{3}{c^5} & \frac{(5-4\nu_m)}{(1-2\nu_m)c^3} & -\frac{3}{c^5} & -1 \\
0 & 0 & 0 & 0 & 0 & 0 & 1 & -\frac{(7-4\nu_m)c^2}{(1-2\nu_m)} & -\frac{2}{c^5} & \frac{2}{c^3} & \frac{2}{c^5} & -1 \\
0 & 0 & 0 & 0 & 0 & 0 & 2\mu_m & \frac{6\nu_m\mu_m c^2}{(1-2\nu_m)} & -\frac{24\mu_m}{c^5} & \frac{4(\nu_m-5)\mu_m}{(1-2\nu_m)c^3} & \frac{24\mu}{c^5} & 0 \\
0 & 0 & 0 & 0 & 0 & 0 & 2\mu_m & -\frac{(14+4\nu_m)\mu_m c^2}{(1-2\nu_m)} & \frac{16\mu_m}{c^5} & \frac{4(1+\nu_m)\mu_m}{(1-2\nu_m)c^3} & -\frac{16\mu}{c^5} & 0
\end{bmatrix}
\begin{bmatrix} A_1 \\ A_2 \\ B_1 \\ B_2 \\ B_3 \\ B_4 \\ C_1 \\ C_2 \\ C_3 \\ C_4 \\ D_3 \\ D_1 \end{bmatrix}
=
\begin{bmatrix} 0 \\ 0 \\ 0 \\ 0 \\ 0 \\ 0 \\ 0 \\ 0 \\ 0 \\ 0 \\ \tau_\infty \\ \tau_\infty \end{bmatrix}
\tag{3.42}
$$

The 12×12 linear system (3.42) may be solved by reducing it to row echelon form.

If we solve this system of equations for D_1 and make the substitution $D_1 = \frac{\tau_\infty}{2\mu}$, we can eliminate τ_∞ and hence obtain a quadratic equation in μ. Therefore, as was the case where no interphase region is present [8], we obtain two solutions for the shear modulus, the correct one being that which is physically feasible.

Solving for each of the unknowns also enables us to find the stress and strain components in each of the phases when the composite is subjected to simple shear.

3.6 A Specific Profile for the Bulk and Shear Moduli of the Interphase Region

We again model the changing properties of the interphase region by the same power law function as in Chapter 2 and [40] that was described in the work of Vörös and Pukánszky [72, 73]. Such a representation has been considered by Jayaraman and Reifsnider [26], Jasiuk and Kouider [25], Wang and Jasiuk [75], and is generally thought to be a fairly accurate representation of the interphase properties while at the same time retaining enough simplicity to obtain an analytical solution. One of the limitations of this type of profile is that we cannot force smoothness at the boundary between interphase and matrix.

If we consider the same power law profile as before, then all the results are analogous to the results for the bulk modulus except that the constants m_1, m_2, m_3 and m_4 are defined differently. For the shear modulus case, these constants are,

$$m_1 = -\frac{3}{5}\left(\frac{9c_1+8c_2}{3c_1+4c_2}\right), \qquad m_2 = \frac{3c_2}{5}\left(\frac{9c_1+8c_2}{3c_1+4c_2}\right)a^P,$$
$$m_3 = \frac{18}{5c_2}\left(\frac{c_1+2c_2}{3c_1+4c_2}\right)a^{-P}, \qquad m_4 = -\frac{18}{5}\left(\frac{c_1+2c_2}{3c_1+4c_2}\right).$$

It is easily shown likewise, that for the constants m_1, m_2, m_3 and m_4 defined above, we get the same solution for $S(x)$, $U(x)$, $T(x)$ and $V(x)$ given by equations that were derived in Chapter 2 and [40]. Note that all other constants appearing in these equations are defined as in Chapter 2 and [40]. Therefore, these solutions enable us to find the effective shear modulus μ_E of the inclusion and interphase which is given by (3.37).

3.7 Results

For the power law profile, we again assume that at the boundary between matrix and interphase, i.e. at $x = b$, that $\kappa(b) = \kappa_m$ and $\mu(b) = \mu_m$. For such a condition we must have $b = aJ^{1/P}$. At $x = a$ we have, $\frac{\mu(a)}{\mu_m} = J$. To compare with the results for the bulk modulus, we plot our results for the shear modulus for the same values of J.

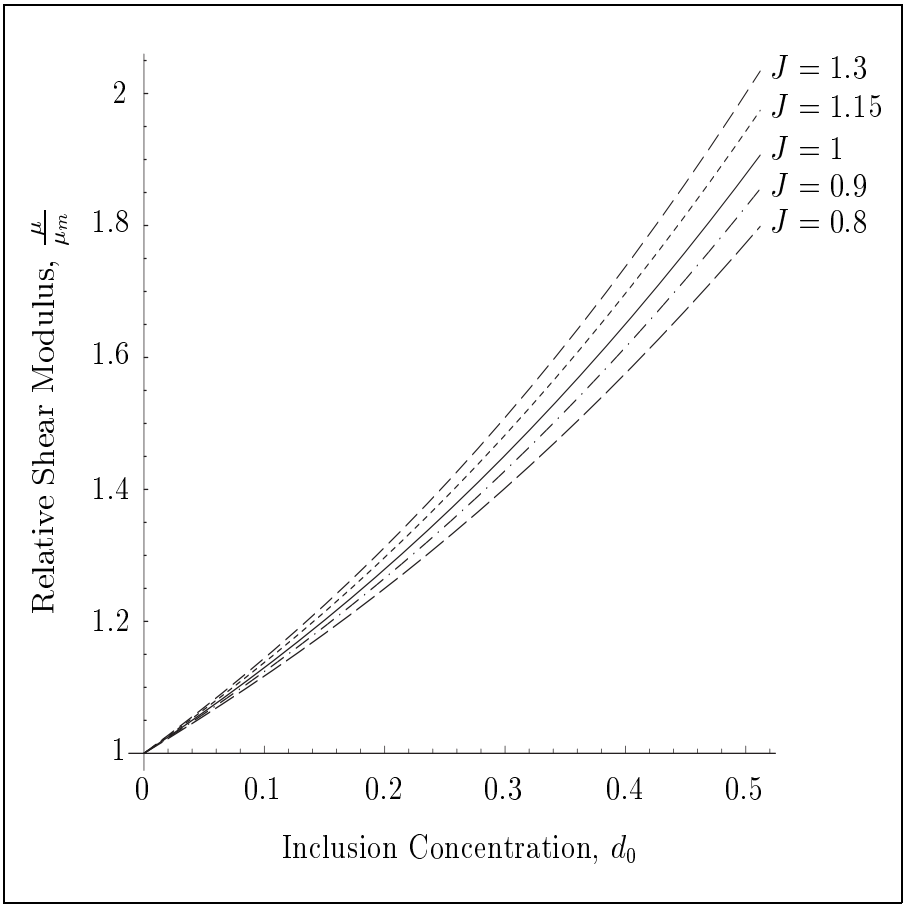

Figure 3.3: The Relative Shear Modulus of a composite as a function of inclusion concentration for various values of J using $\kappa_m = 14$, $\mu_m = 3$, $\kappa_p = 22$ and $\mu_p = 11$. The interphase region was assumed to have a thickness of 25% of the radius of inclusion.

The above results were plotted using the improved model which involves the solution of equation (3.42). Note that the improved model takes into account results from the bulk modulus that we obtained in Chapter 2 and [40]. Shen and Li [60] concluded in their work that their model for the shear modulus was rather accurate when the interphase

properties vary between those of inclusion and matrix. Their results were supported using finite element analysis. For the values of J considered in Figure 3.3, the properties of the interphase do vary between the particle inclusion and matrix. Shen and Li also concluded in their work that their model for the shear modulus was not satisfactory when the interphase is much harder than the matrix and the particle inclusion. Since their model, like the current model, is based on the Mori-Tanaka solution for the shear modulus, one would expect the present model to reflect the same behaviour. However, it is worthwhile for such cases, to consider the behaviour of the improved model which employs the generalised self consistent method.

We compare the improved model to the Mori-Tanaka interphase model by considering the following variations in the interphase properties given in Figures 3.4 and 3.5. Note that we change the properties of the particle inclusion and matrix so that the inclusion is softer than the matrix. Also, we choose various values of J such that the interphase properties are harder than both inclusion and matrix, a similar case considered in the work of Shen and Li [60].

For such an interphase profile we plot the shear modulus as a function of inclusion concentration using the Mori-Tanaka interphase model and the improved model given respectively in Figures 3.6 and 3.7.

We can see from the graphs of Figures 3.6 and 3.7 that the larger the value of J, the greater the variation in the Mori-Tanaka interphase model and the improved model. This behaviour is also reflected in the work of Shen and Li [60] who used a damage parameter to change the properties of the interphase region. This damage parameter is analogous to the parameter J. They measured the change in the strain energy based on the present model to finite element computations. For the shear modulus, it was shown in their work that the larger the damage parameter, the smaller the error in the strain energy between the present method and the finite element computations, a behaviour that is reflected in the current work.

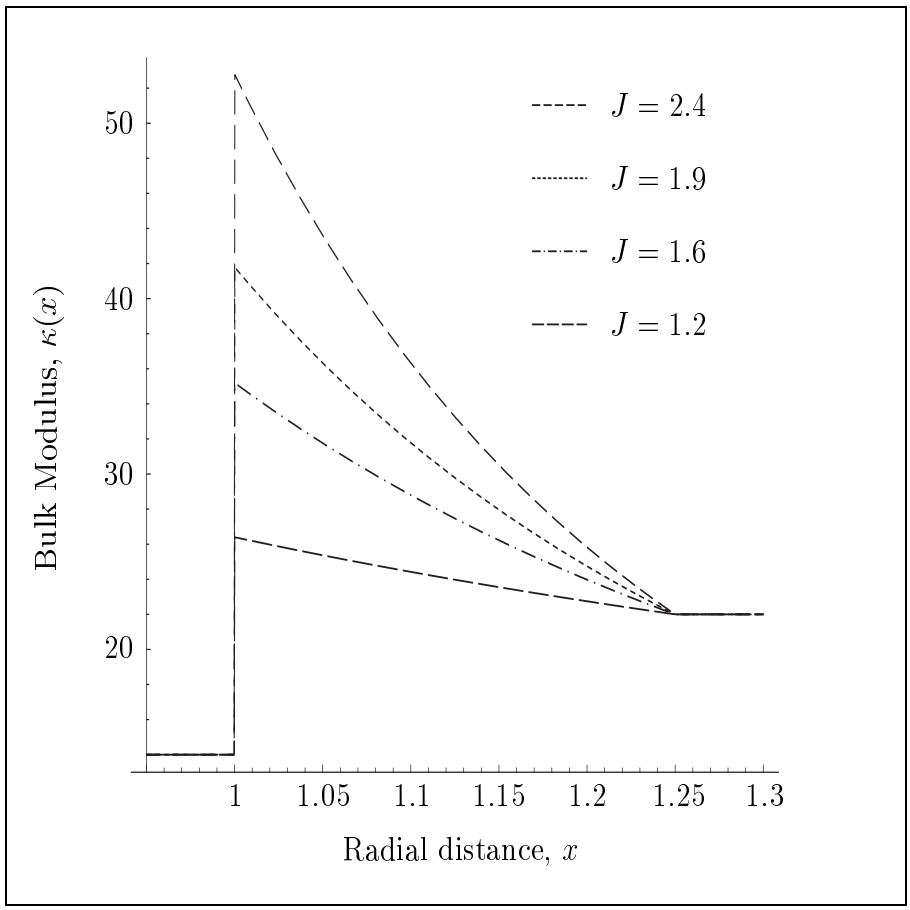

Figure 3.4: The Bulk Modulus as a function of the radial distance, x, from the centre of the inclusion for various values of J using $\kappa_m = 22$, $\mu_m = 11$, $\kappa_p = 14$ and $\mu_p = 3$. The interphase region was assumed to have a thickness of 25% of the radius of inclusion.

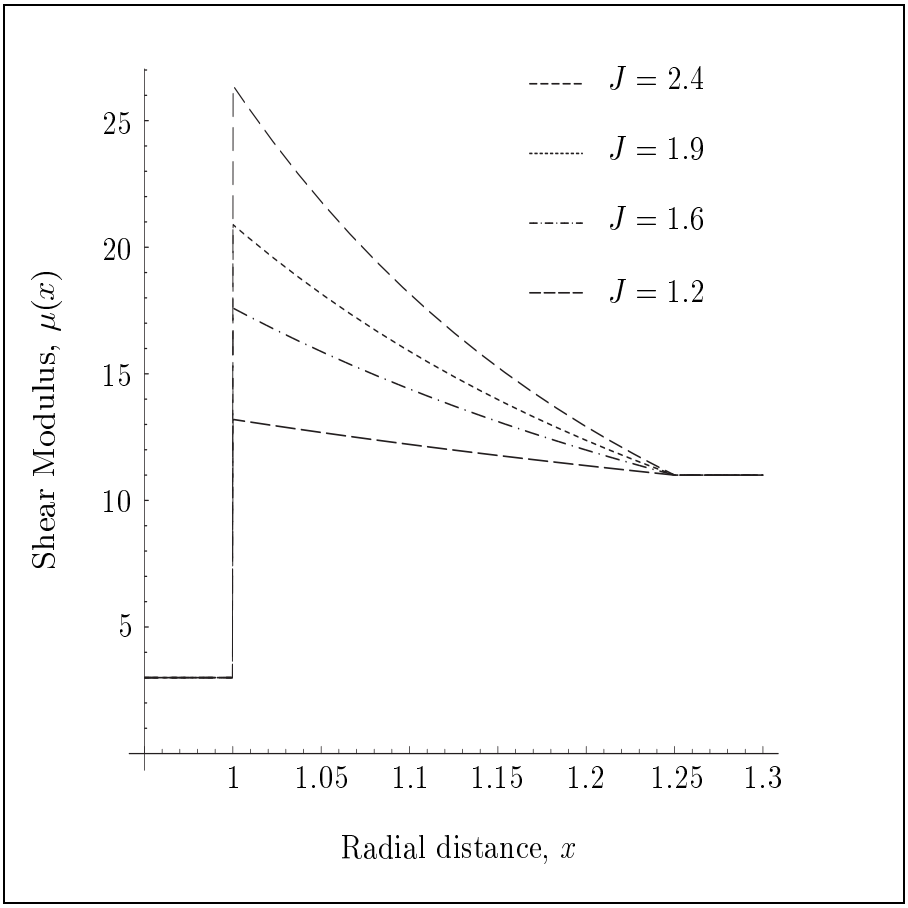

Figure 3.5: The Shear Modulus as a function of the radial distance, x, from the centre of the inclusion for various values of J using $\kappa_m = 22$, $\mu_m = 11$, $\kappa_p = 14$ and $\mu_p = 3$. The interphase region was assumed to have a thickness of 25% of the radius of inclusion.

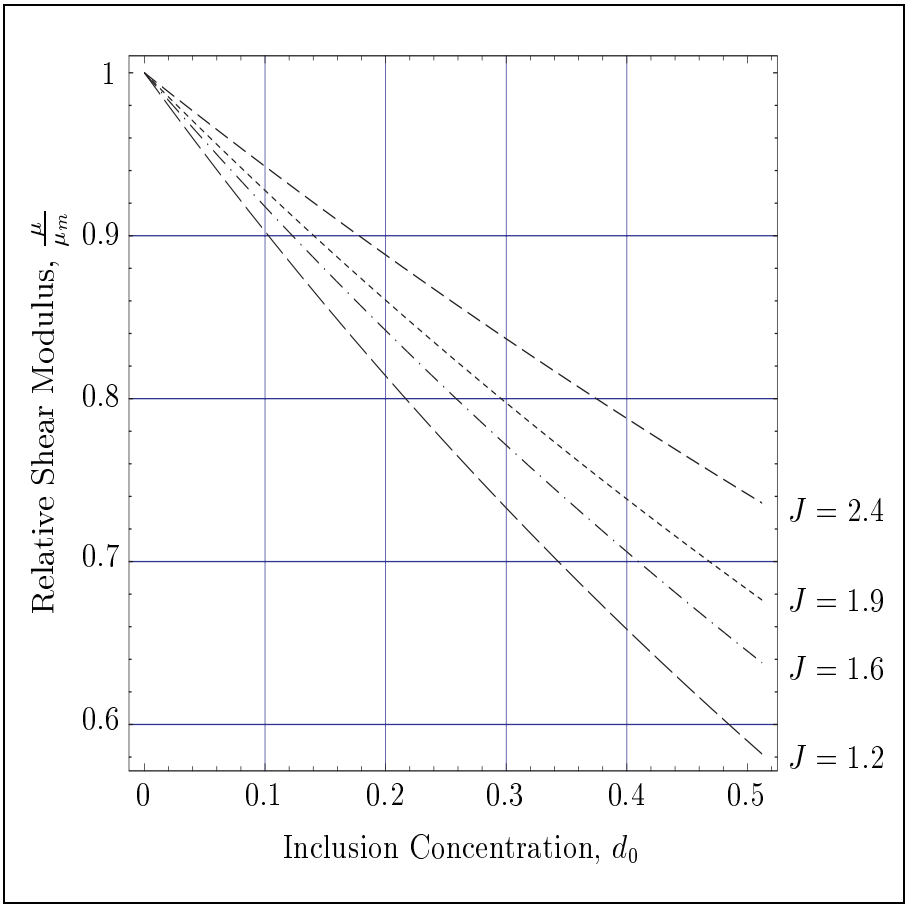

Figure 3.6: The Relative Shear Modulus of a composite as a function of inclusion concentration for various values of J, plotted using the Mori-Tanaka interphase model. The properties of the inclusion and matrix are, $\kappa_m = 22$, $\mu_m = 11$, $\kappa_p = 14$ and $\mu_p = 3$. The interphase region was assumed to have a thickness of 25% of the radius of inclusion.

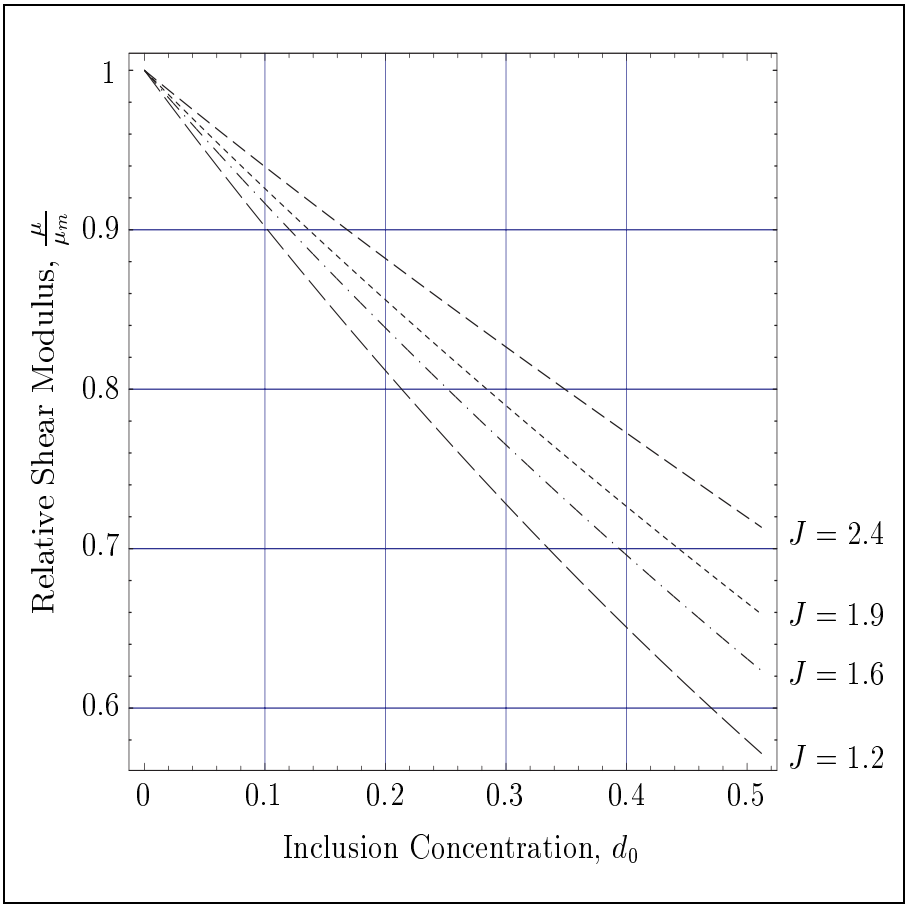

Figure 3.7: The Relative Shear Modulus of a composite as a function of inclusion concentration for various values of J, plotted using the improved GSC homogeneous model. The properties of the inclusion and matrix are, $\kappa_m = 22$, $\mu_m = 11$, $\kappa_p = 14$ and $\mu_p = 3$. The interphase region was assumed to have a thickness of 25% of the radius of inclusion.

3.8 Conclusion

We have obtained an approximation to the shear modulus of a particulate composite with an inhomogeneous interphase using a result obtain by Weng [77] for a 2-phase composite based on the Mori-Tanaka method. As in the bulk modulus case, we were able to obtain an exact solution for the effective shear modulus of the inclusion and interphase for a power law profile, from a coupled pair of differential equations. To account for the fact that the Mori-Tanaka solution is not exact, we employed the generalised self consistent method of Christensen and Lo [8]. We did this by mapping the homogeneous particle consisting of inclusion and interphase back onto a 2-phase composite as was done by Lombardo [37] and by Shen and Li [61]. Such a mapping allowed us to estimate the equivalent homogeneous property of the interphase. The GSC method was then modified to account for this homogeneous interphase region surrounding the inclusion. The accuracy of the improved model seems to depend on how good the estimate is of the equivalent homogeneous properties of the interphase since the method is exact after these properties are known. It is not known how accurate the method is that we use to measure the equivalent homogeneous properties of the interphase. The results however, reflect the behaviour that is expected. That is, when the properties of the interphase vary between inclusion and matrix, then the difference between both models is small or hardly perceived. However, when the inclusion is softer than the matrix and the interphase is harder than both, then the results show a clear difference between both models, a result that is reflected in the work of Shen and Li [60].

Chapter 4

Thermal Expansion Coefficient of a Particulate Composite with an Inhomogeneous Interphase

4.1 Introduction

A particularly important property of composites is the degree of thermal expansion, or how much the material expands with an increase in temperature. This is measured by a thermal expansion coefficient (CTE) which is unique for different materials. This property plays a critical role in the design of electronic packaging used for microelectronic devices. Composites used for the structural components of aircraft or other technological systems that are subject to extreme environments, need a low CTE in order to be stable under a change of temperature.

By utilising bounds obtained by Hashin and Striktman [19] for the elastic moduli, Levin [33] was able to obtain bounds for the CTE of 2-phase composites with isotropic phases. For the case of spherical inclusions, the upper and lower bounds of Levin yield an exact solution for the CTE. Rosen and Hashin [55] extended Levin's results to multiphase anisotropic composites by using thermoelastic energy principles. They also derived an exact expression for the specific heat of a composite with isotropic phases in terms of the phase properties and the composite bulk modulus. By using energy principles of

thermoelasticity, Schapery [59] derived bounds for the CTE of multiphase composites containing isotropic phases. For 2-phase composites, an exact expression was derived identical to that of Levin [33] and Rosen and Hashin [55]. This 2-phase expression was derived in all cases by assuming that perfect bonding exists between the phases. In reality however, perfect bonding does not exist. To treat this problem, Hashin [17] created a thin interphase area surrounding each inclusion with uniform elastic moduli and used a replacement technique to calculate the bulk modulus and CTE. As was the case with the bulk modulus, it is mentioned by Hashin [17] that the 2-phase expression for the CTE can be exploited using this replacement technique.

However, experimental evidence suggests as has been explained by Theocaris [67], that the properties of this interphase region are not uniform but vary radially outward from the centre of the inclusion. Reifsnider [54] has also written extensively on the subject of the interphase mentioning that the properties of this region often vary from point to point within the region making it all the more harder to model its effects. Reifsnider [54] also states that there is evidence to suggest that the properties of the interphase vary radially outward from the centre of the inclusion.

One of the main factors affecting the properties of composite materials is the degree of adhesion between the two phases. This adhesion occurs in a three dimensional region surrounding the inclusion and is known as the interphase or mesophase. The degree of adhesion or adhesion efficiency, depends to a large extent on the surface roughness of the filler. This factor creates stress concentrations, microcracks, impurities, cavities, voids, etc., in the immediate surrounding region, thereby causing a discontinuity of stresses and displacements at various positions in this region. Another factor influencing the formation of the interphase is the polymerisation process that takes place in this region in the formation of polymer composites. During this process, the long polymer chains exhibit less freedom of movement in the region around the inclusion causing an interface layer of denser properties than the bulk matrix. Further evidence for the existence of an interphase region rests on the fact that some composites exhibit crack growth or fracture which would seem to be initiated from the microcracks or voids that are assumed to exist around the inclusion.

One of the difficulties involved in modelling the properties of composite materials is in knowing or determining what the properties of the interphase region are and the size of this region. A large effect on the mechanical and thermal properties of composites has been observed even for relatively small interphase layers. Many have modelled the interphase layer as having a certain definite thickness over all possible volume fractions [75, 25, 9]. It is assumed in much of the literature however, that the thickness of the interphase varies depending on the volume fraction of the inclusions [67, 63, 62]. For polymer composites, the thickness has often been measured at various volume fractions using principles of glass transition temperature and measuring the heat capacity jumps at those temperatures [67, 63, 62]. Theocaris [69] has also used glass transition principles to determine whether the interphase consists of a material that is softer or harder than the pure matrix. These important phenomena are described in further detail later on in this chapter.

Theocaris and Varias [70] attempted to determine the properties of the inhomogeneous interphase region as well as its size by applying Kerner's model [30] and certain interphase profiles for the bulk modulus and CTE. By utilising experimental values for the bulk modulus and CTE of a polyurethane rubber matrix embedded with sodium chloride particles, they were able to estimate the size of the interphase zone and the variation in its properties.

Sideridis and Papanicolaou [63] developed a model to determine the CTE of a particulate composite which takes into account the effects of the interphase. They considered Linear, Hyperbolic, Logarithmic and Parabolic variations in the interphase region and compared their results to the refined law of mixtures which also takes into account the effects of the interphase. In their model they assumed that the properties of the interphase vary from those of particle to matrix.

Thermal expansion coefficients of composites containing aligned fibers surrounded by an inhomogeneous interphase have been studied by Sideridis [62]. He considered a Linear, Hyperbolic and Parabolic variation in the Young's modulus, Poisson's ratio and CTE of the interphase region. The interphase region was assumed to have properties which vary radially outward from the centre of the fiber.

The importance of modeling the interphase region is also emphasised in the work of Kakavas, Anifantis and Papanicolaou [29]. They considered an exponential mode of variation in the properties of the interphase and used them to compute the longitudinal and transverse CTE of a fibre reinforced composite. The interphase region was also assumed to have properties which vary radially outward from the centre of the fiber. Their results showed that the interphase region had little effect in the longitudinal direction but had an important effect in the transverse direction.

Herve [20] has extended the $(n+1)$ phase model of Herve and Zaoui [21] to estimate the thermal conductivity, CTE and specific heats of composite materials containing isotropic spherical inclusions surrounded by n concentric spheres of varying properties. He showed from first principles that the thermal conductivity, CTE and specific heats can be found by solving recursive schemes. A drawback of this model is that the properties of the interphase are not allowed to vary continuously since they have a finite number of layers.

Chaturvedi and Shen [5] have used finite element modeling to determine the CTE of a composite consisting of an epoxy matrix filled with solid or hollow spherical silica particles. In their model the composite is assumed to consist of two phases. One of the drawbacks of using finite element modeling is that it makes it difficult to model the effects of an inhomogeneous interphase.

In this chapter we use the replacement technique proposed by Hashin [17] and Qiu and Weng [52] to find the CTE of a particle inclusion surrounded by an inhomogeneous interphase layer. The technique has been used by Lombardo and Ding [40] to find the bulk modulus and by Lombardo [39] to find the shear modulus of particulate composites with inhomogeneous interphase and by Shen and Li [60, 61]. A similar technique was proposed by Zhong et al. [85] in a two part paper. In part one of this two-part paper, Wu et al. [79], constructed bounds for the elastic moduli of spherical inclusion composites based on the generalised self consistent method. In part two, Zhong et al. [85] model a spherical inclusion surrounded by an inhomogeneous interphase by mapping it onto an effective homogeneous particle of identical size in order to predict the effective moduli. The idea was originated by Garboczi and Berryman [14] who also mapped a particle and surrounding interphase onto an effective homogeneous particle although in their

work the interphase was assumed to be homogeneous. Zhong et al. [85] solved the bulk modulus case exactly for several different profiles for the inhomogeneous interphase. For the effective shear modulus, Zhong et al. [85] employ a differential scheme based on the Hashin-Shtrikman [19] lower bound which is similar to the replacement technique used in Shen and Li [60] as well as Lombardo and Ding [40]. The resulting differential equation is a Riccati equation for the effective shear modulus as a function of the volume fraction of the particle. The differential scheme was found to yield reasonable results which lie between the Hashin-Shtrikman upper and lower bounds.

The replacement method however, to the best of the authors knowledge, has not been used to find the CTE of composites. We begin with a brief discussion of the basic 2-phase expression that lay at the core of the technique and then use it to derive a first order differential equation which maps the inclusion and interphase onto an effective homogeneous particle. A power law profile to model the mechanical properties of the interphase is used as given in the work of Vörös and Pukánszky [72, 73]. The CTE of the interphase is modeled using various linear and quadratic functions. We then compare our results to some other models and with experimental data obtained from the work of Sideridis and Papanicoloau [63] as well as Holliday and Robinson [23].

4.2 Particle Mapping and Preliminary Assumptions

The coefficient of thermal expansion CTE, denoted by α, of a 2-phase composite containing isotropic spherical inclusions surrounded by an isotropic matrix as given by Levin [33], Rosen and Hashin [55] and Schapery [59], is,

$$\alpha_c = \alpha_m + (\alpha_p - \alpha_m) \left(\frac{\left(\frac{1}{\kappa_c}\right) - \left(\frac{1}{\kappa_m}\right)}{\left(\frac{1}{\kappa_p}\right) - \left(\frac{1}{\kappa_m}\right)} \right) \tag{4.1}$$

where κ represents bulk modulus. The subscripts c, m and p represent the composite, matrix and particle inclusion respectively. Note that m and p may be interchanged to give the same result for α_c. Also, the volume fraction of the phases is expressed only through the bulk modulus of the composite κ_c.

We use the same idea as Garboczi and Berryman [14] by mapping the inclusion and surrounding interphase region onto an equivalent homogeneous particle of identical size as shown in Figure 4.1. The difference here lies in the fact that the surrounding interphase region is inhomogeneous.

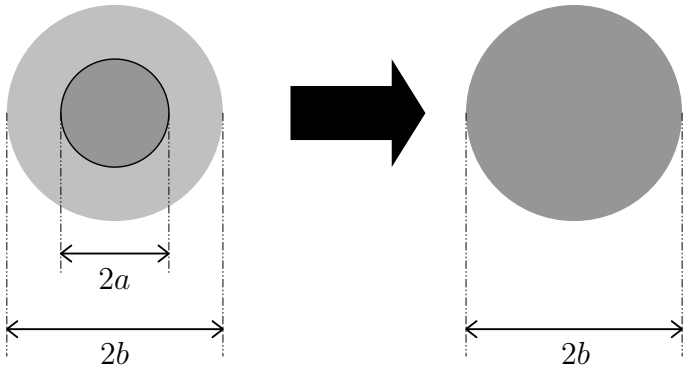

Figure 4.1: A mapping of an inclusion and surrounding interphase onto an effective homogeneous spherical particle of identical size.

As described by Hashin [17], equation (4.1) may be exploited to account for a surrounding interphase region around each of the inclusions, with different properties from the matrix. If we assume first that the surrounding interphase has constant properties α_g, κ_g, and shear modulus μ_g, then the effective coefficient of thermal expansion ECTE,

denoted by α_E, would be given by,

$$\alpha_E = \alpha_g + (\alpha_p - \alpha_g)\left(\frac{\left(\frac{1}{\kappa_E}\right) - \left(\frac{1}{\kappa_g}\right)}{\left(\frac{1}{\kappa_p}\right) - \left(\frac{1}{\kappa_g}\right)}\right)$$

where the subscript E implies the effective property of the inclusion together with the surrounding interphase region. Therefore, by modeling the inclusion and interphase as the new inclusion and replacing this into (4.1), the CTE of the composite would be given by,

$$\alpha_c = \alpha_m + (\alpha_E - \alpha_m)\left(\frac{\left(\frac{1}{\kappa_c}\right) - \left(\frac{1}{\kappa_m}\right)}{\left(\frac{1}{\kappa_E}\right) - \left(\frac{1}{\kappa_m}\right)}\right). \tag{4.2}$$

Suppose now that the CTE and the bulk and shear moduli of the interphase region both vary as continuous functions of x, which represents the radial distance from the centre of the inclusion, that is, we have $\alpha(x)$, $\kappa(x)$ and $\mu(x)$ as functions describing the interphase. We attempt to find the CTE of the composite, i.e. α_c. In order to find α_c from (4.2), we need to determine α_E. Note that for an inhomogeneous interphase, κ_c and κ_E have been determined in Chapter 2 and [40].

Note that if the 2-phase formula given by (4.1) is to be physically valid, then κ_c must lie between κ_p and κ_m. That is, we must have,

$$\kappa_m \leq \kappa_c \leq \kappa_p \qquad \text{or} \qquad \kappa_p \leq \kappa_c \leq \kappa_m.$$

Therefore, when replacing α_p by α_E and κ_p by κ_E as in (4.2), then we must have,

$$\kappa_m \leq \kappa_c \leq \kappa_E \qquad \text{or} \qquad \kappa_E \leq \kappa_c \leq \kappa_m$$

otherwise the 2-phase formula is physically invalid. Now, we have,

$$c = d_0 \frac{b^3}{a^3}$$

where d_0 is the volume fraction of inclusions relative to all phases and c is the volume fraction of the effective particle (consisting of inclusion and interphase) relative to all

phases. Therefore, to ensure the above inequalities hold, we must have $0 \leq c \leq 1$ which implies,

$$0 \leq d_0 \leq \frac{a^3}{b^3}.$$

Therefore, our model for the CTE appears to be valid only over this volume fraction range which is physically realistic since outside this range, there will be pure overlapping of interphases.

4.3 The Inhomogeneous Interphase Model

To account for an inhomogeneous interphase region, we split the interphase into n concentric layers as shown in Figure 4.2.

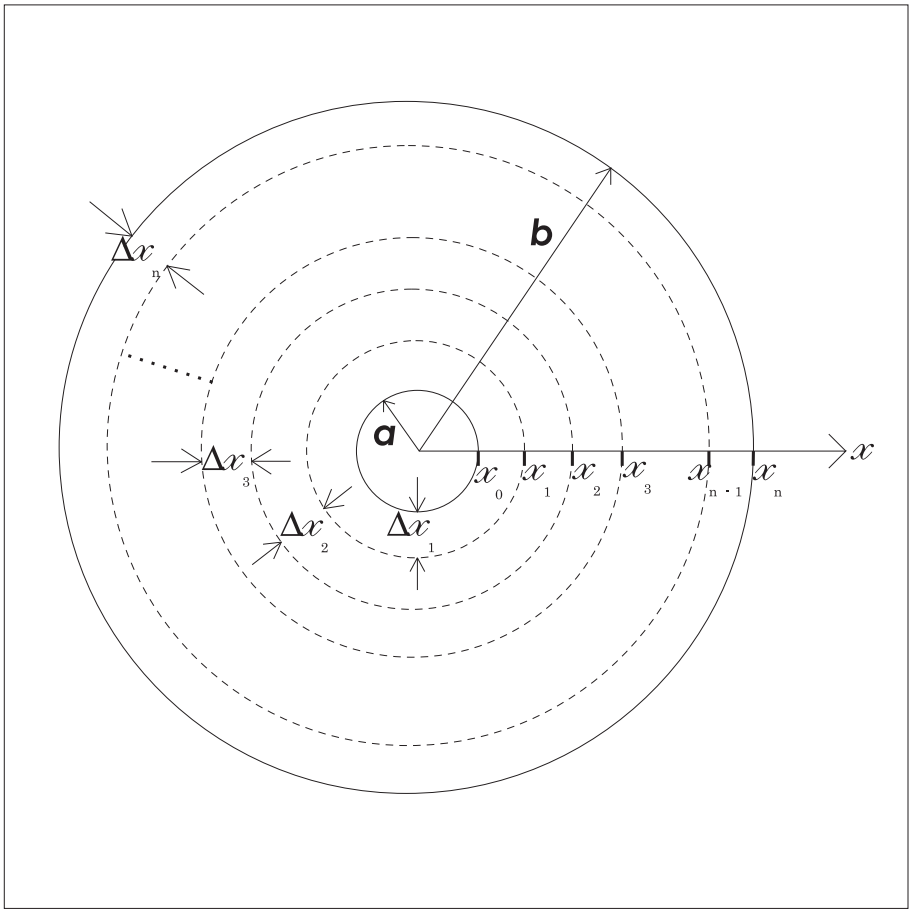

Figure 4.2: Interphase consisting of n regions or layers.

Note that the spherical inclusion has radius a and the interphase has radius b. Consider a partition $\mathcal{P}$ of $[a, b]$ into n subintervals defined by,

$$a = x_0 < x_1 < x_2 < \cdots < x_{i-1} < x_i < \cdots < x_{n-1} < x_n = b.$$

The lengths Δx_1, Δx_2, Δx_3, $\ldots$, Δx_n of the subintervals $[x_0, x_1]$, $[x_1, x_2]$, $[x_2, x_3]$, $\ldots$, $[x_{n-1}, x_n]$ associated with the partition $\mathcal{P}$, presently need not be the same. In each subinterval $[x_{i-1}, x_i]$, choose any point ξ_i; that is $\xi_i \in [x_{i-1}, x_i]$.

The (ECTE) of the inclusion and the first layer of interphase is given by,

$$\alpha_1^E = \alpha(\xi_1) + (\alpha_p - \alpha(\xi_1)) \left(\frac{\left(\frac{1}{\kappa_1^E}\right) - \left(\frac{1}{\kappa(\xi_1)}\right)}{\left(\frac{1}{\kappa_p}\right) - \left(\frac{1}{\kappa(\xi_1)}\right)} \right)$$

where κ_1^E represents the effective bulk modulus of the inclusion and the first layer. Continuiing in this way, we have, for the ECTE α_i^E of the particle up to the i-th layer,

$$\alpha_i^E = \alpha(\xi_i) + \left(\alpha_{i-1}^E - \alpha(\xi_i)\right) \left(\frac{\left(\frac{1}{\kappa_i^E}\right) - \left(\frac{1}{\kappa(\xi_i)}\right)}{\left(\frac{1}{\kappa_{i-1}^E}\right) - \left(\frac{1}{\kappa(\xi_i)}\right)} \right) \tag{4.3}$$

where we take $\alpha_0^E = \alpha_p$. Note that the $(i-1)$-th property is that of the inner composite sphere which is taken as the inclusion phase in the replacement method.

By letting

$$B_i = \left(\frac{\left(\frac{1}{\kappa_i^E}\right) - \left(\frac{1}{\kappa(\xi_i)}\right)}{\left(\frac{1}{\kappa_{i-1}^E}\right) - \left(\frac{1}{\kappa(\xi_i)}\right)} \right)$$

we may rewrite (4.3) as,

$$\alpha_i^E = \alpha(\xi_i)(1 - B_i) + \alpha_{i-1}^E B_i$$

Choose ξ_i to be the right hand endpoint of the subinterval $[x_{i-1}, x_i]$, that is, we shall take $\xi_i = x_i$. Also, let α_i^E be the discrete value of the function $\alpha_E(x)$ at the point x_i, that is, we have $\alpha_i^E = \alpha_E(x_i)$. Similarly for B_i we have $B(x)$, that is, $B_i = B(x_i)$. Note also that $\kappa_i^E = \kappa_E(x_i)$ where $\kappa_E(x)$ is the effective bulk modulus of the inclusion and interphase whose solution is given in Chapter 2 and [40]. Also, we shall let each subinterval of the partition $\mathcal{P}$ have the same width Δx.

Therefore, we have,

$$\alpha_E(x_i + \Delta x) = \alpha(x_i + \Delta x)(1 - B(x_i + \Delta x)) + \alpha_E(x_i) B(x_i + \Delta x)$$

where

$$B(x_i + \Delta x) = \left(\frac{\frac{1}{\kappa_E(x_i + \Delta x)} - \frac{1}{\kappa(x_i + \Delta x)}}{\frac{1}{\kappa_E(x_i))} - \frac{1}{\kappa(x_i + \Delta x)}} \right)$$

and $i \in \{\mathbb{N} : 0 \leq i \leq (n-1)\}$.

Rearranging this equation and dividing through by Δx gives,

$$\frac{\alpha_E(x_i + \Delta x) - \alpha_E(x_i)}{\Delta x} = \left(\frac{\alpha(x_i + \Delta x) - \alpha(x_i)}{\Delta x}\right)(1 - B(x_i + \Delta x)) + (\alpha(x_i) - \alpha_E(x_i))\left(\frac{1 - B(x_i + \Delta x)}{\Delta x}\right).$$

Taking the limit of both sides as $\Delta x \to 0$ gives,

$$\alpha'_E(x_i) = \alpha'(x_i) \lim_{\Delta x \to 0}(1 - B(x_i + \Delta x)) + (\alpha(x_i) - \alpha_E(x_i)) \lim_{\Delta x \to 0}\left(\frac{1 - B(x_i + \Delta x)}{\Delta x}\right).$$

It can be shown that if $\kappa(x)$ and $\kappa_E(x)$ are both smooth, bounded and continuous functions in the interval $[a, b]$, then we have,

$$\lim_{\Delta x \to 0}(1 - B(x_i + \Delta x)) = 0$$

and

$$\lim_{\Delta x \to 0}\left(\frac{1 - B(x_i + \Delta x)}{\Delta x}\right) = \frac{\kappa'_E(x_i)}{(\kappa(x_i) - \kappa_E(x_i))}\frac{\kappa(x_i)}{\kappa_E(x_i)}.$$

Assuming the conditions imposed above, this differential equation for $\alpha_E(x_i)$ is satisfied at all points $x_i \in [a, b]$. Therefore, we have,

$$\alpha'_E(x) + p(x)\alpha_E(x) = \alpha(x)p(x) \tag{4.4}$$

where

$$p(x) = \left(\frac{\kappa'_E(x)\kappa(x)}{(\kappa(x) - \kappa_E(x))\kappa_E(x)}\right).$$

Equation (4.4) is a first order linear differential equation in $\alpha_E(x)$. Note that $\kappa_E(x)$ represents the effective bulk modulus of the inclusion together with the interphase at position x, whereas $\kappa(x)$ simply represents the bulk modulus of the interphase at x. Also note that the function $\alpha(x)$ represents the behaviour of the thermal expansion coefficient in the interphase region.

From the work in Chapter 2 and [40] it can be shown that,

$$\kappa_E(x) = \frac{\kappa_0 S(x) + T(x)}{\kappa_0 U(x) + V(x)}$$

where $S(x)$, $T(x)$, $U(x)$ and $V(x)$ are found by solving a pair of coupled first order differential equations.

The boundary conditions for the differential equations for $S(x)$, $T(x)$, $U(x)$ and $V(x)$ are such that at $x = a$ we have $\kappa_E(a) = \kappa_0$. Likewise, for the differential equation given by (4.4), we have as the boundary condition,

$$\alpha_E(a) = \alpha_0$$

where α_0 is the CTE of the inclusion.

4.3.1 The General Solution

Using the integrating factor method, the solution to differential equation (4.4) at $x = b$, which is the ECTE of the inclusion and interphase, is given by,

$$\alpha_E(b) = \alpha(b) + e^{-\int_a^b p(x)\,dx}\,(\alpha_0 - \alpha(a) - I) \tag{4.5}$$

where

$$I = \int_a^b \alpha'(t) e^{\int_a^t p(\tau)\,d\tau}\,dt.$$

The CTE of the composite can then easily be found by using expression (4.2) for α_c.

4.4 A Specific Profile for the Interphase Region

We shall extend the results of Chapter 2 and [40] for the CTE of a composite by considering the same power law profile for the mechanical properties of the inhomogeneous interphase as given in the work of Vörös and Pukánszky [72, 73]. That is, we take

$$\lambda(x) = \lambda_m f(x) \qquad \text{and} \qquad \mu(x) = \mu_m f(x)$$

where

$$f(x) = J\left(\frac{a}{x}\right)^P.$$

$\lambda(x)$ and $\mu(x)$ are the Lamé coefficients describing the mechanical properties of the interphase region which is assumed to be isotropic and dependent only on x which represents the radial distance from the centre of the inclusion.

The constants λ_m and μ_m represent the Lamé coefficients of the matrix which is assumed to be a homogeneous and isotropic material. Also, for such a representation, the poisson's ratio of the interphase will be a constant ν_m, equal to the poisson's ratio of the matrix.

The constant J represents the modulus at the surface of the inclusion relative to the modulus of the matrix, while the constant P represents the rate at which the modulus of the interphase changes with respect to x. It will be assumed that at the boundary between interphase and matrix, that the moduli of the interphase match those of the matrix. In such a case we have, $b = aJ^{1/P}$. In using this representation, it is however not necessary that the moduli of the interphase region at either boundary match the inclusion or matrix, although such conditions may be imposed if that is the desired effect.

The constants λ_m, μ_m and J are positive by definition while the power P may be either positive or negative.

It can be shown that the integral appearing in the integrating factor of the differential equation (4.4) is given by,

$$\int p(x)\,dx = \ln\left|\frac{\kappa_E(x)}{\kappa(x)-\kappa_E(x)}\right| + \int \frac{\kappa'(x)}{(\kappa(x)-\kappa_E(x))}\,dx \tag{4.6}$$

From Chapter 2 and [40] we have,

$$S(x) = r_1 x^{\lambda_1} + r_2 x^{\lambda_2} \qquad \text{and} \qquad T(x) = t_1 x^{\lambda_1} + t_2 x^{\lambda_2}$$

where r_1, r_2, t_1, t_2, λ_1 and λ_2 are constants which are themselves functions of the problem parameters. Let

$$U(x) = u_1 x^{\lambda_1 + P} + u_2 x^{\lambda_2 + P} \qquad \text{and} \qquad V(x) = v_1 x^{\lambda_1 + P} + v_2 x^{\lambda_2 + P}$$

where

$$u_1 = \frac{(\lambda_1 - m_1) r_1}{m_2}, \qquad u_2 = \frac{(\lambda_2 - m_1) r_2}{m_2},$$
$$v_1 = \frac{(\lambda_1 - m_1) t_1}{m_2}, \qquad v_2 = \frac{(\lambda_2 - m_1) t_2}{m_2}.$$

The constants m_1 and m_2 are also defined in Chapter 2 and [40] and are functions of the problem parameters. By defining constants

$$f_1 = \kappa_0 r_1 + t_1, \qquad f_2 = \kappa_0 r_2 + t_2,$$
$$d_1 = \kappa_0 u_1 + v_1, \qquad d_2 = \kappa_0 u_2 + v_2,$$

as well as,

$$h_1 = (\kappa_m J a^P) d_1 \qquad \text{and} \qquad h_2 = (\kappa_m J a^P) d_2,$$

it can be shown that the integral appearing in (4.6) is given by,

$$\int \frac{\kappa'(x)}{(\kappa(x) - \kappa_E(x))}\, dx = (-P h_1) I_1 + (-P h_2) I_2$$

where

$$I_1 = \int \frac{1}{x((h_1 - f_1) + (h_2 - f_2) x^{-q})}\, dx$$

and

$$I_2 = \int \frac{1}{x((h_1 - f_1)x^q + (h_2 - f_2))}\, dx.$$

By making the substitution $u = (h_1 - f_1) + (h_2 - f_2)x^{-q}$, it can be shown that

$$I_1 = \frac{1}{q(h_1 - f_1)} \ln \left| \left(\frac{h_1 - f_1}{h_2 - f_2} \right) x^q + 1 \right|.$$

By making the substitution $u = (h_1 - f_1)x^q + (h_2 - f_2)$, it can be shown that

$$I_2 = \frac{1}{q(h_2 - f_2)} \ln \left| \frac{(h_1 - f_1)x^q}{(h_1 - f_1)x^q + (h_2 - f_2)} \right|.$$

After some algebraic manipulation, we may write the integrating factor as,

$$e^{\int p(x)\, dx} = \frac{1}{|h_1 - f_1|} \left| \left(f_1 + f_2 x^{-q}\right) \left(1 + \frac{1}{\beta} x^{-q}\right)^{\gamma_1 - 1} (1 + \beta x^q)^{\gamma_2} \right|$$

where we have defined,

$$\gamma_1 = \frac{P h_2}{q(h_2 - f_2)}, \qquad \gamma_2 = \frac{-P h_1}{q(h_1 - f_1)}$$

and

$$\beta = \left(\frac{h_1 - f_1}{h_2 - f_2} \right).$$

It can be shown that for all values of the parameters, we have the condition,

$$\gamma_1 + \gamma_2 = 1. \tag{4.7}$$

This condition is not obvious from the definitions of γ_1 and γ_2 but is very useful as we shall now see. If we have the condition $\kappa(a) = \kappa_0$, then there is a singularity in differential equation (4.4). In this special case we always have $\beta a^q = -1$ which if it weren't for the condition (4.7), would cause a singularity in the integrating factor at $x = a$. However, by imposing (4.7) we may remove this singularity and re-write the integrating factor as,

$$e^{\int p(x)\, dx} = \left| \frac{\beta^{1-\gamma_1}}{h_1 - f_1} \right| |f_1 x^{\eta_1} + f_2 x^{\eta_2}| \tag{4.8}$$

where,

$$\eta_1 = q(1-\gamma_1) \qquad \text{and} \qquad \eta_2 = -q\gamma_1.$$

4.4.1 A Linear Thermal Expansion Coefficient for the Interphase

Given the above profile for the mechanical properties of the inhomogeneous interphase, the integrating factor to differential equation (4.4) is given in closed form by (4.8). If the CTE of the interphase varies as some function of x, that is, $\alpha(x)$, then it is assumed that the differential equation (4.4) can be solved for various of these functions.

Therefore, if we assume that the CTE of the interphase is described by a linear function, that is,

$$\alpha(x) = \varepsilon_0 + \varepsilon_1 x,$$

then the integral appearing in (4.5) becomes,

$$I = \varepsilon_1 \int_a^b e^{\int_a^t p(\tau)\, d\tau}\, dt.$$

Once this integral has been evaluated it then becomes a simple matter of following the procedure in section 4.3.1 to determine the CTE of the composite.

Letting $g(x) = e^{\int p(x)\, dx}$ we have,

$$I = \frac{\varepsilon_1}{g(a)} \left| \frac{\beta^{1-\gamma_1}}{h_1 - f_1} \right| \int_a^b \left| f_1 t^{\eta_1} + f_2 t^{\eta_2} \right| \, dt.$$

This integral may be easily evaluated numerically once the parameters are known.

We may choose ε_1 and ε_0 such that $\alpha(a) = \alpha_0$ and $\alpha(b) = \alpha_m$. This ensures a linear variation in the CTE of the interphase from the particle inclusion to matrix. Therefore we have,

$$\varepsilon_0 = \frac{\alpha_0 b - \alpha_m a}{b-a} \qquad \text{and} \qquad \varepsilon_1 = \frac{\alpha_m - \alpha_0}{b-a}.$$

4.4.2 A Quadratic Thermal Expansion Coefficient for the Interphase

If we assume that the CTE of the interphase is described by a quadratic function, that is,

$$\alpha(x) = \varepsilon_0 + \varepsilon_1 x + \varepsilon_2 x^2,$$

then given that $g(x) = e^{\int p(x)\,dx}$, the integral appearing in (4.5) becomes,

$$I = \frac{1}{g(a)} \left| \frac{\beta^{1-\gamma_1}}{h_1 - f_1} \right| \left(\varepsilon_1 \int_a^b \left| f_1 t^{\eta_1} + f_2 t^{\eta_2} \right| \, dt + 2\varepsilon_2 \int_a^b \left| f_1 t^{\eta_1+1} + f_2 t^{\eta_2+1} \right| \, dt \right)$$

This integral may also be easily evaluated numerically once values for the problem parameters are known.

Quadratic 1

A realistic quadratic profile for $\alpha(x)$ would be to choose $\alpha(a) = \alpha_0$, $\alpha(b) = \alpha_m$ and $\alpha'(b) = 0$. The first two conditions ensures that the CTE of the interphase varies from that of the particle inclusion to that of the matrix while the last condition ensures a smooth transition at the interphase/matrix boundary. Imposing these conditions gives,

$$\varepsilon_0 = \alpha_m + b^2 \frac{(\alpha_0 - \alpha_m)}{(a-b)^2}, \qquad \varepsilon_1 = -2b \frac{(\alpha_0 - \alpha_m)}{(a-b)^2}, \qquad \varepsilon_2 = \frac{\alpha_0 - \alpha_m}{(a-b)^2}.$$

Quadratic 2

A second possibly realistic quadratic profile for $\alpha(x)$ would be to choose $\alpha(a) = \alpha_0$, $\alpha(b) = \alpha_m$ and $\alpha'(a) = 0$. The first two conditions have the same effect as before, ensuring that the (CTE) of the interphase varies from that of the particle inclusion to that of the matrix while the last condition ensures a smooth transition at the inclusion/interphase boundary. Imposing these conditions gives,

$$\varepsilon_0 = \alpha_0 + a^2 \frac{(\alpha_m - \alpha_0)}{(a-b)^2}, \qquad \varepsilon_1 = -2a \frac{(\alpha_m - \alpha_0)}{(a-b)^2}, \qquad \varepsilon_2 = \frac{\alpha_m - \alpha_0}{(a-b)^2}.$$

The three variations of the (CTE) of the inhomogeneous interphase are shown in Figure 4.3.

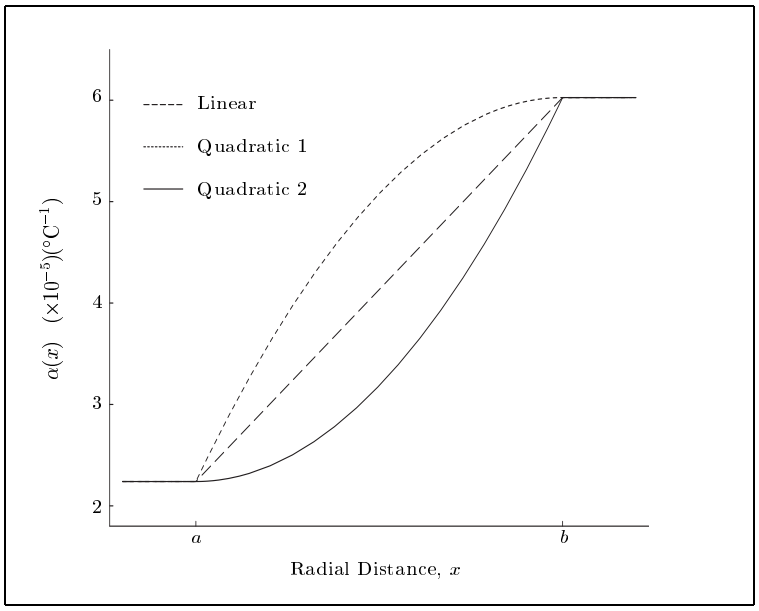

Figure 4.3: CTE profile of the Inhomogeneous Interphase.

4.5 Thickness and Bonding Characteristics of the Interphase

In the following results we have made the simplifying assumption that the thickness of the interphase remains fixed regardless of the volume fraction of the composite, unlike the work of Sideridis and Papanicolaou [63]. In their work they have used glass transition phenomena to measure the interphase thickness or volume fraction which they believe to be a function of the filler volume fraction. Such a conclusion is the result of work done by Lipatov [34] and has also been incorporated into many models [67, 63, 62, 64] having an inhomogeneous interphase. It therefore seems worthwhile to briefly discuss here some of the aspects of this Lipatov theory since it seems widely used.

Below a certain temperature known as the glass transition temperature T_g, polymers are said to be in a glass like state where motion of the polymer molecules is very restricted and hindered by the neighboring molecules. The molecules still exhibit motion in this region however the motion is weak due to their relatively low kinetic energy. Above the glass transition temperature, the molecules are more free to move and rotate and the polymer exhibits rubber like behaviour. Unlike metals, as the temperature of the polymer is increased above T_g, the softening of the polymer occurs gradually over a large temperature range, approximately $20°C$ above T_g. There is a relatively large change in the polymer's stiffness properties as the temperature moves from the glassy state to the rubbery state. The polymer exhibits viscoelastic behaviour most noteably around this temperature.

It has been observed that for a certain volume fraction of filler, an increase in the glass transition temperature of a polymer composite causes an increase of the total surface of the filler. This is due to the fact that an increase in T_g implies that neighbouring polymer molecules bond with the molecules at the surface of the inclusion and since their movement is more restricted, this causes the formation of a denser interphase region. Therefore, the volume fraction of the strong phase increases causing a change in the overall viscoelastic behaviour of the polymer composite.

It has been postulated that the size of the interphase region that forms around the

inclusion often has a somewhat significant thickness due to the fact that their is a significant change in T_g with the presence of filler. Also, since the value of T_g is mainly due to the presence of the polymer matrix, a change in T_g would imply a change in the characteristics of the matrix.

When the volume fraction v_f, of the inclusions increases, it has been observed that the value of T_g also increases. It is believed that this is due to the fact that as v_f increases, the number of polymer molecules reacting with the surface of the inclusions also increases causing a larger portion of the bulk polymer to be more restricted in movement, thereby causing an increase in T_g.

There has been experimental evidence [69] which has detected a decrease in the value of T_g for some polymer composites suggesting a poorer quality of adhesion between inclusion and matrix as the main factor. This has also been supported by Theocaris and Spathis [69] using theoretical evidence.

The extent of the interphase can be measured by observing that there is a jump in the specific heat capacity around the glass transition temperature for certain amounts of filler. It has also been observed that these jumps vary according to the amount of filler in the composite.

By measuring the heat capacity jumps one can use Lipatov theory to measure the size of the interphase. The size of the interphase region that forms in polymer composites depends on the inclusion concentration according to this theory. It is believed that this is due to the fact that as the filler content is increased, the number of polymer molecules in the vincinity of the filler surface, which are also restricted of movement, is also increased. This implies that the volume fraction of the interphase will also be increased. According to Lipatov theory, the interphase volume fraction is given by,

$$v_i = 3v_f \frac{\Delta r_i}{r_f}$$

where the subscripts f and i represent filler and interphase repsectively, r represents radius, Δr_i represents the thickness of the interphase and v represents volume fraction. Δr_i can be found from the relationship,

$$\left(\frac{\Delta r_i + r_f}{r_f}\right)^3 - 1 = \lambda_i \frac{\upsilon_f}{1-\upsilon_f}$$

where the quantity λ_i is given by,

$$\lambda_i = 1 - \frac{\Delta {C_p}^{Fill}}{\Delta {C_p}^{Unf}}.$$

$\Delta {C_p}^{Fill}$ and $\Delta {C_p}^{Unf}$ represent the change in the specific heat capacity near the glass transition temperature of the filled and unfilled polymer respectively.

Using these principles Sideridis and Papanicolaou [63] derived the following expression representing the interphase volume fraction for a composite consisting of an epoxy resin embedded with spherical particles of aluminium whose properties are given in Table 4.1:

$$\upsilon_i = -1.241{\upsilon_f}^3 + 1.324{\upsilon_f}^2 + -0.083\upsilon_f$$

where $\upsilon_f \in [0, 0.75]$. Therefore, using the fact that

$$\upsilon_i = \left(\frac{b^3}{a^3} - 1\right)\upsilon_f,$$

we have on average $b = 1.056a$ which implies that the interphase for this composite on average has a thickness of 5.6% of the radius of inclusion for the above specified volume fraction range.

It is also possible to use glass transition behaviour to get some idea as to the type of bonding that is occurring in the interphase region. Experimental evidence suggests that the addition of a filler into a polymeric matrix may either increase or decrease the glass transition temperature of the composite relative to that of the polymer. When the composite has a larger T_g than the matrix, it can be concluded that the bonding between filler and matrix occuring in the interphase region is *strong*. Also when the bonding in the interphase is *weak*, the T_g of the composite is reduced. Therefore, measurement of T_g of polymer composites is an effective way of knowing the bonding characteristics of the interphase.

In our model we assume like the model of Sideridis and Papanicoloau [63] that quantities such as the bulk modulus and CTE of the interphase match those of the particle

inclusion and matrix at their respective boundaries.

4.6 Results

We compare the current results to some other simple theoretical 2-phase models as well as some models incorporating an interphase and to experimental results obtained from Sideridis and Papanicolaou [63] as well as Holliday and Robinson [23]. The composites used in their experiments consisted of spherical filler particles of Aluminium embedded in an epoxy resin at various filler volume fractions. The material properties are given in Table 4.1.

For the experiment of Sideridis and Papanicolaou [63], specimens containing various volume fractions were tested on a DUPont 990 thermomechanical analyser in order to measure the thermal expansion coefficient. Three samples per volume fraction were tested and an average value was obtained. The experimental values of Sideridis and Papnicolaou [63] as well as those of Holliday and Robinson [23] are given in Table 4.2.

The results of the current model were plotted against the simple rule of mixtures and the model of Levin [33] which neglect the effects of the interphase. Our results were also compared against the interphase model of Sideridis and Papanicolaou [63] as well as the refined law of mixtures. Note that the result for the refined law of mixtures which has an integral representation of the solution can also be obtained using the replacement method with the simple rule of mixtures result. The CTE of a particulate composite obtained using this refined law of mixtures model is given by,

$$\alpha_c = \alpha_f c_f + \alpha_m c_m + \frac{3c_f}{a^3}\int_a^b \alpha(r) r^2\, dr.$$

The model of Sideridis and Papanicolaou [63] is based on the principles of the theory of elasticity and makes the assumption that the properties of the interphase match those of the particle and matrix at their respective boundaries, whereas the current model does not. They considered Linear, Hyperbolic, Logarithmic and Parabolic variations in the interphase region and compared their results to the refined law of mixtures as well as other 2-phase models. The CTE obtained using their model is given by,

Property	Aluminium	Epoxy Resin
Young's modulus (N/m^2)	70×10^9	3.5×10^9
Bulk modulus (N/m^2)	73×10^9	4.2×10^9
Poisson's ratio	0.34	0.36
Thermal expansion coefficient ($^\circ C^{-1}$)	22.4×10^{-6}	60.26×10^{-6}

Table 4.1: Properties of the constituent materials

$$\alpha_c = \alpha_m - \frac{3(1-\nu_m)(1-c_m)E_i c_i[E_f(\alpha_i - \alpha_0)C + E_m c_m(\alpha_m - \alpha_i)A]}{(AD - BC)E_m c_m}$$

where,

$$\begin{aligned} A &= [(1-c_m)(1+\nu_i) + 2(1-2\nu_i)c_f]E_f + 2(1-2\nu_f)c_i E_i \\ B &= 3(1-c_m)(1-\nu_i)E_f \\ C &= 3(1-\nu_i)E_m c_f c_m \\ D &= [2(1-c_m)(1-2\nu_m) + (1+\nu_m)]E_i c_i + [c_f(1+\nu_i) + 2(1-2\nu_i)(1-c_m)]E_m c_m \end{aligned}$$

The subscripts f, i, and m refer to filler, interphase and matrix respectively and c denotes volume fraction. Note that ν and E represent Poisson's ratio and Young's modulus respectively. In order to evaluate E_i, α_i and ν_i we need to find,

$$M_i = \frac{3}{b^3 - a^3}\int_a^b M_i(r)r^2\,dr$$

where M represents E, α or ν and M_i represents the average value of the interphase.

Their model showed good agreement with the experimental results of Holliday and Robinson but not with their own. It was believed that there was a high degree of agglomeration of particles in the composites that were prepared in their laboratory which explained why their experimental values lied well below most of the theoretical predictions. The results are presented in Figures 4.4 and 4.5. The results for the interphase

Filler volume fraction, d_0	Sideridis and Papanicolaou [63], CTE	Holliday and Robinson [23], CTE
0.0	60.0×10^{-6}	58.0×10^{-6}
0.10	49.04×10^{-6}	53.05×10^{-6}
0.15	44.02×10^{-6}	50.02×10^{-6}
0.20	40.04×10^{-6}	48.2×10^{-6}
0.25	36.9×10^{-6}	46.04×10^{-6}
0.30	34.4×10^{-6}	44.03×10^{-6}
0.40	-	40.3×10^{-6}
0.50	-	36.6×10^{-6}
0.60	-	34.03×10^{-6}
0.70	-	32.02×10^{-6}

Table 4.2: Experimental Results measured for CTE

thickness of 25% of the radius of inclusion shown in Figure 4.4 is a hypothetical interphase thickness.

All the results were plotted in the volume fraction range of $0 \leq d_0 \leq \frac{a^3}{b^3}$ which seems to be the maximum range at which the current model would be valid although it is worthwhile to note that even within this range there is a high chance of overlapping of interphase regions, particularly near $d_0 = \frac{a^3}{b^3}$. The CTE of the interphase was modelled using a linear variation whereas the bulk modulus was modelled by the power function considered in section 4.4. The value of J was taken to be $J = \frac{\kappa_0}{\kappa_m}$.

It can be seen from the graphs in Figures 4.4 and 4.5 that the present model lies well below the 2-phase model of Levin [33] and the simple rule of mixtures. Note that for all the interphase models considered, the radius of the inclusion does not effect the results in any way since it is the thickness of the interphase relative to this radius which is the important factor. For an interphase with a thickness of 25% of the radius of inclusion, the graph shows well the distinction between the theoretical models.

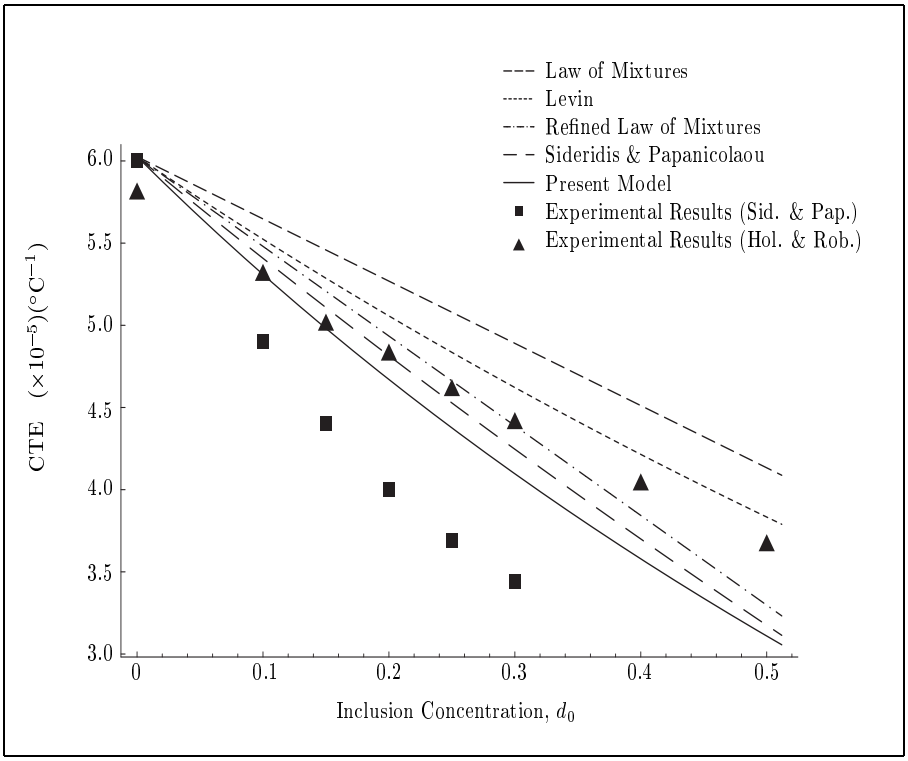

Figure 4.4: Results of the present model in comparison to other theoretical models and experimental results of Table 4.2. The interphase was assumed to have a thickness of 25% of the radius of inclusion and had a linear variation of the CTE representing the inhomogeniety. Also $J = \frac{\kappa_0}{\kappa_m}$.

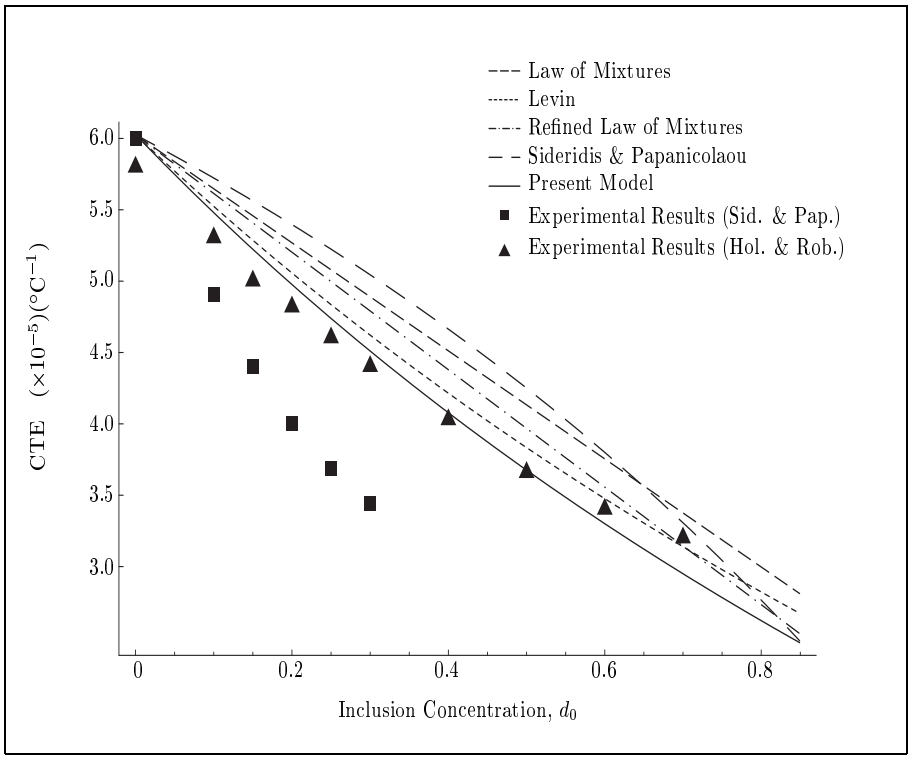

Figure 4.5: Results of the present model in comparison to other theoretical models and experimental results of Table 4.2. The interphase was assumed to have a thickness of 5.6% of the radius of inclusion and had a linear variation of the CTE representing the inhomogeniety. Also $J = \frac{\kappa_0}{\kappa_m}$.

For an interphase with a thickness of 5.6% of the radius of inclusion, which is the average calculated from the results of Sideridis and Papanicolaou [63], the present model provided a good fit to the experimental data of Holliday and Robinson, particularly in the low to medium volume fraction range. For the higher volume fraction range, the experimental data seemed to deviate away from the present model. This may be due to the fact that there is an overlapping of interphase regions in this range of volume fractions.

To examine the effects of different profiles for the CTE of the interphase region we considered the 3 types of variations given in Figure 4.3. The results are plotted against the experimental results of Holliday and Robinson [23] in Figure 4.6.

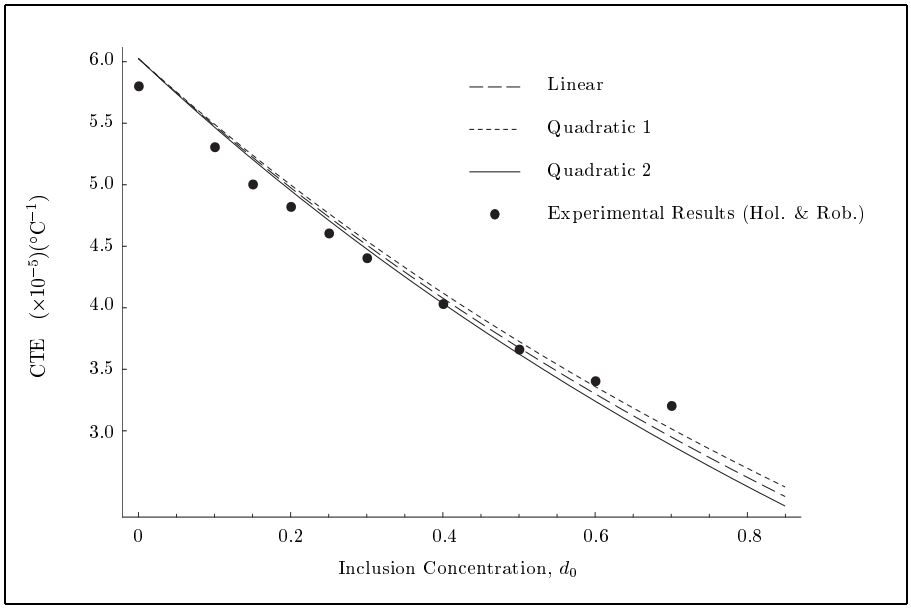

Figure 4.6: Results of the present model for the 3 profiles considered in Figure 4.3. The interphase was assumed to have a thickness of 5.6% of the radius of inclusion and $J = \frac{\kappa_0}{\kappa_m}$.

It can be seen from Figure 4.6 that the linear variation lies in between both quadratic variations as expected. A cubic variation in the CTE of the interphase was also considered which joined smoothly at the two boundaries, however the results of this profile are not shown here as they were very similar to the results for the linear variation. It can be seen from this graph that for $d_0 \in [0, 0.5]$, Quadratic 2 seemed to provide the best fit to the experimental data, although the other profiles also show a relatively good fit. For

$d_0 \in [0.5, 0.8]$, none of the profiles seem to adequately represent the experimental data. A possible reason for this could be that the interphase regions are beginning to overlap which the current model does not take into account. It is also important to note that the experimental data of Holliday and Robinson may not be very accurate near $d_0 = 0$ since at this volume fraction, which represents the pure matrix, their measured CTE was 5.8×10^{-5} whereas the value measured in Table 4.1 is 6.026×10^{-5}.

To examine the effects of the mechanical properties of the interphase region, we considered a linear variation for the CTE and varied the parameter J. The results are given in Figure 4.7.

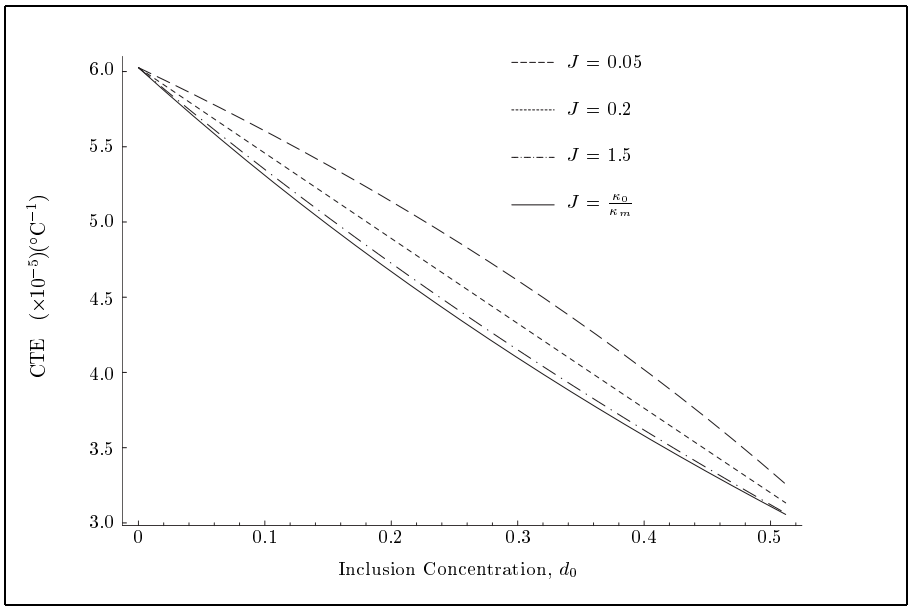

Figure 4.7: Results of the present model for different values of the parameter J. The interphase was assumed to have a thickness of 25% of the radius of inclusion and had a linear variation for the CTE.

For the results in Figure 4.7, four values of J were chosen in order to highlight the differences in the CTE of composites in terms of the mechanical properties of the interphase. The results show that for very soft interphases, that is $J = 0.05$ and $J = 0.2$, the CTE of the composite is much larger for all values of the inclusion concentration that are considered. The results also show that the harder interphase has the effect of lowering the CTE. It is important to note that a hard interphase does not alter the CTE by much.

For example, if we consider the curves for $J = \frac{\kappa_0}{\kappa_m} \approx 3.3$ and $J = 1.5$, then the results for these curves do not seem to differ substantially. This suggests that for composites with the given properties of Table 4.1, a hard interphase is not necessary in obtaining a low CTE since an interphase of stiffness properties of the same order of magnitude as the matrix is sufficient for the desired purpose. Also, if we take larger and larger values for J, the curves are close to the curve corresponding to $J = \frac{\kappa_0}{\kappa_m}$.

4.7 Conclusion

In summary we have been able to use the replacement technique of Hashin [17] and Qiu and Weng [52] to determine the coefficient of thermal expansion of a particulate composite. At the very foundation of the model is the 2-phase result of Levin [33] which we have been able to extend for inhomogeneous interphases. We were able to do this by mapping the inclusion and inhomogeneous interphase onto an equivalent homogeneous particle of identical size. This was achieved by splitting the interphase region into n concentric layers and applying the replacement method. In the limit as $n \to \infty$ we end up with a first order linear differential equation which models the mapping. This differential equation we found in terms of a function $\kappa_E(x)$ for the inhomogeneous interphase. Therefore, the solution for the CTE depends on the solution for the bulk modulus of the equivalent homogeneous particle. This bulk modulus is given by the solution of a pair of coupled first order linear differential equations derived in chapter 2 and in [40] or by a first order non-linear differential equation derived by Shen and Li [60]. For a power law profile that is described in the work of Vörös and Pukánszky [72, 73], an exact solution is derived for the coefficient of thermal expansion of a particulate composite. For the CTE of the interphase we considered linear and quadratic functions although the results could have easily been extended for higher order polynomials or for other functions. Our solution was also valid for a wide range of volume fraction of inclusions d_0 but not over the whole range since there is a forbidden overlapping of interphases as $d_0 \to 1$.

The results of the model compared reasonably well against other 2-phase models and with some interphase models as well as with the experimental results of Holliday and Robinson [23]. The composite that was considered consisted of an epoxy matrix filled with aluminium spherical particles. The interphase thickness was measured by using results in the work of Sideridis and Papanicolaou [63] who used principles of glass transition temperature.

The results for different interphase profiles for the CTE were presented graphically as well as the effect of the mechanical properties that are represented by the parameter J. It is shown for the profile considered how the mechanical properties influence the CTE of

the epoxy/aluminium composite. The present model showed large differences in the CTE for soft interphases $J < 1$ but relatively small changes for hard interphases $J > 1$.

Chapter 5

A Two-way Particle Mapping for Calculation of the Effective Dielectric Response of Graded Spherical Composites

5.1 Introduction

Recently, research tends to suggest that the dielectric properties of the interphase are also inhomogeneous, varying with respect to the radial distance from the centre of the spherical inclusion [56, 57]. Such an inhomogeneous transition is due to the bonding mechanisms occurring in the space between the inclusion and matrix. A controlled design of the spatial varying property also enables one to control the overall property of composites.

Results for the dielectric constant have been published for 2-phase composites in which perfect bonding is assumed to exist between the inclusion and the matrix. The first of these results are from Maxwell-Garnett theory [43] with the same result derived later by Hashin using the composite spheres assemblage model [15]. This same result can also be used for the electrical and thermal conductivity, magnetic permeability and diffusivity, provided that the spherical inclusions and matrix are isotropic.

There has been a first principles approach developed by Dong, Gu and Yu [10] to find

the effective dielectric response of composites with a dilute suspension of graded spherical particles. Use of this approach however is difficult for any arbitrary graded profile since the solution procedure is dependent on finding the exact solution to the governing differential equations. Therefore Yu, Gu and Huang [82] developed a differential effective dipole approximation (DEDA), which can be applied to any arbitrary graded profile at least numerically. Although DEDA showed good agreement with the first principles approach, it was not known how good this approximation was at the time of its invention. It has been recently shown by Yu and Gu [81] that for graded spherical particles, DEDA is in fact exact. In this paper it is shown that the equations derived using the replacement method [22] on the Maxwell-Garnett mixing rule, coincide with the results of DEDA. These results however, are only valid for a low concentration of suspended inclusions since the interaction among the inclusions has been neglected in the construction of these models.

Vo and Shi [74] measured the dielectric properties of composites as a function of inclusion concentration using a proposed theoretical model based on effective medium theory. The dielectric property of composites and its dependence on the filler concentration is taken into account in their model. Therefore, their model is valid over all volume fractions and showed good agreement with experimental results. It was also proven to contain the Maxwell-Garnett result as an asymptotic limit. Their model however cannot account for a variation in the properties of the interphase region but instead measures the property of the interphase by a single constant. One of the difficulties in modeling the interphase region of composite materials is to know what properties of the interphase best model reality. If the properties of the interphase are being modeled by a single constant, then how that constant is chosen becomes an important factor. If the properties of the interphase are modeled by a smooth variation, then choosing an appropriate function becomes an issue of importance. The more parameters that are included in such a function, the greater is the freedom of choice of the dielectric profile, however it then becomes a harder problem to solve. The equations appearing in this chapter and in [38] are applied to three different profiles which model the inhomogeniety of the interphase. If one knows or can estimate the variation in the dielectric property, then, an effective way of determining

the equivalent homogeneous property is shown. A way to incorporate the inhomogenous model with Vo and Shi's [74] homogeneous model is therefore proposed.

5.2 Analytical Model

5.2.1 A Spherical Inclusion Surrounded by an Inhomogeneous Interphase

The Maxwell-Garnett approximation [43] of the dielectric constant of a composite consisting of isotropic spherical inclusions embedded in an isotropic matrix is given by,

$$\varepsilon = \varepsilon_m + \frac{c}{\frac{1}{\varepsilon_p - \varepsilon_m} + \frac{(1-c)}{3\varepsilon_m}} \tag{5.1}$$

where ε_m is the dielectric constant of the matrix, ε_p is the dielectric constant of the inclusions and c is their volume fraction. Hashin [16] also derived the same result using the composite spheres assemblage model. Expression (5.1) can also be used to model thermal and electrical conductivity, magnetic permeability and diffusivity [19].

If we consider each spherical inclusion to be surrounded by an isotropic inhomogeneous interphase region of finite size whose properties vary as a function of the radial distance from the centre of the inclusion, then as in chapters 2 and 3, we may derive a pair of governing differential equations which models the effective dielectric constant ε_E of the inclusion and interphase. A full derivation of these equations is given in Appendix B. The governing differential equations for the dielectric constant are therefore,

$$S'(x) = -\frac{2}{x}S(x) + \frac{2}{x}\varepsilon(x)U(x) \tag{5.2}$$

$$U'(x) = \frac{1}{x\varepsilon(x)}S(x) - \frac{1}{x}U(x) \tag{5.3}$$

with conditions $S(a) = 1$, $U(a) = 0$ and $x \in [a, b]$, along with,

$$T'(x) = -\frac{2}{x}T(x) + \frac{2}{x}\varepsilon(x)V(x) \tag{5.4}$$

$$V'(x) = \frac{1}{x\varepsilon(x)}T(x) - \frac{1}{x}V(x) \tag{5.5}$$

with conditions $T(a) = 0$, $V(a) = 1$ and $x \in [a, b]$.

The function $\varepsilon(x)$ represents the dielectric variation of the interphase region where x represents the radial distance from the centre of the inclusion. Note that the constant a represents the radius of the inclusion while the constant b represents the radius of the outer boundary of the interphase from the centre of the inclusion. Therefore the interphase has thickness $(b-a)$. Also note that the differential equations given by (5.2) and (5.3) are similar to (5.4) and (5.5) and differ only in the boundary conditions. Therefore, only one pair of equations need to be solved with appropriate care taken when accounting for the boundary conditions. The effective dielectric constant of the inclusion and interphase is then given by,

$$\varepsilon_E(b) = \frac{\varepsilon_p S(b) + T(b)}{\varepsilon_p U(b) + V(b)}. \tag{5.6}$$

Such a result is obtained by splitting the interphase region into n concentric layers, applying the replacement method [52, 17] on expression (5.1) and then letting $n \to \infty$. The result is that the inclusion together with its surrounding inhomogeneous interphase region is mapped onto a homogeneous spherical particle of identical size.

The above results are useful because we are able to model the interphase inhomogeneity by smooth, bounded and continuous functions of x as opposed to using a discontinuous step like graded interface as was used in [56]. Also, the above results are applicable to any arbitrary profile for the interphase region.

The dielectric properties of a composite filled with such *effective particles* consisting of inclusion and surrounding interphase, is then easily found by letting $\varepsilon_p = \varepsilon_E$ and $c = d_0 \frac{b^3}{a^3}$ in expression (5.1). Note that here c is the volume fraction of the effective particles expressed in terms of the volume fraction of the inclusions d_0.

5.2.2 Comparing with DEDA

It is easily shown that the above model coincides with the Tartar formula [45] and with differential effective dipole approximation (DEDA) [82] which was recently shown to be exact for spherical particles by Yu and Gu [81]. To show this, one must simply recognize that the effective dielectric constant at position x is given by,

$$\varepsilon_E(x) = \frac{\varepsilon_p S(x) + T(x)}{\varepsilon_p U(x) + V(x)}.$$

If we differentiate this expression and use the equations that define $S(x)$, $T(x)$, $U(x)$ and $V(x)$, we find that we recover the Tartar formula and DEDA which is given by,

$$\frac{d}{dx}[x\varepsilon_E(x)] + \frac{[\varepsilon_E(x)]^2}{\varepsilon(x)} = 2\varepsilon(x). \tag{5.7}$$

Like DEDA, the present model can be applied to arbitrary graded profiles and is exact for spherical particles. DEDA is derived by computing the dipole moment of a single coated spherical particle, unlike the current method. Therefore, the methods of derivation are different, yet the same result emerges. Also, the Tartar formula seems to be derived from an assemblage of spheres and not from an isolated spherical particle like DEDA and the replacement method.

Given that the same result has emerged, one may be inclined to ask what advantage the present method has over DEDA. That is, do equations (5.2) and (5.3) have any superiority over equation (5.7)? First it is worthwhile to note that equations (5.2) and (5.3) are two first order linear eqautions while equation (5.7) is a Riccati single first order equation but nonlinear. The two first order linear equations may be converted to a single second order linear equation while the nonlinear Riccati equation may also be converted to a second order linear equation via a simple transformation. Both sets of differential equations seem to be of the same level of complexity so there does not appear to be any advantage in using one over the other. Therefore, the present equations simply offer an alternative to equation (5.7).

5.3 Some Specific Profiles

5.3.1 A Power Law Profile

Suppose the dielectric properties of the interphase region vary according to the power law function given by,

$$\varepsilon(x) = \varepsilon_m J \left(\frac{a}{x}\right)^P, \tag{5.8}$$

where J represents the dielectric constant at the surface of the inclusion relative to that of the matrix while the constant P represents the rate at which the dielectric properties change with respect to x. Note that J is real and positive by definition while the constant P is real but may be either positive or negative.

Substitution of the power law function (5.8) into equations (5.2) and (5.3) gives upon conversion to a second order differential equation in $S(x)$,

$$S''(x) + \frac{(P+4)}{x} S'(x) + \frac{2P}{x^2} S(x) = 0 \tag{5.9}$$

where $S(a) = 1$ and $S'(a) = -\frac{2}{a}$. Making the substitution $x = e^t$ converts equation (5.9) to,

$$S''(t) + (P+3)S'(t) + 2PS(t) = 0 \tag{5.10}$$

The characteristic equation of this DE has roots given by,

$$\lambda_1 = \frac{-(P+3) + \sqrt{P^2 - 2P + 9}}{2}, \qquad \lambda_2 = \frac{-(P+3) - \sqrt{P^2 - 2P + 9}}{2}.$$

Note that λ_1 and λ_2 are both real and distinct for all values of P.

Therefore, the solution to (5.9) is given by,

$$S(x) = Ax^{\lambda_1} + Bx^{\lambda_2} \tag{5.11}$$

where,

$$A = \frac{1}{a^{\lambda_1}} \left(\frac{\lambda_2 + 2}{\lambda_2 - \lambda_1}\right), \qquad B = \frac{1}{a^{\lambda_2}} \left(\frac{\lambda_1 + 2}{\lambda_1 - \lambda_2}\right).$$

Rearranging equation (5.2) enables us to find $U(x)$ as,

$$U(x) = \frac{1}{\varepsilon_m J a^P} \left\{ \left(\frac{\lambda_1}{2} + 1 \right) A x^{\lambda_1 + P} + \left(\frac{\lambda_2}{2} + 1 \right) B x^{\lambda_2 + P} \right\}. \tag{5.12}$$

Similarly, equations (5.4) and (5.5) give,

$$T(x) = C x^{\lambda_1} + D x^{\lambda_2} \tag{5.13}$$

and

$$V(x) = \frac{1}{\varepsilon_m J a^P} \left\{ \left(\frac{\lambda_1}{2} + 1 \right) C x^{\lambda_1 + P} + \left(\frac{\lambda_2}{2} + 1 \right) D x^{\lambda_2 + P} \right\} \tag{5.14}$$

where

$$C = \frac{1}{a^{\lambda_1}} \left(\frac{2\varepsilon_m J}{\lambda_1 - \lambda_2} \right), \qquad D = \frac{1}{a^{\lambda_2}} \left(\frac{2\varepsilon_m J}{\lambda_2 - \lambda_1} \right).$$

5.3.2 An Exponential Profile

Suppose the dielectric properties of the interphase region vary according to the exponential function given by,

$$\varepsilon(x) = \alpha e^{\beta x}.$$

Here α and β are analogous to the parameters J and P respectively of the power law profile. Substitution of this function into (5.2) and (5.3) and converting to a second order differential equation in S gives,

$$x S''(x) + (4 - \beta x) S'(x) - 2\beta S(x) = 0 \tag{5.15}$$

where $S(a) = 1$ and $S'(a) = -\frac{2}{a}$.
Making the substitution $t = \beta x$ converts this differential equation to,

$$t S''(t) + (4 - t) S'(t) - 2t S(t) = 0. \tag{5.16}$$

We may use the method of Frobenius to solve (5.16). Since $t = 0$ is a regular singular point of (5.16), we look for solutions of the form,

$$S(t) = \sum_{m=0}^{\infty} a_m t^{m+c}. \tag{5.17}$$

Substitution of (5.17) into (5.16) gives a recurrence relation in a_m given by,

$$a_{m+1} = \frac{(m+c+2)}{(m+c+1)(m+c+4)} a_m. \tag{5.18}$$

The indicial equation has roots given by $c = 0$ and $c = -3$. Note that $c = -3$ fails to give a solution to (5.18). Solving the recurrence relation (5.18) for the case $c = 0$ and substituting into (5.17) gives,

$$S(t) = 3! a_0 \sum_{m=0}^{\infty} \frac{(m+1)}{(m+3)!} t^m. \tag{5.19}$$

Integrating expression (5.19) with respect to t gives,

$$\int S(t)\, dt = 3! a_0 \left(\frac{e^t}{t^2} - \frac{1}{t^2} - \frac{1}{t} - \frac{1}{2} \right) + C, \qquad \forall t.$$

Differentiating this expression and substituting $t = \beta x$ gives,

$$S(x) = D \left\{ \frac{e^{\beta x}(\beta x - 2)}{x^3} + \frac{(\beta x + 2)}{x^3} \right\},$$

where D is an arbitrary constant. It can be shown that $\frac{e^{\beta x}(\beta x-2)}{x^3}$ and $\frac{(\beta x+2)}{x^3}$ are two independent solutions of the differential equation (5.15). Therefore, the general solution to (5.15) is given by,

$$S(x) = C_1 \frac{(\beta x + 2)}{x^3} + C_2 \frac{e^{\beta x}(\beta x - 2)}{x^3} \tag{5.20}$$

and the function $U(x)$ is given by,

$$U(x) = -\frac{C_1}{\alpha} \frac{e^{-\beta x}}{x^3} + \frac{C_2}{\alpha} \left\{ \frac{\beta}{2} \left(\frac{\beta x - 2}{x^2} \right) + \frac{1}{x^3} \right\}. \tag{5.21}$$

The constants C_1 and C_2 are defined by,

$$C_1 = \frac{-\omega_2}{\gamma_2\omega_1 - \gamma_1\omega_2}, \qquad C_2 = \frac{\omega_1}{\gamma_2\omega_1 - \gamma_1\omega_2}$$

where,

$$\gamma_1 = \left(\frac{\beta a + 2}{a^3}\right), \qquad \gamma_2 = e^{\beta a}\left(\frac{\beta a - 2}{a^3}\right),$$
$$\omega_1 = -\frac{e^{-\beta a}}{a^3}, \qquad \omega_2 = \left\{\frac{\beta}{2}\left(\frac{\beta a - 2}{a^2}\right) + \frac{1}{a^3}\right\}.$$

Similarly, we have,

$$T(x) = D_1\frac{(\beta x + 2)}{x^3} + D_2\frac{e^{\beta x}(\beta x - 2)}{x^3} \tag{5.22}$$

and

$$V(x) = -\frac{D_1}{\alpha}\frac{e^{-\beta x}}{x^3} + \frac{D_2}{\alpha}\left\{\frac{\beta}{2}\left(\frac{\beta x - 2}{x^2}\right) + \frac{1}{x^3}\right\}, \tag{5.23}$$

where

$$D_1 = \frac{-\gamma_2\alpha}{\omega_2\gamma_1 - \omega_1\gamma_2}, \qquad D_2 = \frac{\gamma_1\alpha}{\omega_2\gamma_1 - \omega_1\gamma_2}.$$

5.3.3 An Exponential-Power Law Profile

Suppose the dielectric properties of the interphase region vary according to the function given by,

$$\varepsilon(x) = cx^P e^{\beta x}. \tag{5.24}$$

Such a function is useful in that it enables us to control three different parameters, that is, c, P and β, thereby giving us a wider class of functions than the previous two profiles.

Substituting (5.24) into (5.2) and (5.3) and converting to a second order equation in $S(x)$ gives,

$$x^2S''(x) + x(4 - P - \beta x)S'(x) - 2(P + \beta x)S(x) = 0 \tag{5.25}$$

Letting $z = |\beta|x$ and substituting into (5.25) gives,

$$S''(z) + \frac{1}{z}(4 - P - \text{sign}(\beta)z)S'(z) - \frac{2}{z^2}(P + \text{sign}(\beta)z)S(z) = 0 \tag{5.26}$$

We can transform this differential equation by making use of the following theorem [3]:

The change of variable

$$S(z) = w(z)\exp\left(-\frac{1}{2}\int Q\,dz\right)$$

transforms

$$S'' + QS' + RS = 0 \qquad \text{into} \qquad w'' + \left(R - \frac{1}{2}Q' - \frac{1}{4}Q^2\right)w = 0.$$

Therefore, letting,

$$S(z) = w(z)z^{\frac{1}{2}(P-4)}e^{\frac{1}{2}\text{sign}(\beta)z} \tag{5.27}$$

transforms equation (5.26) into Whittaker's equation [1],

$$w''(z) + \left[-\frac{1}{4} + \frac{\kappa}{z} + \frac{\left(\frac{1}{4} - \mu^2\right)}{z^2}\right]w(z) = 0, \tag{5.28}$$

where,

$$\kappa = -\text{sign}(\beta)\frac{P}{2}, \qquad \text{and} \qquad \mu = \frac{1}{2}\sqrt{9 + 2P + P^2}.$$

The solution to (5.28) is given by,

$$w(z) = A_1 M_{\kappa,\mu}(z) + B_1 W_{\kappa,\mu}(z)$$

where $M_{\kappa,\mu}(z)$ and $W_{\kappa,\mu}(z)$ are Whittaker's functions and A_1 and B_1 are arbitrary constants. Therefore, the solution to equation (5.25) is given by,

$$S(x) = x^{\frac{1}{2}(P-4)}e^{\frac{1}{2}\beta x}(A_2 M_{\kappa,\mu}(|\beta|x) + B_2 W_{\kappa,\mu}(|\beta|x)) \tag{5.29}$$

where A_2 and B_2 are arbitrary constants. The Whittaker functions are defined by,

$$M_{\kappa,\mu}(z) = e^{-\frac{1}{2}z} z^{\frac{1}{2}+\mu} M(\frac{1}{2} + \mu - \kappa, 1 + 2\mu, z)$$
$$W_{\kappa,\mu}(z) = e^{-\frac{1}{2}z} z^{\frac{1}{2}+\mu} U(\frac{1}{2} + \mu - \kappa, 1 + 2\mu, z)$$

where $M(a, b, z)$ and $U(a, b, z)$ are Kummer's functions which are defined by,

$$M(a, b, z) = \sum_{n=0}^{\infty} \frac{(a)_n z^n}{(b)_n n!}$$

and

$$U(a, b, z) = \frac{\pi}{\sin \pi b} \left\{ \frac{M(a, b, z)}{\Gamma(1 + a - b)\Gamma(b)} - z^{1-b} \frac{M(1 + a - b, 2 - b, z)}{\Gamma(a)\Gamma(2 - b)} \right\}.$$

Note that,

$$(a)_n = a(a + 1)(a + 2) \ldots (a + n - 1), \qquad (a)_0 = 1.$$

Also, we have the following special properties for the Kummer functions:

$$\frac{d}{dz} M(a, b, z) = \frac{a}{b} M(a + 1, b + 1, z)$$

and

$$\frac{d}{dz} U(a, b, z) = -aU(a + 1, b + 1, z).$$

In terms of Kummer's functions, we may rewrite the solution to equation (5.25) as,

$$S(x) = x^{\frac{1}{2}P+\mu-\frac{3}{2}} e^{\frac{1}{2}(\text{sign}(\beta)-1)|\beta|x} \Big\{ AM(\frac{1}{2} + \mu - \kappa, 1 + 2\mu, |\beta|x) + BU(\frac{1}{2} + \mu - \kappa, 1 + 2\mu, |\beta|x) \Big\} \tag{5.30}$$

where A and B are arbitrary constants which can be found by using the boundary conditions, $S(a) = 1$ and $S'(a) = -\frac{2}{a}$. The solution for $U(x)$ is then found by rearranging equation (5.2). The constants A and B are given by,

$$A = \frac{\gamma_1 U_a^{(2)} - \gamma_2 U_a^{(1)}}{U_a^{(2)} M_a^{(1)} - U_a^{(1)} M_a^{(2)}} \qquad \text{and} \qquad B = \frac{\gamma_2 M_a^{(1)} - \gamma_1 M_a^{(2)}}{U_a^{(2)} M_a^{(1)} - U_a^{(1)} M_a^{(2)}}$$

where,

$$\begin{aligned}
M_a^{(1)} &= M(\frac{1}{2} + \mu - \kappa, 1 + 2\mu, |\beta| a), \\
U_a^{(1)} &= U(\frac{1}{2} + \mu - \kappa, 1 + 2\mu, |\beta| a), \\
M_a^{(2)} &= \frac{\left(\frac{1}{2} + \mu - \kappa\right)}{(1 + 2\mu)} M(\frac{3}{2} + \mu - \kappa, 2 + 2\mu, |\beta| a), \\
U_a^{(2)} &= -\left(\frac{1}{2} + \mu - \kappa\right) U(\frac{3}{2} + \mu - \kappa, 2 + 2\mu, |\beta| a), \\
\gamma_1 &= a^{-\frac{1}{2}P - \mu + \frac{3}{2}} e^{-\frac{1}{2}(\text{sign}(\beta) - 1)|\beta| a}, \\
\gamma_2 &= \frac{1}{|\beta|} \gamma_1 \left\{ -\frac{\left(\frac{1}{2}P + \mu + \frac{1}{2}\right)}{a} - \frac{1}{2}(\text{sign}(\beta) - 1)|\beta| \right\}.
\end{aligned}$$

Therefore, the solution for $T(x)$ is given by,

$$\begin{aligned}
T(x) = x^{\frac{1}{2}P + \mu - \frac{3}{2}} e^{\frac{1}{2}(\text{sign}(\beta) - 1)|\beta| x} \Big\{ & C_1 M(\frac{1}{2} + \mu - \kappa, 1 + 2\mu, |\beta| x) \\
& + C_2 U(\frac{1}{2} + \mu - \kappa, 1 + 2\mu, |\beta| x) \Big\}
\end{aligned} \tag{5.31}$$

and the solution for $V(x)$ is found from equation (5.4) where C_1 and C_2 are constants given by,

$$C_1 = \frac{U_a^{(1)} \gamma_3}{U_a^{(1)} M_a^{(2)} - U_a^{(2)} M_a^{(1)}}, \qquad C_2 = \frac{-M_a^{(1)} \gamma_3}{U_a^{(1)} M_a^{(2)} - U_a^{(2)} M_a^{(1)}}$$

where,

$$\gamma_3 = \frac{2c}{|\beta|} a^{\frac{1}{2}P - \mu + \frac{1}{2}} e^{\frac{1}{2}(\text{sign}(\beta) + 1)|\beta| a}.$$

5.4 The Equivalent Homogeneous Interphase

5.4.1 A Reverse Mapping

The Maxwell-Garnett dilute concentration solution for the dielectric constant is given by expression (5.1). We have been able to manipulate this expression using the replacement method in order to account for an inhomogeneous interphase region surrounding each inclusion. That is, we map the inclusion and surrounding inhomomgeneous interphase onto an effective spherical particle of identical size with dielectric constant denoted by $\varepsilon_E(b)$. Once we have found $\varepsilon_E(b)$ for an inhomomgeneous interphase, we can determine a constant value ε_i for the dielectric constant of the interphase by doing a reverse mapping as shown in Figure 5.1, that is, we map a homogeneous sphere of radius b onto a two-phase sphere of identical size by solving,

$$\varepsilon_E(b) = \varepsilon_i + \frac{\left(\frac{a^3}{b^3}\right)}{\frac{1}{\varepsilon_p - \varepsilon_i} + \frac{\left(1-\frac{a^3}{b^3}\right)}{3\varepsilon_i}}, \tag{5.32}$$

to determine the value of ε_i.

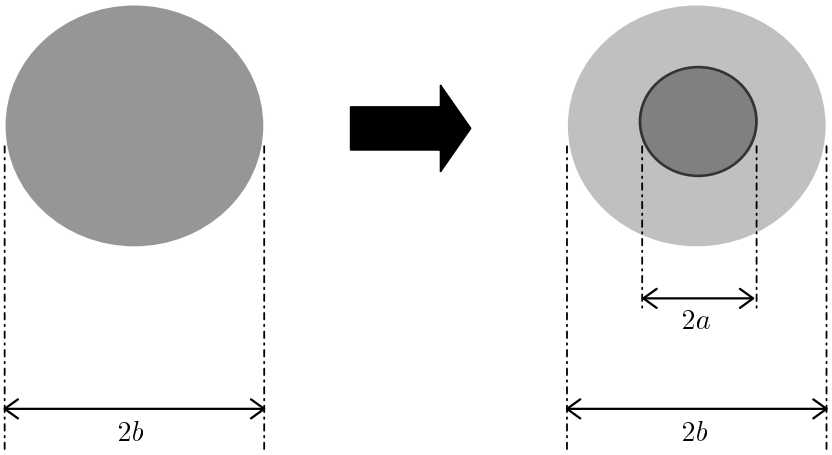

Figure 5.1: A mapping of a homogeneous particle consisting of inclusion and interphase onto a 2-phase composite.

Thus, for an inhomogeneous interphase, the present method gives us a way of finding the equivalent homogeneous property of the interphase.

5.4.2 Incorporating Other Models

Since we now know what the equivalent homogenous property of the interphase is, we may incorporate this result into other existing 3-phase models, which assume a homogeneous interphase surrounding each inclusion. We therefore propose here a way of fusing two different models together, an inhomogeneous and a homogeneous interphase model. We refer to this joining process as the fused model.

For instance, the value ε_i calculated from expression (5.32) can be used in the Vo and Shi [74] model. The advantage of using the Vo and Shi model is that full volume fraction packing of spherical inclusions is allowed and the size of the interphase region may also vary as a function of inclusion concentration. The work of Theocaris [67] has also suggested that for polymer composites in particular, the size of the interphase region depends on the inclusion concentration. Therefore, the Vo and Shi model allows us to account for this phenomena whereas the inhomogenous interphase model does not. According to the Vo and Shi model, the dielectric constant of a particulate composite is given by,

$$\varepsilon_C = \frac{h + 2l}{h - l} \tag{5.33}$$

where

$$h = \left\{ 1 + 2\frac{(\varepsilon_m - \varepsilon_i)(\varepsilon_i - \varepsilon_p)}{(2\varepsilon_m + \varepsilon_i)(2\varepsilon_i + \varepsilon_p)}\frac{a^3}{b^3} \right. \quad - \quad 2\frac{(\varepsilon_m - 1)(\varepsilon_m - \varepsilon_i)}{(\varepsilon_m + 2)(2\varepsilon_m + \varepsilon_i)}\frac{b^3}{c^3}$$
$$\left. - \quad 2\frac{(\varepsilon_m - 1)(\varepsilon_m + 2\varepsilon_i)(\varepsilon_i - \varepsilon_p)}{(\varepsilon_m + 2)(2\varepsilon_m + \varepsilon_i)(2\varepsilon_i + \varepsilon_p)}\frac{a^3}{b^3} \right\},$$

$$l = \left\{ \frac{(\varepsilon_m - 1)}{(\varepsilon_m + 2)} j - \frac{(2\varepsilon_m + 1)n}{(\varepsilon_m + 2)(2\varepsilon_m + \varepsilon_i)}\frac{b^3}{c^3} \right\},$$

$$j = \left\{ 1 + 2\frac{(\varepsilon_m - \varepsilon_i)(\varepsilon_i - \varepsilon_p)}{(2\varepsilon_m + \varepsilon_i)(2\varepsilon_i + \varepsilon_p)}\frac{a^3}{b^3} \right\}$$

and

$$n = \left\{ (\varepsilon_m - \varepsilon_i) + \frac{(\varepsilon_m + 2\varepsilon_i)(\varepsilon_i - \varepsilon_p)}{(2\varepsilon_i + \varepsilon_p)}\frac{a^3}{b^3} \right\}.$$

The subscripts m, i and p stand for matrix, interphase and particle inclusion respectively. The parameters a and b are as defined in our inhomogeneous interphase model while the parameter c represents the radial distance from the centre of the inclusion to the outer boundary of the matrix phase of a representative composite sphere. The parameters a, b and c are related to each other through the parameters k and d_0 where k is the interphase volume constant and d_0 is the volume fraction of filler, that is,

$$\frac{a^3}{b^3} = \frac{(1+kd_0)}{(1+k)}, \tag{5.34}$$

$$\frac{a^3}{c^3} = d_0, \tag{5.35}$$

and

$$\frac{b^3}{c^3} = d_0 \left\{ 1 + k\frac{(1-d_0)}{(1+kd_0)} \right\}. \tag{5.36}$$

It is important to note that if the interphase volume constant in (5.33) is set to zero, that is, $k = 0$, then as has been stated by Vo and Shi [74], their model tends to the Maxwell-Garnett approximation given by (5.1). As a result of this, if we ignore (5.34) and (5.36) and allow $b = constant \times a$, then under the mapping (5.32), the Vo and Shi Model given by (5.33) converges to our inhomogeneous interphase model. Therefore, the Vo and Shi model and the inhomogeneous interphase model are the same when the size of the interphase remains fixed over all filler concentrations.

As was mentioned before, the advantage of using the Vo and Shi model is that full volume fraction packing may be assumed and the interphase volume fraction varies as a function of inclusion concentration, a phenomenon supported by the work of Theocaris [67]. By rearranging equation (5.34), the paramater b may be expressed by,

$$b = a\frac{(1+k)^{\frac{1}{3}}}{(1+kd_0)^{\frac{1}{3}}}. \tag{5.37}$$

For the Vo and Shi model to be implemented, one must know the value of ε_i and k. For any given set of experimental data, the model may be applied by choosing a variety of combinations for ε_i and k which best fit the data. The disadvantage here is that there are

many combinations of ε_i and k to choose from so one does not know which combination to use. However, if one knows a suitable choice for the value of ε_i, then this only presents us with the problem of choosing the value of k which may be found from experiment. For example, Todd and Shi [71] found a function for ε_i in terms of k for a given set of data. For polymer composites, Theocaris [67] has proposed a way of measuring the size of the interphase with respect to volume fraction using principles of glass transition temperature.

We propose here a way to choose the interphase dielectric constant ε_i for a given value of k by using our inhomogeneous interphase model. If we average the parameter b over the domain $0 \leq d_0 \leq 1$, then we have,

$$b_{AV} = \frac{3a}{2k}\left\{(1+k) - (1+k)^{\frac{1}{3}}\right\}.$$

Therefore, for any given k, the value for b_{AV} used in our inhomogeneous interphase model gives us a value for ε_i via the mapping (5.32), which we may then use in the Vo and Shi model along with our original k.

5.5 Results

5.5.1 Power Law Profile

For the power law profile, we choose the parameters J and P such that the properties of the interphase vary from those of the inclusion to those of the matrix, that is, we have $\varepsilon(a) = \varepsilon_p$ and $\varepsilon(b) = \varepsilon_m$.

Figures 5.2 and 5.3 represent the theoretical results of the fused model versus the experimental data [53] of two ceramic filled epoxy composites. The ceramic filler consisted of Lead magnesium niobate-lead titanate with a dielectric constant at room temperature given by, $\varepsilon_p = 17800$. A commercial epoxy known as Shipley photoepoxy with $\varepsilon_m = 3$ was used in Composite (I) and a developed in-house epoxy with $\varepsilon_m = 4$ was used in Composite (II).

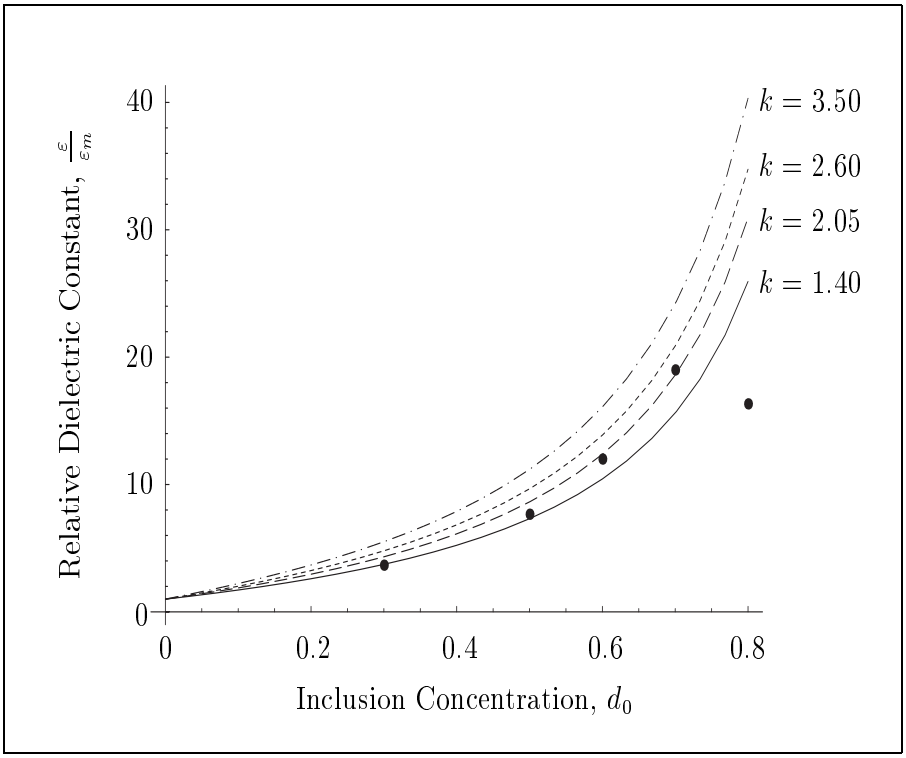

Figure 5.2: Theoretical results of the Relative Dielectric Constant versus the experimental data of Composite (I) [53] as a function of inclusion concentration for various values of k using the fused model and the Power Law Profile.

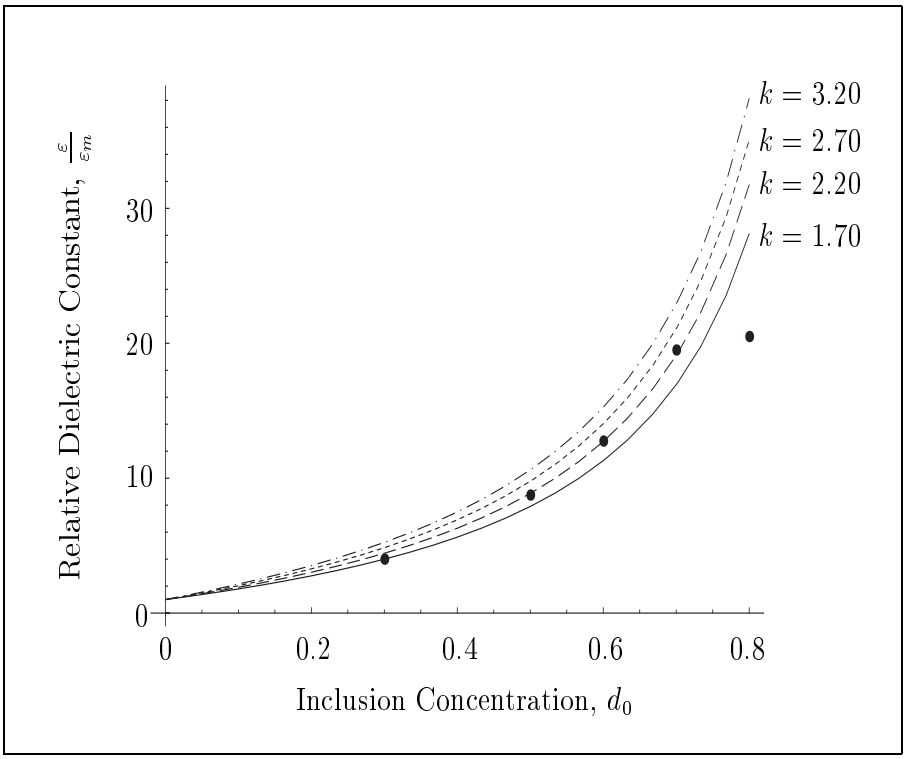

Figure 5.3: Theoretical results of the Relative Dielectric Constant versus the experimental data of Composite (II) [53] as a function of inclusion concentration for various values of k using the fused model and the Power Law Profile.

It can be seen from Figure 5.2 that $k = 2.05$ gives the best fit to the experimental data of Composite (I) and from Figure 5.3 it can be seen that $k = 2.20$ gives the best fit for Composite (II). Such values of k found are different to the ones found by Vo and Shi [74] who also made estimates of the interphase dielectric constant.

5.5.2 Exponential Profile

For the exponential profile, we choose the parameters α and β such that the properties of the interphase again vary from those of the inclusion to those of the matrix. Such a choice for α and β produces a profile very similar to the power law. Therefore, for the exponential profile, the theoretical results of the fused model versus the experimental data [53] of Composite (I) and (II) are fairly close to Figures 5.2 and 5.3, the difference being negligible.

5.5.3 Exponential-Power Law Profile

For the power-exponential profile, we can choose the parameters such that the properties of the interphase again vary from those of the inclusion to those of the matrix, however, since there are three parameters that define this profile, there are several possibile curves which can account for this, clearly showing the advantages of using such a profile. Therefore, we choose the parameters c and β such that we have $\varepsilon(a) = \varepsilon_p$ and $\varepsilon(b) = \varepsilon_m$ and allow the parameter P to vary. For a specific value of $k = 3.20$, we can plot several results by allowing the parameter P to vary. Figure 5.4 shows the profiles for the inhomogeneous interphase for several values of P and Figure 5.5 shows the theoretical results versus the experimental data of composite (II) [53] for those values of P. Alternatively, for a specific value of $P = 350$, Figure 5.6 shows results obtained by allowing the parameter k to vary.

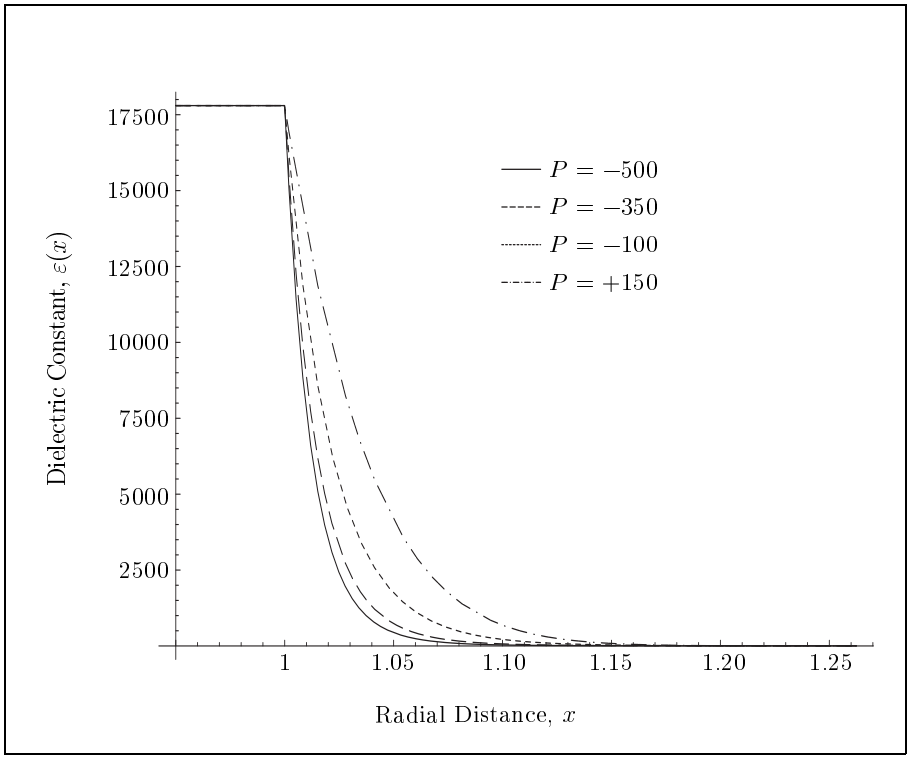

Figure 5.4: The Exponential-Power law Profile for the Dielectric Constant of the inhomogeneous interphase region for various values of P. Note that here $k = 3.20$.

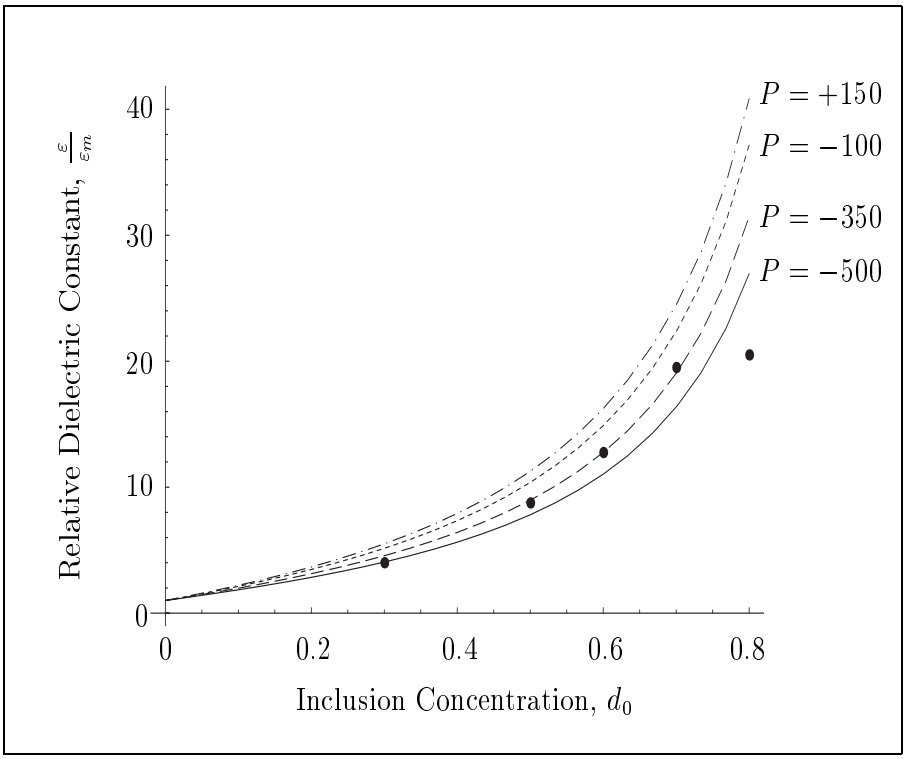

Figure 5.5: Theoretical results of the Relative Dielectric Constant versus the experimental data of Composite (II) [53] as a function of inclusion concentration for various values of P using the fused model and the Exponential-Power Law Profile. Note that here $k = 3.20$.

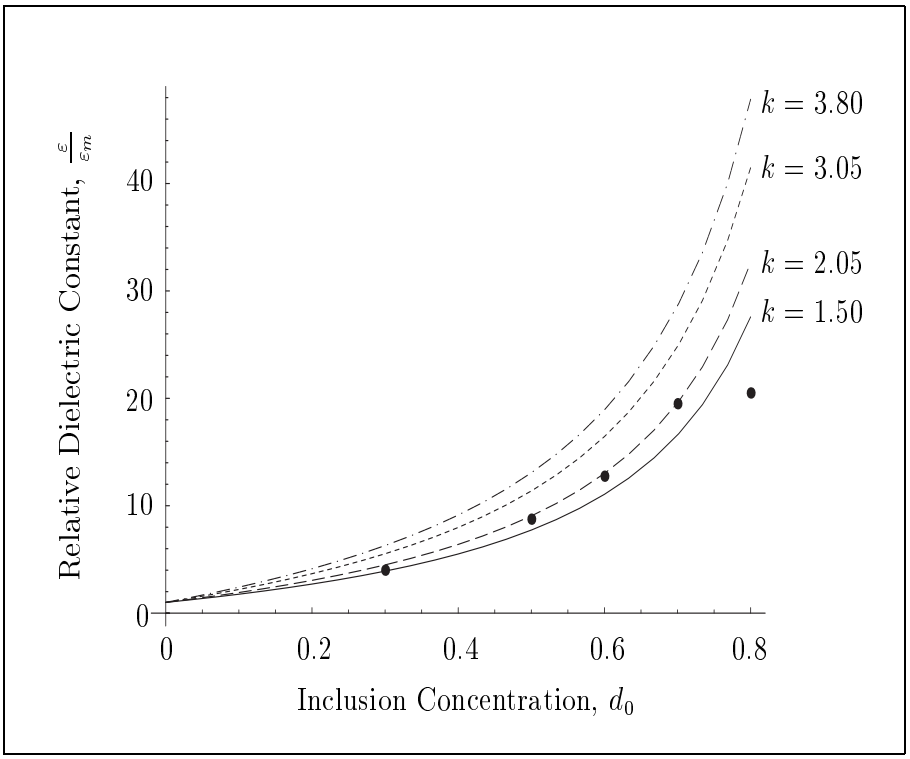

Figure 5.6: Theoretical results of the Relative Dielectric Constant versus the experimental data of Composite (II) [53] as a function of inclusion concentration for various values of k using the fused model and the Exponential-Power Law Profile. Note that here $P = 350$.

5.5.4 Suitability of the Gradation Profiles

One of the difficulties involved in modeling the interphase in composite materials is to know what its properties are. The interphase properties depend to a large extent on the properties of the individual materials that make up the composite. Other factors may come into play as well, for instance, if the composite was prepared with the aid of coupling agents. Therefore, since the materials for different composites vary, the bonding between the constituent materials is of a different nature for each composite. The properties of the interphase depend to a large extent on the bonding that is occurring between each of the phases. Since the properties of the composite depend to a large extent on this bonding, knowledge of the nature of the interphase becomes an important issue. In fact, Lesko et al. [32] have written

> The lack of quantitative knowledge of interphase properties is the *Achilles' heel* of the field.

For the three different profiles considered, the parameters were chosen such that the dielectric properties of the interphase vary from those of the particle inclusion to the matrix. Vo and Shi [74] have applied their interphase model to the same data with much success and concluded that the properties of the interphase lie somewhere between the property of the inclusion and matrix. It therefore seems somewhat reasonable to assume the dielectric properties of the interphase to vary from inclusion to matrix although such an assumption may be easily challenged. For the elastic properties of composites, this assumption is often made, [67] although for the dielectric properties of the interphase, there does not seem to be much reported in the literature.

5.6 Conclusion

In this chapter we have determined the dielectric properties of composites containing spherical inclusions surrounded by an inhomogenous interphase region. We did this by mapping the inclusion together with its interphase onto a homogeneous spherical particle by applying the replacement method. The same approach was used in chapters 2, 3 and4 to determine other properties of a particulate composite. The differential equations derived for the dielectric constant are generalised for a wide class of functions describing the inhomogeneous properties of the interphase region and were found to coincide with the results of DEDA [82] and the Tartar formula [45].

By doing a reverse mapping of a homogeneous sphere onto a 2-phase composite, it was shown how the inhomogeneous interphase model may be incorporated into the model of Vo and Shi [74]. The model of Vo and Shi offers advantages in that the size of the interphase region is allowed to vary in size as a function of inclusion concentration, a result that is supported by the work of Theocaris [67]. We called this process of joining the two models together as the fused model. The advantage of this is that some of the limitations posed by each individual model are effectively eliminated.

We have plotted the results for the different profiles against experimental data by choosing different values for the parameters and the agreement is excellent. However, knowing what values to assign to these parameters may sometimes be a difficult task. Nonetheless, it seems that if we are to apply the model well, we need to know two important things, that is, the size of the interphase as a function of inclusion concentration, and the profile that best describes the inhomogeneous dielectric properties of the interphase region.

Chapter 6

Some Useful Results for the Bulk and Shear Modulus of a Functionally Graded Particulate Composite

6.1 Introduction

Modeling the elastic moduli of composite materials is a very active area of research amongst the composite community. The consideration of the interphase in modeling the elastic moduli as well as other properties is becoming increasingly important especially with the discovery of nanoparticles and nanotubes. For example, for a given volume fraction of inclusions, the volume fraction of the interphase region increases as the size of the inclusions is reduced. Therefore, the role of the interphase becomes greater as the size of the inclusions decrease and so for nanocomposites in particular, their properties largely depend on the properties of this interphase.

The properties of the interphase may either serve to strengthen the composite as a whole or it may even weaken it. There are many instances where the interphase properties have played the role of strengthening the overall material. An example of a weak interphase appears to occur in the manufacturing of polyimide/silica nanocomposites. Odegard, Clancy and Gates [48] attempted to determine the elastic properties of such composites and found that for very small nanoparticles of silica, the elastic properties of

the composite had a lower value than those of the polyimide matrix alone. Therefore, very small nanoparticles of silica seem to offer poor reinforcement. This may help to explain why the dielectric properties of such composites are quite high relative to the dielectric properties of the constituents. It appears that there is increased dipole polarizability in the interphase region resulting in an increase in the dielectric constant of the composite. An increase in the dipole polarizability implies that the molecules in the interphase region are more free to rotate and orient themselves in an applied electric field. Therefore, it seems as though there is poor bonding in the interphase region due to this phenomenon, which may help to explain why the elastic properties of such composites have a lower value than the bulk polymer.

In this work we model the bulk and shear modulus of composite materials containing spherical inclusions where the interphase properties are described using two different profiles. In the first case we assume the properties vary linearly and in the second case as a product of a general power law and exponential function. The results are first generalised and expressed in terms of definite integrals where one of the property profiles (i.e. the bulk or shear modulus) is assumed to be constant. When both the bulk and shear modulus of the interphase are assumed to vary linearly, the governing differential equations become rather complex. For example, Weng [78] solved the bulk modulus problem for particle and fiber reinforced composites in terms of hypergeometric functions where the matrix properties were assumed to vary linearly. Ding and Weng [9] also considered the same type of composite but with one of the matrix properties held constant. For the linear case the results presented in this work which are of closed form but assume that one of the interphase properties (i.e. the bulk or shear modulus) is held constant. These results are therefore similar to results published by Ding and Weng [9]. The difference however lies in the fact that Ding and Weng [9] considered the matrix itself to be functionally graded.

Ozmusul and Picu [51] used a finite element modeling approach where the interphase is assumed to have a linearly varying Young's modulus. A unit cell model is used in which the interphase is discretized into a number of steps or layers having constant moduli. The authors also mention that much current research tends to suggest that the interphase region plays a larger role for nanocomposites.

Jasiuk and Kouider [25] considered a unidirectional fiber reinforced composite where two profiles for the interphase are considered. The first case considered is when the Young's modulus of the interphase varies as a general power law with constant Poisson's ratio and the second case where the Young's moduli and Poisson's ratio vary as linear functions. For the general power law, an exact solution is derived for the displacement of a composite cylinder subject to displacement boundary conditions. For the linear profile, a series form for the solution is derived. Perfect bonding is assumed at the particle and interphase boundary and at the interphase matrix boundary. For the power law profile, authors obtain results for both the transverse bulk and shear modulus. The shear modulus is analyzed using the Generalised Self Consistent method. For the linear profile Jasiuk and Kouider obtained results for the transverse bulk modulus and axial shear modulus. The transverse shear modulus appears to be a much harder problem for the linear profile.

For an interphase region which has a constant Poisson's ratio, the governing differential equations which describe both the bulk and shear properties are simplified and the result of Lutz and Zimmerman [42] are recovered, which show that the bulk modulus problem is the same as the conductivity problem when the Poisson's ratio is set to zero. For constant Poisson's ratio, we solve both the bulk and shear problem for the power-exponential profile. It seems as though there is no researcher thus far who has yet considered the power-exponential profile as applied to the bulk and shear modulus. Such a profile however has been considered by Wei and Tang [76], in the modeling of the dielectric response of graded cylindrical composites.

The equations governing the bulk modulus properties are known to be exact unlike the governing equations for the shear modulus. However, for the interphase profiles considered, that is, profiles which vary between the particle and matrix moduli, the governing equations for the shear modulus have been shown to be very accurate, for example see chapter 3. For profiles outside this range which are quite possible considering the example mentioned earlier of the polyimide/silica nanocomposites, we can utilize the technique described in chapter 3 to deal with such profiles.

6.2 Bulk Modulus of a Composite

The bulk modulus of an inclusion with a surrounding inhomogeneous interphase of finite thickness is governed by a pair of differential equations that were derived in chapter 2 and by Lombardo and Ding [40]. We restate these differential equations here for reference. They are,

$$S'(x) = -\frac{3}{x}\left(\frac{4\mu(x)}{3\kappa(x)+4\mu(x)}\right)S(x) + \frac{3}{x}\left(\frac{4\kappa(x)\mu(x)}{3\kappa(x)+4\mu(x)}\right)U(x) \tag{6.1}$$

$$U'(x) = \frac{3}{x}\left(\frac{3}{3\kappa(x)+4\mu(x)}\right)S(x) - \frac{3}{x}\left(\frac{3\kappa(x)}{3\kappa(x)+4\mu(x)}\right)U(x) \tag{6.2}$$

where $S(a) = 1$, $U(a) = 0$ and $x \in [a, b]$.

The functions $\kappa(x)$ and $\mu(x)$ represent the bulk and shear modulus of the inhomogeneous interphase respectively. These functions are assumed to be smooth, bounded and continuous.

The functions $T(x)$ and $V(x)$ are found by replacing S with T and U with V in equations (6.1) and (6.2), where $T(a) = 0$, $V(a) = 1$ and $x \in [a, b]$.

The bulk modulus of the inclusion and interphase is then given by,

$$\kappa_E = \frac{\kappa_0 S(b) + T(b)}{\kappa_0 U(b) + V(b)}, \tag{6.3}$$

where κ_0 is the bulk modulus of the inclusion. Note that a represents the radius of the inclusion, b represents the distance from the centre of the inclusion to the outer boundary of the interphase and E stands for effective spherical particle.

If we convert equations (6.1) and (6.2) into a second order differential equation in $U(x)$, we get,

$$U''(x) + P_1(x)U'(x) + Q_1(x)U(x) = 0 \tag{6.4}$$

where

$$P_1(x) = \frac{4}{x} + \frac{3\kappa'(x) + 4\mu'(x)}{3\kappa(x) + 4\mu(x)}$$

and

$$Q_1(x) = \frac{9\kappa'(x)}{x(3\kappa(x) + 4\mu(x))}.$$

The boundary conditions are given by,

$$U(a) = 0 \qquad \text{and} \qquad U'(a) = \frac{3}{a}\left(\frac{3}{3\kappa(a) + 4\mu(a)}\right). \tag{6.5}$$

Similarly, in order to find $T(x)$ and $V(x)$, replace U with V in equation (6.4). The boundary conditions for the differential equation in V would be,

$$V(a) = 1 \qquad \text{and} \qquad V'(a) = -\frac{3}{a}\left(\frac{3\kappa(a)}{3\kappa(a) + 4\mu(a)}\right). \tag{6.6}$$

6.2.1 Constant Bulk Modulus of the Interphase

If we let $\kappa(x) = \kappa_g$ a constant, then equation (6.4) becomes,

$$U''(x) + \left(\frac{4}{x} + \frac{4\mu'(x)}{3\kappa_g + 4\mu(x)}\right) U'(x) = 0 \tag{6.7}$$

which when solved subject to the boundary conditions (6.5) gives,

$$U(x) = 9a^3 \int_a^x \frac{dt}{t^4(3\kappa_g + 4\mu(t))}. \tag{6.8}$$

Substitution into equation (6.2) gives,

$$S(x) = \frac{a^3}{x^3} + 9a^3\kappa_g \int_a^x \frac{dt}{t^4(3\kappa_g + 4\mu(t))}. \tag{6.9}$$

Similarly, replacing U with V in (6.7) and solving it subject to the boundary conditions (6.6) gives,

$$V(x) = 1 - 9a^3\kappa_g \int_a^x \frac{dt}{t^4(3\kappa_g + 4\mu(t))} \tag{6.10}$$

and

$$T(x) = \kappa_g - \frac{a^3\kappa_g}{x^3} - 9a^3{\kappa_g}^2 \int_a^x \frac{dt}{t^4(3\kappa_g + 4\mu(t))}. \tag{6.11}$$

Therefore, the functions (6.8)-(6.11) enable us to determine the effects of the variable shear modulus on the bulk modulus of a composite. Note that only one integral needs to be solved which should be much easier than the original coupled system for a wide class of functions for $\mu(x)$. Also, in order for these integrals to yield reasonable results for the bulk modulus of a composite, an appropriate choice of the constant κ_g must be made. Given a variable bulk modulus $\kappa(x)$ for the interphase, we seek a suitable way of approximating this function by a constant. An appropriate choice would be to use the average value of the interphase taken from the rule of mixtures. This value is given by,

$$\kappa_g = \frac{3}{(b^3 - a^3)} \int_a^b x^2 \kappa(x)\, dx$$

and may be obtained by applying the replacement method on the simple rule of mixtures.

A Linear Profile for the Shear Modulus of the Interphase

If we let $\mu(x) = \alpha x + \beta$ be a linear function describing the inhomogeneous shear properties of the interphase, then the integral appearing in the functions (6.8)-(6.11) is given by,

$$\int_a^x \frac{dt}{t^4(3\kappa_g + 4\mu(t))} = \frac{1}{3\gamma}\left(\frac{1}{a^3} - \frac{1}{x^3}\right) + \frac{16\alpha^2}{\gamma^3}\left(\frac{1}{a} - \frac{1}{x}\right) + \frac{2\alpha}{\gamma^2}\left(\frac{1}{x^2} - \frac{1}{a^2}\right) + \frac{64\alpha^3}{\gamma^4}\left\{ \ln\left(\frac{a}{x}\right) + \ln\left(\frac{4\alpha x + \gamma}{4\alpha a + \gamma}\right) \right\}$$

where $\gamma = 3\kappa_g + 4\beta$. The above expression holds provided that $\gamma \neq 0$. If $\gamma = 0$ then we have,

$$\int_a^x \frac{dt}{t^4(3\kappa_g + 4\mu(t))} = \frac{1}{16\alpha}\left(\frac{1}{a^3} - \frac{1}{x^3}\right).$$

The effective bulk modulus, κ_E, of the inclusion and interphase is then given by expression (6.3).

6.2.2 Constant Shear Modulus of the Interphase

If we let $\mu(x) = \mu_g$ a constant, then equation (6.4) becomes,

$$xU''(x) + \left(4 + \frac{3x\kappa'(x)}{3\kappa(x) + 4\mu_g}\right) U'(x) + \frac{9\kappa'(x)}{(3\kappa(x) + 4\mu_g)} U(x) = 0. \tag{6.12}$$

If we make the substitution $z(x) = xU'(x)+3U(x)$, then this differential equation becomes,

$$z'(x) + \frac{3\kappa'(x)}{(3\kappa(x) + 4\mu_g)} z(x) = 0$$

which is first order in z. Solving this first order differential equation in $z(x)$ implies that,

$$U'(x) + \frac{3}{x} U(x) = \frac{C}{x(3\kappa(x) + 4\mu_g)}$$

where C is an arbitrary constant. Solving this first order differential equation in $U(x)$ when subject to the boundary conditions (6.5) gives,

$$U(x) = \frac{9}{x^3} \int_a^x \frac{t^2}{(3\kappa(t) + 4\mu_g)} \, dt. \tag{6.13}$$

Substitution into equation (6.2) gives,

$$S(x) = 1 - \frac{12\mu_g}{x^3} \int_a^x \frac{t^2}{(3\kappa(t) + 4\mu_g)} \, dt. \tag{6.14}$$

Similarly, replacing U with V in (6.12) and solving it subject to the boundary conditions (6.6) gives,

$$V(x) = \frac{a^3}{x^3} - \frac{12\mu_g}{x^3} \int_a^x \frac{t^2}{(3\kappa(t) + 4\mu_g)} \, dt \tag{6.15}$$

and

$$T(x) = \frac{4}{3}\mu_g \left(1 - \frac{a^3}{x^3}\right) - \frac{16{\mu_g}^2}{x^3} \int_a^x \frac{t^2}{(3\kappa(t) + 4\mu_g)} \, dt. \tag{6.16}$$

Similarly, the functions (6.13)-(6.16) enable us to determine the effects of the variable bulk modulus of the interphase on the bulk modulus of a composite. Note that only one integral needs to be solved which should be much easier than the original coupled system for a wide class of functions for $\kappa(x)$. Also, in order for these integrals to yield reasonable results for the bulk modulus of a composite, an appropriate choice of the constant μ_g must

be made. Given a variable shear modulus $\mu(x)$ for the interphase, we approximate this function by the average value of the interphase taken from the rule of mixtures. That is,

$$\mu_g = \frac{3}{(b^3 - a^3)} \int_a^b x^2 \mu(x)\, dx$$

A Linear Profile for the Bulk Modulus of the Interphase

If we let $\kappa(x) = \alpha x + \beta$ be a linear function describing the inhomogeneous bulk modulus of the interphase, then the integral appearing in the functions (6.13)-(6.16) is given by,

$$\int_a^x \frac{t^2}{(3\kappa(t) + 4\mu_g)}\, dt = \frac{(3\beta + 4\mu_g)^2}{(3\alpha)^3} \ln\left(\frac{3\alpha x + 3\beta + 4\mu_g}{3\alpha a + 3\beta + 4\mu_g}\right) + \frac{(x^2 - a^2)}{6\alpha} - \frac{(3\beta + 4\mu_g)}{(3\alpha)^2}(x - a)$$

provided that $\alpha \neq 0$. When $\alpha = 0$ we have,

$$\int_a^x \frac{t^2}{(3\kappa(t) + 4\mu_g)}\, dt = \frac{(b^3 - a^3)}{3(3\beta + 4\mu_g)}.$$

The effective bulk modulus, κ_E, of the inclusion and interphase is then given by expression (6.3).

6.3 Shear Modulus of a Composite

An approximation to the shear modulus of an inclusion with a surrounding inhomogeneous interphase of finite thickness is governed by a pair of differential equations that were derived in chapter 3 and in [39]. We restate these differential equations here for reference. They are,

$$S'(x) = -\frac{3}{5x}\left(\frac{9\kappa(x)+8\mu(x)}{3\kappa(x)+4\mu(x)}\right)S(x) + \frac{3\mu(x)}{5x}\left(\frac{9\kappa(x)+8\mu(x)}{3\kappa(x)+4\mu(x)}\right)U(x) \tag{6.17}$$

$$U'(x) = \frac{18}{5x\mu(x)}\left(\frac{\kappa(x)+2\mu(x)}{3\kappa(x)+4\mu(x)}\right)S(x) - \frac{18}{5x}\left(\frac{\kappa(x)+2\mu(x)}{3\kappa(x)+4\mu(x)}\right)U(x) \tag{6.18}$$

where $S(a) = 1$, $U(a) = 0$ and $x \in [a, b]$.

Again, the functions $\kappa(x)$ and $\mu(x)$ represent the bulk and shear modulus of the inhomogeneous interphase respectively and are assumed to be smooth, bounded and continuous.

Also, the functions $T(x)$ and $V(x)$ are found by replacing S with T and U with V in equations (6.17) and (6.18), where $T(a) = 0$, $V(a) = 1$ and $x \in [a, b]$.

The shear modulus of the inclusion and interphase is then given by,

$$\mu_E = \frac{\mu_0 S(b) + T(b)}{\mu_0 U(b) + V(b)}, \tag{6.19}$$

where μ_0 is the shear modulus of the inclusion. If we convert equations (6.17) and (6.18) into a second order differential equation in $U(x)$, we get,

$$U''(x) + P_2(x)U'(x) + Q_2(x)U(x) = 0 \tag{6.20}$$

where

$$P_2(x) = \frac{4}{x} + \frac{\mu'(x)}{\mu(x)} + \frac{3\kappa'(x)+4\mu'(x)}{3\kappa(x)+4\mu(x)} - \frac{\kappa'(x)+2\mu'(x)}{\kappa(x)+2\mu(x)}$$

and

$$Q_2(x) = \frac{18}{5x}\frac{\mu'(x)(\kappa(x)+2\mu(x))}{\mu(x)(3\kappa(x)+4\mu(x))}.$$

The boundary conditions are given by,

$$U(a) = 0 \qquad \text{and} \qquad U'(a) = \frac{18}{5a\mu(a)} \left(\frac{\kappa(a) + 2\mu(a)}{3\kappa(a) + 4\mu(a)} \right). \tag{6.21}$$

Similarly, in order to find $T(x)$ and $V(x)$, replace U with V in equation (6.20). The boundary conditions for this differential equation in V would be,

$$V(a) = 1 \qquad \text{and} \qquad V'(a) = -\frac{18}{5a} \left(\frac{\kappa(a) + 2\mu(a)}{3\kappa(a) + 4\mu(a)} \right). \tag{6.22}$$

6.3.1 Constant Bulk Modulus of the Interphase

Note that if we let $\kappa(x) = \kappa_g$ a constant, then it is not obvious how to obtain an integral form of the solution to the differential equation (6.20).

6.3.2 Constant Shear Modulus of the Interphase

If we let $\mu(x) = \mu_g$ a constant, then equation (6.20) becomes,

$$U''(x) + P_2(x)U'(x) = 0 \tag{6.23}$$

which when solved subject to the boundary conditions (6.21) gives,

$$U(x) = \frac{18a^3}{5\mu_g} \int_a^x \frac{\kappa(t) + 2\mu_g}{t^4(3\kappa(t) + 4\mu_g)}\, dt. \tag{6.24}$$

Substituting this solution for $U(x)$ into differential equation (6.18) gives,

$$S(x) = \frac{a^3}{x^3} + \frac{18a^3}{5} \int_a^x \frac{\kappa(t) + 2\mu_g}{t^4(3\kappa(t) + 4\mu_g)}\, dt. \tag{6.25}$$

Similarly, replacing U with V in (6.23) and solving it subject to the boundary conditions (6.22) gives,

$$V(x) = 1 - \frac{18a^3}{5} \int_a^x \frac{\kappa(t) + 2\mu_g}{t^4(3\kappa(t) + 4\mu_g)}\, dt \tag{6.26}$$

and

$$T(x) = \mu_g - \frac{a^3\mu_g}{x^3} - \frac{18a^3\mu_g}{5}\int_a^x \frac{\kappa(t)+2\mu_g}{t^4(3\kappa(t)+4\mu_g)}\,dt. \tag{6.27}$$

The functions (6.24)-(6.27) enable us to determine the effects of the variable bulk modulus of the interphase on the shear modulus of a composite. Note that only one integral needs to be solved which should be much easier than the original coupled system for a wide class of functions for $\kappa(x)$. Also, in order for these integrals to yield reasonable results for the shear modulus of a composite, an appropriate choice of the constant μ_g must be made. Given a variable shear modulus $\mu(x)$ for the interphase, we again approximate this function by the average value of the interphase taken from the rule of mixtures given by,

$$\mu_g = \frac{3}{(b^3-a^3)}\int_a^b x^2\mu(x)\,dx.$$

A Linear Profile for the Bulk Modulus of the Interphase

If we let $\kappa(x) = \alpha x + \beta$ be a linear function describing the inhomogeneous bulk modulus of the interphase, then the integral appearing in the functions (6.24)-(6.27) is given by,

$$\int_a^x \frac{\kappa(t)+2\mu_g}{t^4(3\kappa(t)+4\mu_g)}\,dt = \frac{3\alpha^2(3\gamma_1-\gamma_2)}{{\gamma_2}^3}\left(\frac{1}{a}-\frac{1}{x}\right) + \frac{\alpha(3\gamma_1-\gamma_2)}{2{\gamma_2}^2}\left(\frac{1}{x^2}-\frac{1}{a^2}\right) + \frac{\gamma_1}{3\gamma_2}\left(\frac{1}{a^3}-\frac{1}{x^3}\right) + \frac{9\alpha^3(3\gamma_1-\gamma_2)}{{\gamma_2}^4}\left\{\ln\left(\frac{a}{x}\right)+\ln\left(\frac{3\alpha t+\gamma_2}{3\alpha a+\gamma_2}\right)\right\}$$

where $\gamma_1 = \beta + 2\mu_g$ and $\gamma_2 = 3\beta + 4\mu_g$. Note, if $\gamma_2 = 0$ we have,

$$\int_a^x \frac{\kappa(t)+2\mu_g}{t^4(3\kappa(t)+4\mu_g)}\,dt = \frac{1}{9}\left(\frac{1}{a^3}-\frac{1}{x^3}\right) + \frac{\gamma_1}{12\alpha}\left(\frac{1}{a^4}-\frac{1}{x^4}\right)$$

The effective shear modulus, μ_E, of the inclusion and interphase is then given by expression (6.19).

6.4 Constant Poisson's Ratio of the Interphase

If for some function $f(x)$ we have $\kappa(x) = \kappa_m f(x)$ and $\mu(x) = \mu_m f(x)$, then the Poisson's ratio of the inhomogeneous interphase will be constant, equal to that of the matrix. Note that the subscript m stands for matrix. In such a situation, the coupled system given by equations (6.1) and (6.2) and similarly (6.17) and (6.18) become,

$$S'(x) = \frac{m_1}{x} S(x) + \frac{m_2}{x} f(x) U(x) \tag{6.28}$$

$$U'(x) = \frac{m_3}{x f(x)} S(x) + \frac{m_4}{x} U(x) \tag{6.29}$$

where for the bulk modulus case we have,

$$m_1^\kappa = -3\left(\frac{4\mu_m}{3\kappa_m + 4\mu_m}\right), \qquad m_2^\kappa = 3\left(\frac{4\kappa_m\mu_m}{3\kappa_m + 4\mu_m}\right),$$
$$m_3^\kappa = 3\left(\frac{3}{3\kappa_m + 4\mu_m}\right), \qquad m_4^\kappa = -3\left(\frac{3\kappa_m}{3\kappa_m + 4\mu_m}\right),$$

and for the shear modulus case we have,

$$m_1^\mu = -\frac{3}{5}\left(\frac{9\kappa_m + 8\mu_m}{3\kappa_m + 4\mu_m}\right), \qquad m_2^\mu = \frac{3\mu_m}{5}\left(\frac{9\kappa_m + 8\mu_m}{3\kappa_m + 4\mu_m}\right),$$
$$m_3^\mu = \frac{18}{5\mu_m}\left(\frac{\kappa_m + 2\mu_m}{3\kappa_m + 4\mu_m}\right), \qquad m_4^\mu = -\frac{18}{5}\left(\frac{\kappa_m + 2\mu_m}{3\kappa_m + 4\mu_m}\right).$$

It can be easily shown that for both cases, this coupled system converts to the following second order differential equation in $S(x)$;

$$S''(x) + \frac{1}{x}\left(4 - x\frac{f'(x)}{f(x)}\right) S'(x) + \frac{m_1^j}{x}\frac{f'(x)}{f(x)} S(x) = 0 \tag{6.30}$$

where $S(a) = 1$, $S'(a) = \frac{m_1^j}{a}$ and $j \in \{\kappa, \mu\}$.

Also, the conductivity of an inclusion and surrounding interphase is governed by a pair of differential equations that were derived in chapter 5. Converting this pair of equations into a second order differential equation in $S(x)$ gives,

$$S''(x) + \frac{1}{x}\left(4 - x\frac{\varepsilon'(x)}{\varepsilon(x)}\right)S'(x) - \frac{2}{x}\frac{\varepsilon'(x)}{\varepsilon(x)}S(x) = 0$$

where $S(a) = 1$, $S'(a) = -\frac{2}{a}$. If we set $m_1^\kappa = -2$, then this implies $\nu_m = 0$, where ν represents the Poisson's ratio. Therefore, for a composite which has an inhomogeneous interphase with Poisson's ratio equal to zero and also $\nu_m = 0$, then the conductivity problem is the same as the bulk modulus problem. This result was first discovered by Lutz and Zimmerman [42].

Also, if we set $m_1^\kappa = m_1^\mu$, then this implies $\nu_m = 0.2$. Therefore, for a composite which has an inhomogeneous interphase with Poisson's ratio equal to 0.2 and also $\nu_m = 0.2$, then the bulk modulus problem is the same as the shear modulus problem. It is however important to note that the solution for the shear modulus given here is an approximation only, since the differential equations given by (6.17) and (6.18) are based on the 2-phase Mori-Tanaka solution for the shear modulus.

6.4.1 An Exponential-Power Law Profile

Suppose the function $f(x)$ describing the properties of the interphase region varies according to,

$$f(x) = cx^P e^{\beta x}. \tag{6.31}$$

Such a function is more useful than the general power law profile described in [40], in that it enables us to control three different parameters, that is, c, P and β, thereby giving us a wider class of functions.

Substituting this function into differential equation (6.30) gives,

$$x^2S''(x) + x(4 - P - \beta x)S'(x) + m_1^j(P + \beta x)S(x) = 0. \tag{6.32}$$

The solution to equation (6.32) where $m_1^j = -2$ was derived in chapter 5 where we considered this same profile for the dielectric properties. For general values of m_1^j the solution procedure is the same, therefore we simply state here the solution which is given by,

$$S(x) = x^{\frac{1}{2}P+\lambda-\frac{3}{2}} e^{\frac{1}{2}(\mathrm{sign}(\beta)-1)|\beta|x} \Big\{ A\, M(\frac{1}{2}+\lambda-\omega, 1+2\lambda, |\beta|x) + B\, U(\frac{1}{2}+\lambda-\omega, 1+2\lambda, |\beta|x) \Big\}$$

where M and U are Kummer's functions which are defined by,

$$M(a,b,z) = \sum_{n=0}^{\infty} \frac{(a)_n z^n}{(b)_n n!}$$

and

$$U(a,b,z) = \frac{\pi}{\sin \pi b} \left\{ \frac{M(a,b,z)}{\Gamma(1+a-b)\Gamma(b)} - z^{1-b} \frac{M(1+a-b, 2-b, z)}{\Gamma(a)\Gamma(2-b)} \right\}.$$

Note that,

$$(a)_n = a(a+1)(a+2)\ldots(a+n-1), \qquad (a)_0 = 1,$$

and other special properties of the Kummer functions are described in [1].

The parameters ω and λ are given by,

$$\omega = \left(2 - \frac{P}{2} + m_1^j\right) \mathrm{sign}(\beta), \qquad \text{and} \qquad \lambda = \frac{1}{2}\sqrt{9 - 4\left(m_1^j + \frac{3}{2}\right)P + P^2}.$$

Note that it can be easily shown that λ is real for all values of m_1^j. Also A and B are arbitrary constants which can be found by using the boundary conditions, $S(a) = 1$ and $S'(a) = \frac{m_1^j}{a}$.

The solution for $U(x)$ is then found by rearranging equation (6.28). The constants A and B are given by,

$$A = \frac{\gamma_1 U_a^{(2)} - \gamma_2 U_a^{(1)}}{U_a^{(2)} M_a^{(1)} - U_a^{(1)} M_a^{(2)}} \qquad \text{and} \qquad B = \frac{\gamma_2 M_a^{(1)} - \gamma_1 M_a^{(2)}}{U_a^{(2)} M_a^{(1)} - U_a^{(1)} M_a^{(2)}}$$

where,

$$
\begin{aligned}
M_a^{(1)} &= M(\frac{1}{2}+\lambda-\omega, 1+2\lambda, |\beta|a),\\
U_a^{(1)} &= U(\frac{1}{2}+\lambda-\omega, 1+2\lambda, |\beta|a),\\
M_a^{(2)} &= \frac{\left(\frac{1}{2}+\lambda-\omega\right)}{(1+2\lambda)} M(\frac{3}{2}+\lambda-\omega, 2+2\lambda, |\beta|a),\\
U_a^{(2)} &= -\left(\frac{1}{2}+\lambda-\omega\right) U(\frac{3}{2}+\lambda-\omega, 2+2\lambda, |\beta|a),\\
\gamma_1 &= a^{-\frac{1}{2}P-\lambda+\frac{3}{2}} e^{-\frac{1}{2}(\mathrm{sign}(\beta)-1)|\beta|a},\\
\gamma_2 &= \frac{1}{|\beta|}\gamma_1 \left\{ -\frac{\left(\frac{1}{2}P+\lambda-\frac{3}{2}-m_1^j\right)}{a} - \frac{1}{2}(\mathrm{sign}(\beta)-1)|\beta| \right\}.
\end{aligned}
$$

The solution for $T(x)$ is given by,

$$
T(x) = x^{\frac{1}{2}P+\lambda-\frac{3}{2}} e^{\frac{1}{2}(\mathrm{sign}(\beta)-1)|\beta|x} \Big\{ C\, M(\frac{1}{2}+\lambda-\omega, 1+2\lambda, |\beta|x) + D\, U(\frac{1}{2}+\lambda-\omega, 1+2\lambda, |\beta|x) \Big\}
$$

and the solution for $V(x)$ is found from equation (6.28) after replacing S with T and U with V. The arbitrary constants C and D can be found by using the boundary conditions, $T(a) = 1$ and $T'(a) = \frac{m_2^j f(a)}{a}$, which give,

$$
C = \frac{U_a^{(1)}\gamma_3}{U_a^{(1)}M_a^{(2)} - U_a^{(2)}M_a^{(1)}}, \qquad D = \frac{-M_a^{(1)}\gamma_3}{U_a^{(1)}M_a^{(2)} - U_a^{(2)}M_a^{(1)}}
$$

where,

$$
\gamma_3 = \frac{m_2^j c}{|\beta|} a^{\frac{1}{2}P-\lambda+\frac{1}{2}} e^{\frac{1}{2}(\mathrm{sign}(\beta)+1)|\beta|a}.
$$

SiC	$\kappa_p = 247.47$	$\mu_p = 209.40$
Al	$\kappa_m = 66.96$	$\mu_m = 25.67$

Table 6.1: Properties of the constituent materials measured in GPa.

6.5 Results

The following results were computed for a composite containing spherical inclusions of silicon-carbide and 6061-T6 aluminium as the matrix phase. These properties are shown in Table 6.1 and are taken from Ding and Weng, [9]. Also the interphase thickness was assumed to be 10% of the radius of inclusion.

6.5.1 Results of Section 6.2.1.

Figure 6.1 shows the effects of the linear profile $\mu(x) = \alpha x + \beta$ on the bulk modulus of the composite as a function of the parameter α for various values of κ_g. The value of β was chosen such that the shear modulus matches at the boundary between interphase and matrix, that is, $\mu(b) = \mu_m$. The parameter α was chosen such that,

$$-\frac{\mu_p - \mu_m}{b - a} \leq \alpha \leq 0,$$

which ensures that at all points in the interphase, the shear modulus of the interphase always lies between the shear modulus of the inclusion and matrix. Note that κ_g was chosen such that $\kappa_m \leq \kappa_g \leq \kappa_p$.

Figure 6.1 shows that for larger values of κ_g, the bulk modulus of the composite does not change much with respect to α. However, as the value of κ_g approaches κ_m, the graph clearly shows a greater variation in the bulk modulus of the composite with respect to α.

For a specific value of $\alpha = -\frac{\mu_p - \mu_m}{b-a}$, figure 6.2 shows clearly the variation of the bulk modulus of the composite as a function of inclusion concentration for various values of κ_g.

For two distinct values of κ_g, figures 6.3 and 6.4 show the variation in the bulk modulus of the composite as a function of inclusion concentration for various values of α. The linear

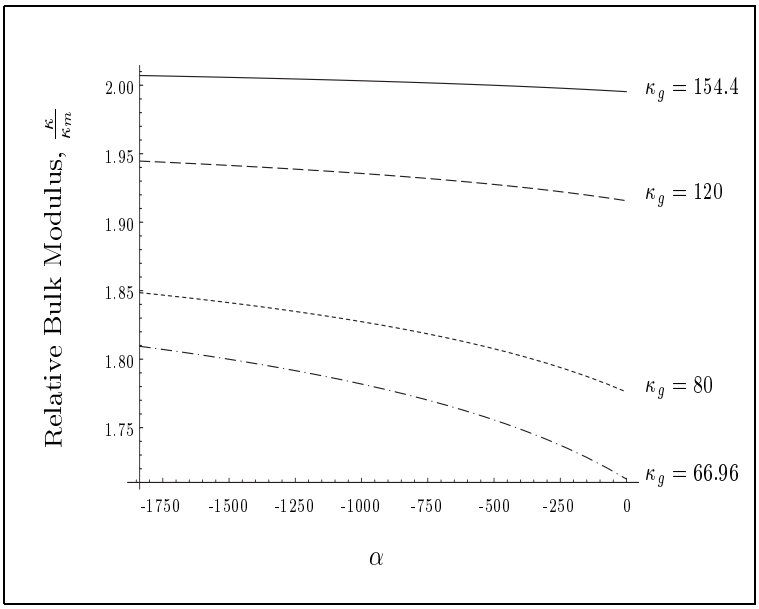

Figure 6.1: Relative bulk modulus of a composite as a function of α for various values of κ_g. The interphase profile was assumed to have a constant bulk modulus, κ_g and a linear shear modulus, $\mu(x) = \alpha x + \beta$. Note, the inclusion concentration was taken to be $d_0 = 0.5$.

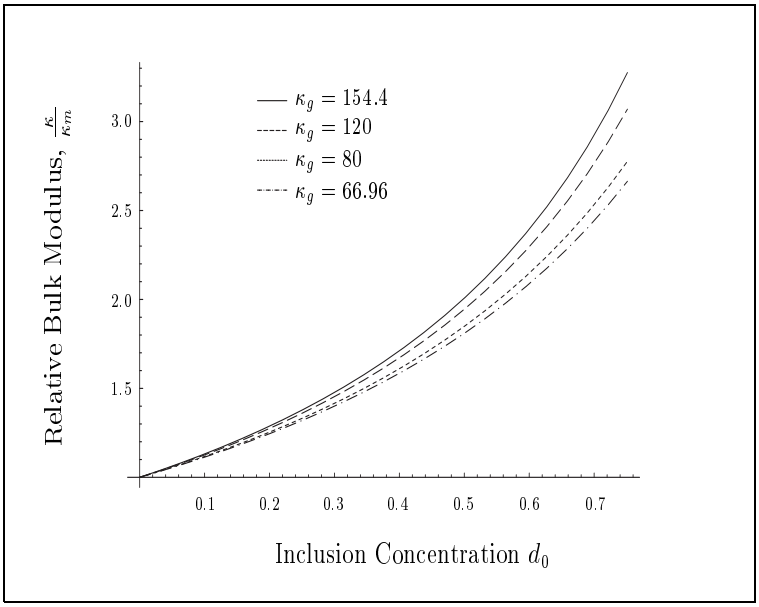

Figure 6.2: Relative bulk modulus of a composite as a function of inclusion concentration d_0 for various values of κ_g. Note that $\mu(x) = \alpha x + \beta$ and that $\alpha = -1837.3$.

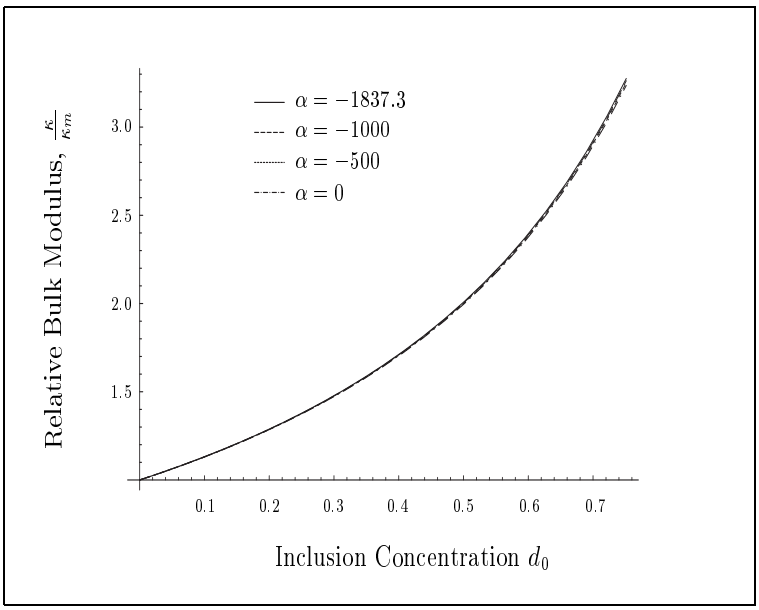

Figure 6.3: Relative bulk modulus of a composite as a function of inclusion concentration d_0 for various values of α. Note that $\mu(x) = \alpha x + \beta$ and that $\kappa_g = 154.4$.

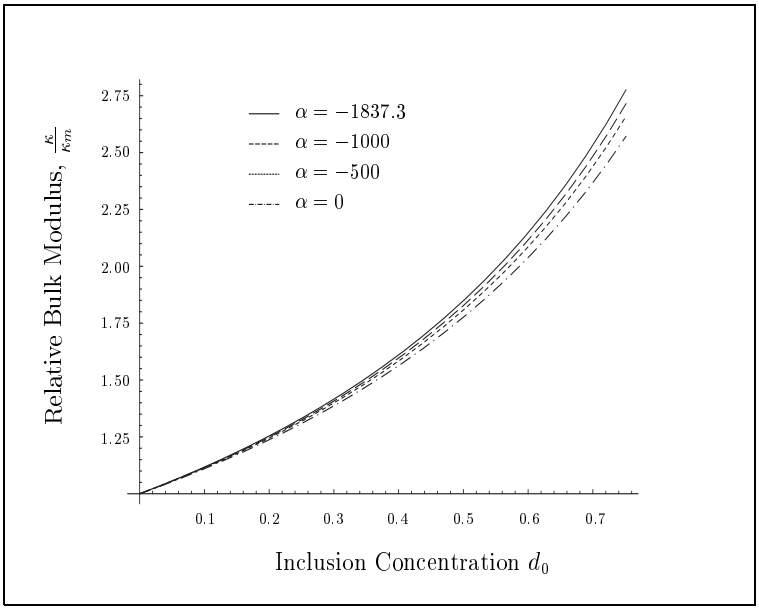

Figure 6.4: Relative bulk modulus of a composite as a function of inclusion concentration d_0 for various values of α. Note that $\mu(x) = \alpha x + \beta$ and that $\kappa_g = 80$.

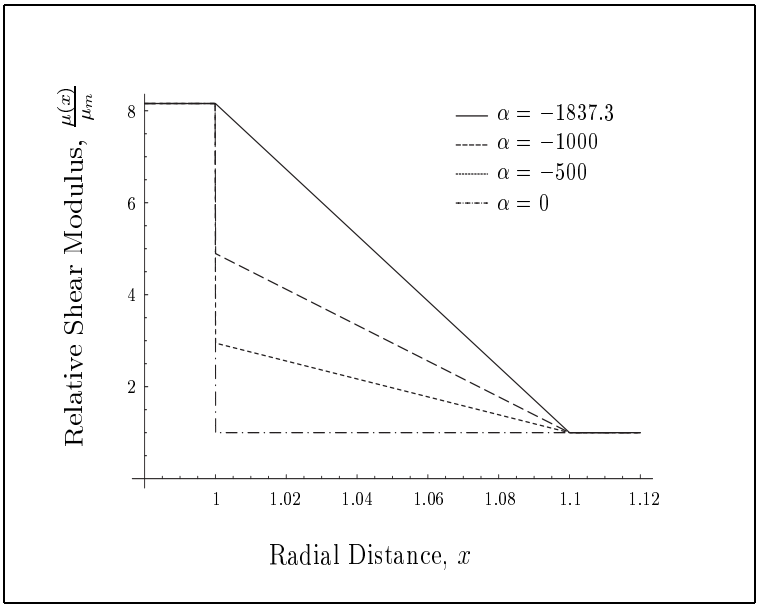

Figure 6.5: Relative shear modulus of the interphase region for various values of the parameter α.

profile of the shear modulus for these values of α are plotted in figure 6.5. From these two graphs it can be clearly seen that for $\kappa_g = 154.4$, a variation in the linear shear modulus of the interphase does not have much of an effect on the bulk modulus of the composite, whereas for $\kappa_g = 80$, a variation in the linear profile for the shear modulus does effect the bulk modulus of the composite. This effect seems consistent with the results plotted in figure 6.1. In figure 6.1 it was shown that there is a greater variation in the bulk modulus of the composite with respect to α as the value of κ_g approaches κ_m. Therefore, figures 6.3 and 6.4 support this fact.

6.5.2 Results of Section 6.2.2.

Figure 6.6 shows the effects of the linear profile $\kappa(x) = \alpha x + \beta$ on the bulk modulus of the composite as a function of the parameter α for various values of μ_g. Again, the value of β was chosen such that the bulk modulus matches at the boundary between interphase and matrix, that is, $\kappa(x) = \kappa_m$. The parameter α was chosen such that,

$$-\frac{\kappa_p - \kappa_m}{b-a} \leq \alpha < 0,$$

which ensures that at all points in the interphase, the bulk modulus of the interphase always lies between the bulk modulus of the inclusion and matrix. Note that μ_g was chosen such that $\mu_m \leq \mu_g \leq \mu_p$.

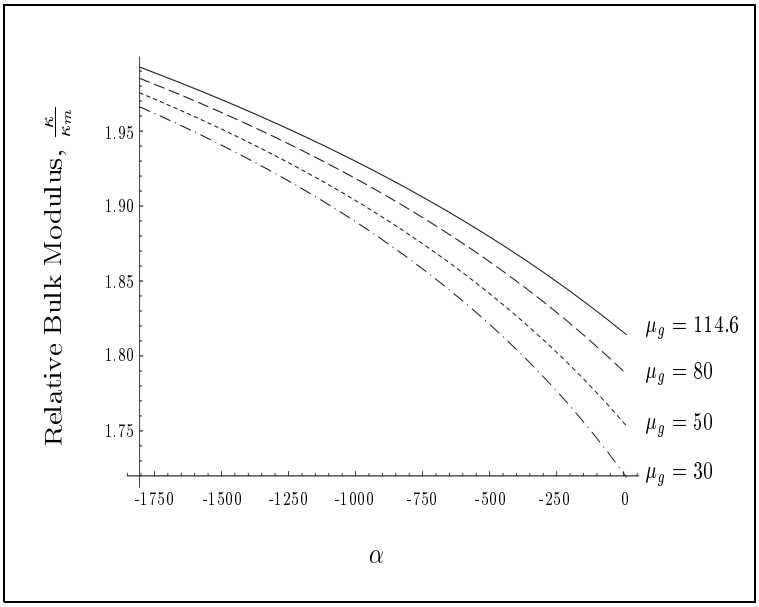

Figure 6.6: Relative bulk modulus of a composite as a function of α for various values of μ_g. The interphase profile was assumed to have a constant shear modulus, μ_g and a linear bulk modulus, $\kappa(x) = \alpha x + \beta$. Note, the inclusion concentration was taken to be $d_0 = 0.5$.

Figure 6.6 clearly shows that the bulk modulus of the composite changes significantly with respect to α for various values of μ_g.

For a specific value of $\alpha = -\frac{\kappa_p - \kappa_m}{b-a}$, figure 6.7 shows a small variation in the bulk modulus of the composite as a function of inclusion concentration for various values of μ_g. As the value of α is increased to $\alpha = -250$ as shown in figure 6.8, there is a greater variation in the bulk modulus of the composite for the same values of μ_g considered in figure 6.7. This result seems consistent from the graph shown in figure 6.6.

Figure 6.9 shows a clear difference in the variation of the bulk modulus of the composite

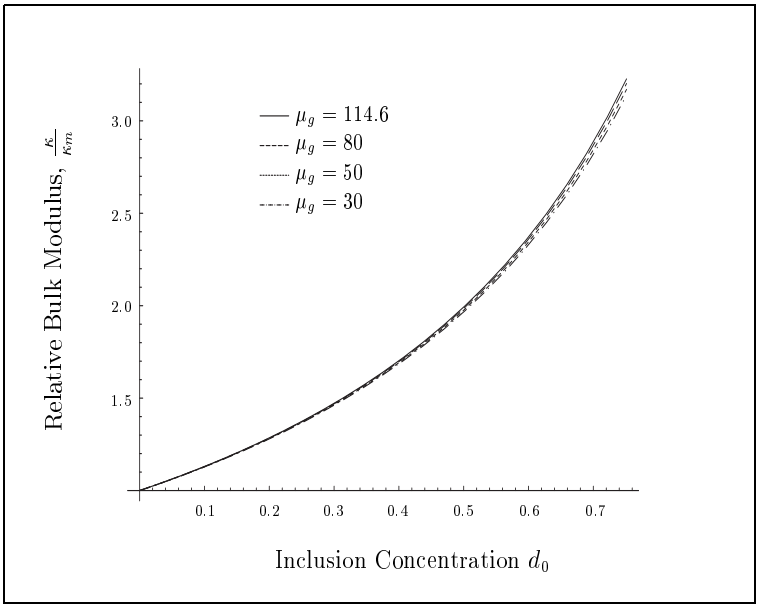

Figure 6.7: Relative bulk modulus of a composite as a function of inclusion concentration d_0 for various values of μ_g. Note that $\kappa(x) = \alpha x + \beta$ and that $\alpha = -1805.1$.

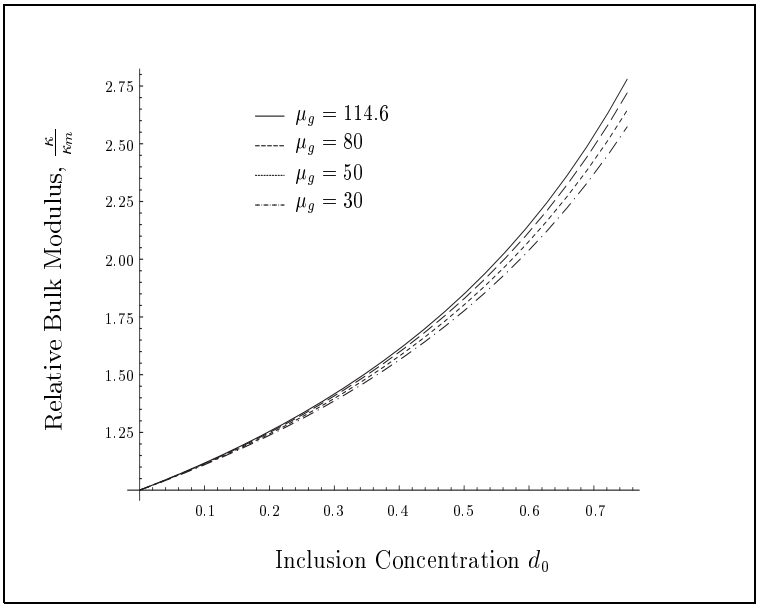

Figure 6.8: Relative bulk modulus of a composite as a function of inclusion concentration d_0 for various values of μ_g. Note that $\kappa(x) = \alpha x + \beta$ and that $\alpha = -250$.

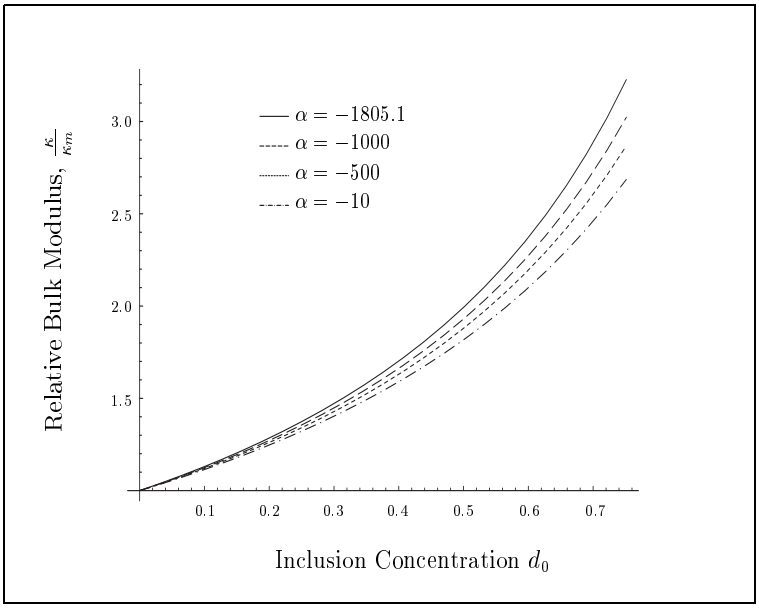

Figure 6.9: Relative bulk modulus of a composite as a function of inclusion concentration d_0 for various values of α. Note that $\kappa(x) = \alpha x + \beta$ and that $\mu_g = 114.6$.

in terms of the inclusion concentration for various values of α with $\mu_g = 114.6$. The linear profile of the bulk modulus of the interphase for these values of α are plotted in figure 6.10.

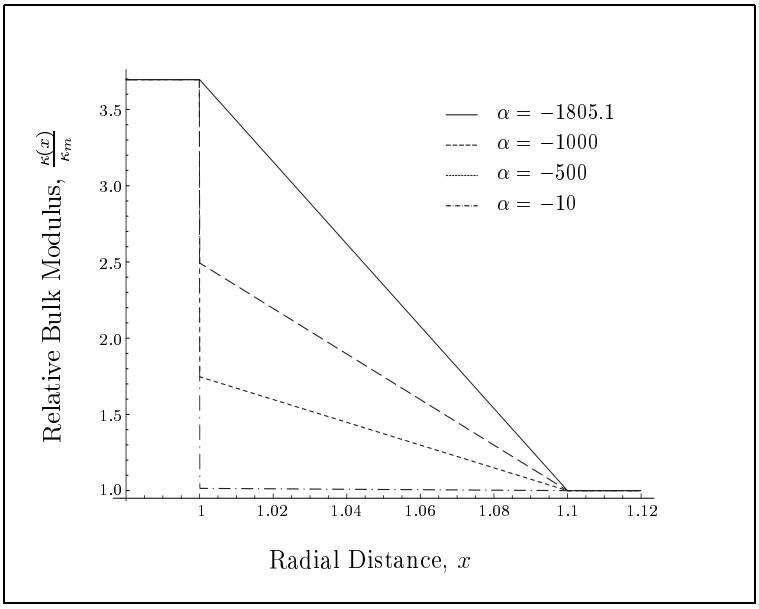

Figure 6.10: Relative bulk modulus of the interphase region for various values of the parameter α.

6.5.3 Results of Section 6.3.2.

Figure 6.11 shows the effects of the linear profile $\kappa(x) = \alpha x + \beta$ on the shear modulus of the composite as a function of the parameter α for various values of μ_g. Again, the value of β was chosen such that the bulk modulus matches at the boundary between interphase and matrix, that is, $\kappa(x) = \kappa_m$. The parameter α was chosen such that,

$$-\frac{\kappa_p - \kappa_m}{b - a} \leq \alpha < 0,$$

which ensures that at all points in the interphase, the bulk modulus of the interphase always lies between the bulk modulus of the inclusion and matrix. Note that μ_g was chosen such that $\mu_m \leq \mu_g \leq \mu_p$.

Note that the Mori-Tanaka solution for the shear modulus is not exact and therefore the differential equations represented by (6.17) and (6.18) do not give the exact solution to the shear modulus of an inclusion surrounded by an inhomogeneous interphase. However, under certain conditions, the shear modulus that is derived based on these equations is a rather good approximation to the actual solution. For example, see [60] and work done in

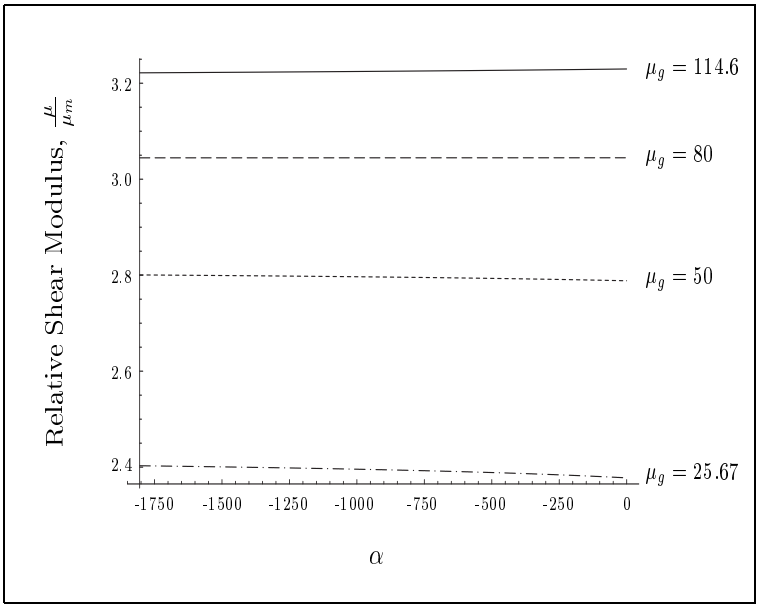

Figure 6.11: Relative shear modulus of the interphase region as a function of the parameter α for various values of μ_g.

chapter 3. For the linear variations considered in figure 6.12 and for the range of values considered for μ_g, the results for the shear modulus presented here are believed to be reasonably accurate. For different linear variations than those considered in figure 6.12, or for μ_g outside the range considered here, it may be an advantage to use the mapping method that is discussed in chapter 3 and in [39].

Figure 6.11 shows that there is no significant change in the shear modulus of the composite with respect to the parameter α for all the μ_g considered. Therefore, it appears that a linear variation in the bulk modulus has little effect on the shear modulus of the composite, provided that the linear variation are like those considered in figure 6.12. That is, the bulk modulus of the interphase varies linearly between inclusion and matrix and matches at the interphase/matrix interface. Figures 6.13 and 6.14 also support this fact since there does not seem to be much variation between the curves for different values of α, particularly in figure 6.13 where $\mu_g = 114.62$.

For a specific value of $\alpha = -\frac{\kappa_p - \kappa_m}{b-a}$, figure 6.15 shows a large variation in the shear modulus of the composite as a function of inclusion concentration for various values of

μ_g. Therefore, for the profiles considered, it appears that the parameter μ_g has a much larger influence on the shear modulus of the composite.

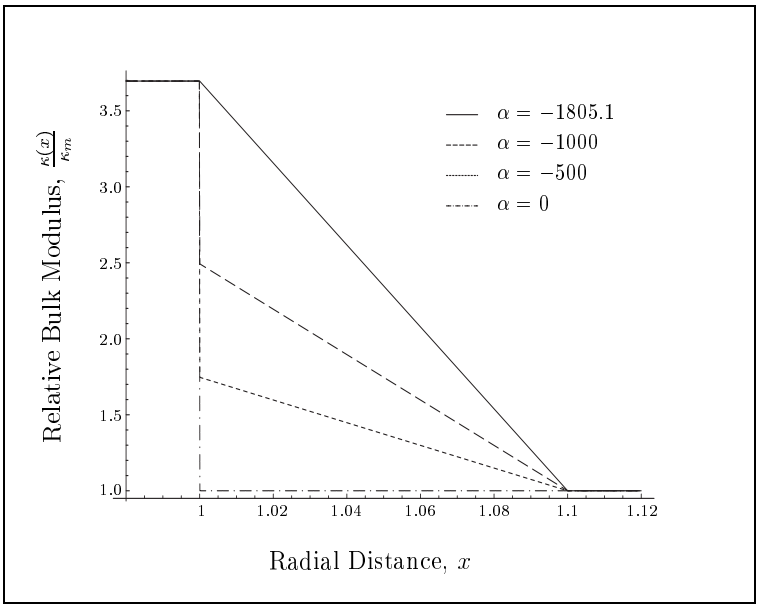

Figure 6.12: Relative bulk modulus of the interphase region as a function of the radial distance x.

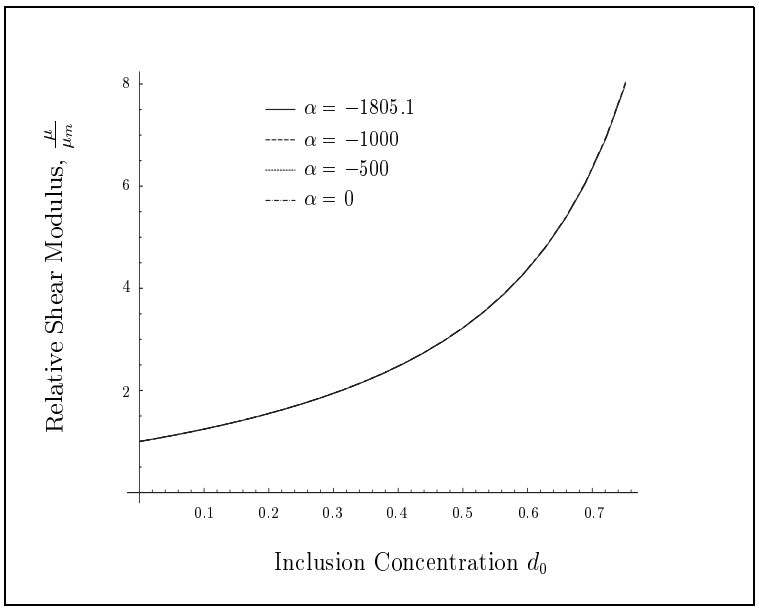

Figure 6.13: Relative shear modulus of the interphase region as a function of inclusion concentration for various values of the parameter α. Note $\mu_g = 114.62$.

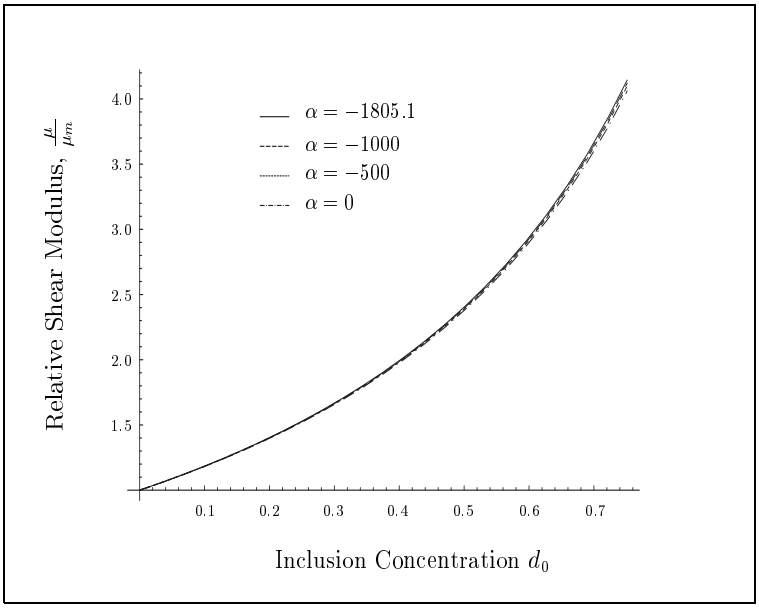

Figure 6.14: Relative shear modulus of the interphase region as a function of inclusion concentration for various values of the parameter α. Note $\mu_g = 25.67$.

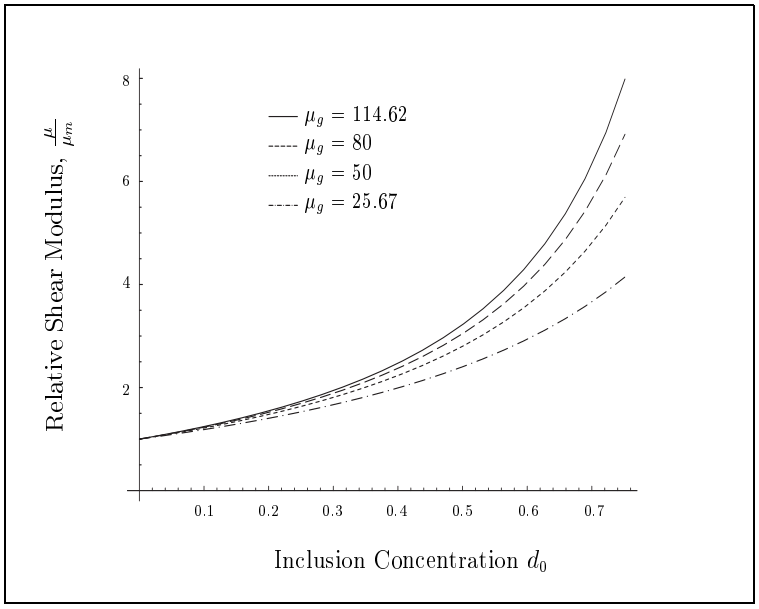

Figure 6.15: Relative shear modulus of the interphase region as a function of inclusion concentration for various values of the parameter μ_g. Note $\alpha = -1805.1$.

6.5.4 Results of Section 6.4.

The Bulk Modulus

For the power exponential profile, the parameters were chosen so that the bulk modulus of the interphase matches the inclusion at $x = a$ and the matrix at $x = b$. Some curves for the interphase are shown in figure 6.16 where the parameter P is allowed to vary.

The remaining parameters β and c are chosen so that we get the appropriate matching at the inclusion/interphase and interphase/matrix interface. Thus, the variation in the parameter P produces a variation in the curve which begins and ends at those two points. This is the advantage that the exponential/power law profile has over the general power law profile considered previously (see chapters 2, 3, 4). The disadvantage however of both of these profiles is that it is not possible to match at the inclusion/interphase and interphase/matrix interface for both the bulk and shear modulus at the same time. Therefore, since we are discussing the bulk modulus properties of the composite, it seems reasonable that we allow the interphase bulk modulus to match the inclusion at $x = a$ and the matrix at $x = b$ as opposed to the interphase shear modulus.

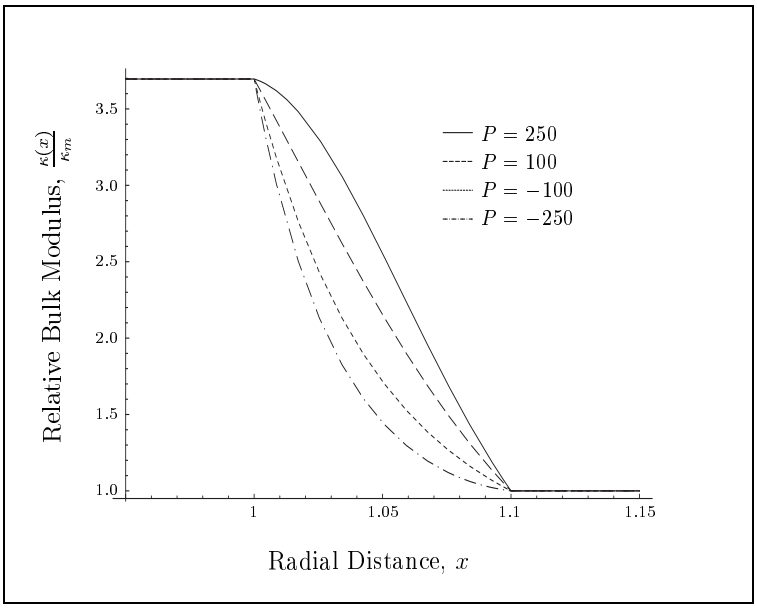

Figure 6.16: Relative bulk modulus of the interphase region as a function of the radial distance x, for different values of the parameter P in the power exponential profile.

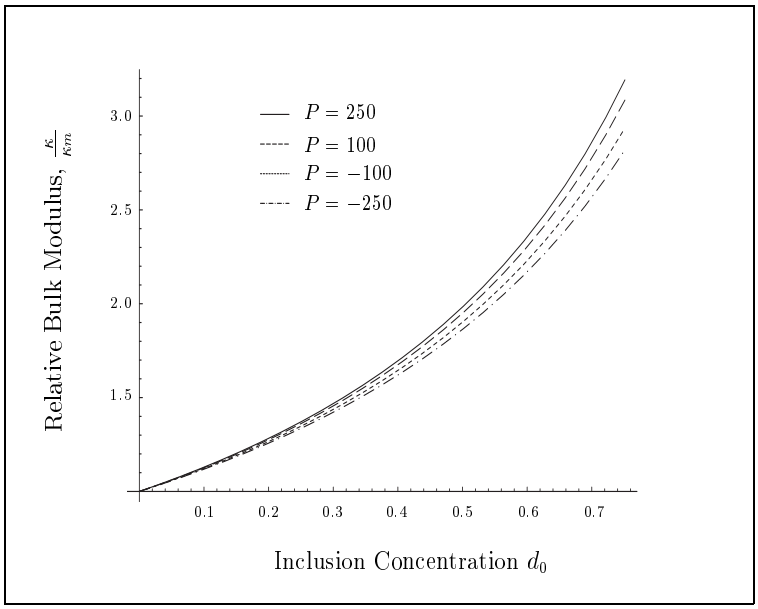

Figure 6.17: Relative bulk modulus of the composite as a function of inclusion concentration for different values of the parameter P.

The results of figure 6.17 show the curves for the relative bulk modulus as a function of inclusion concentration for those profiles considered in figure 6.16. The results show what we would expect to happen. For $P = -250$ which represents the softest interphase considered, the results of figure 6.17 show that the curve lies below each of the other curves. As the interphase gets harder for the different profiles considered, the results of figure 6.17 reflect the behavior that is expected, i.e. that bulk modulus increases.

The Shear Modulus

For the power exponential profile, the parameters were chosen so that the shear modulus of the interphase matches the inclusion at $x = a$ and the matrix at $x = b$. Some curves for the interphase are shown in figure 6.18 where the parameter P is allowed to vary.

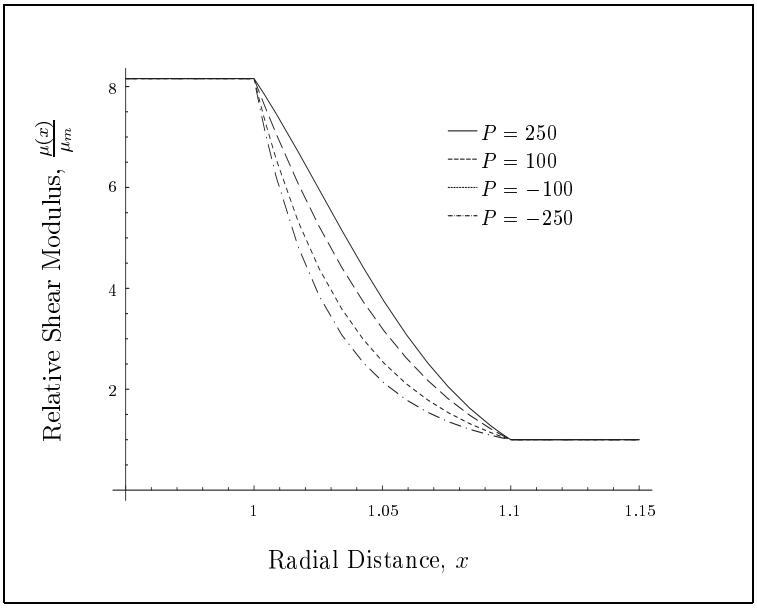

Figure 6.18: Relative shear modulus of the interphase region as a function of the radial distance x, for different values of the parameter P in the power exponential profile.

Note that since we are discussing the shear properties of the composite, it seems reasonable that we allow the interphase shear modulus to match the inclusion at $x = a$ and the matrix at $x = b$ as opposed to the interphase bulk modulus which we considered in the previous section.

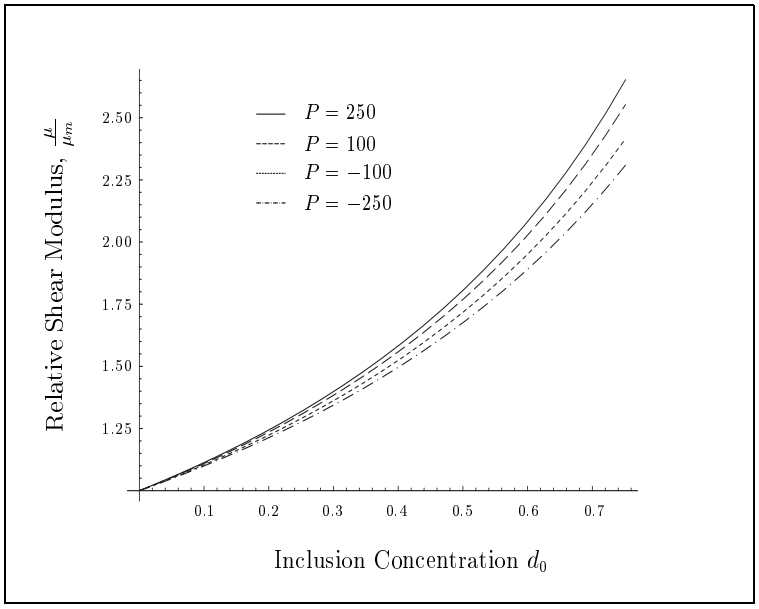

Figure 6.19: Relative shear modulus of the composite as a function of inclusion concentration for different values of the parameter P.

The results of figure 6.19 show the curves for the relative shear modulus as a function of inclusion concentration for those profiles considered in figure 6.18. The results again show what we would expect to happen. For $P = -250$ which represents the softest interphase considered, the results of figure 6.19 show that the curve lies below each of the other curves. As the interphase gets harder for the different profiles considered, the results of figure 6.19 reflect the behavior that is expected, i.e. that shear modulus increases.

Again, it is worth noting that for the profiles considered in figure 6.19, the results for the shear modulus presented here are believed to be reasonably accurate. For different profiles than those considered in figure 6.19 it may be an advantage to use the mapping method that is discussed in chapter 3.

6.6 Conclusion

In this chapter we have been able to utilize the results obtained in chapters 2 and 3 to obtain a general integral representation of the effective bulk or shear modulus of a particle inclusion surrounded by an inhomogeneous interphase. These results of course hold when either the bulk or shear modulus of the interphase is held constant. We were unable to determine an integral representation for the shear modulus of a composite where the bulk modulus of the interphase is held constant. For all other cases we were able to use these integral representations to account for a linear variation in the property of the interphase. The results showed the effects of the linear variation of one of the property profiles while the other is held constant. The case where both the bulk and shear modulus of the interphase both vary linearly was not considered and may be useful in obtaining greater insight into the nature of the role of a linearly varying interphase. This case may be considered in the future.

The effect of a constant Poisson's ratio on the governing differential equations for the bulk and shear modulus was also examined. It was shown that for a constant Poisson's ratio of the interphase equal to zero and also $\nu_m = 0$, the bulk modulus problem is the same as the conductivity problem given in chapter 5, which is the same result obtained originally by Lutz and Zimmerman [42]. Also if we set $\nu_i = \nu_m = 0.2$ it was shown that the bulk modulus problem is the same as the shear modulus problem given the differential equations stated in this work.

For a power-exponential profile, a solution for the bulk and shear modulus of the effective particle consisting of inclusion and interphase is obtained in terms of Kummer functions. Results were plotted for various values of the profile parameters and showed a clear distinction between them.

Chapter 7

Conclusion

7.1 Summary of the Research Presented

It has been demonstrated using the replacement method how to use 2-phase results to account for an inhomogeneous interphase region surrounding each spherical inclusion. We were able to do this for the bulk and shear modulus, the thermal expansion coefficient as well as the conductivity properties of composites consisting of a matrix phase with spherical inclusions embedded within it.

It was found that the results for the bulk modulus are exact since the 2-phase result that was utilised is exact for the bulk modulus case. For the shear modulus however, the 2-phase result that was used to account for the interphase was the Mori-Tanaka solution which is not exact. Therefore, the differential equations that were derived for the shear modulus are not exact, however, it has been shown by reference to the results of Shen and Li [60] that these differential equations are accurate for certain profiles of the inhomogeneous interphase. It was revealed by Shen and Li [60] using finite element computations, that when the inhomogeneous properties vary between those of the inclusion and matrix, that the differential equations obtained give accurate results with minimal error. However, for profiles outside this region, Shen and Li [60] revealed that the errors were large. Therefore, to account for these profiles, a technique was employed whereby the inhomogeneous interphase was mapped onto an equivalent homogeneous interphase. Once the equivalent homogeneous property was determined, the modified Generalised Self

Consistent Method was employed, which is exact for the shear modulus. It was shown that this technique improved the accuracy of the results for such profiles, however, how much the accuracy was improved was not investigated. Shen and Li [61] in a follow-up paper however, have also employed the same technique and proved that for such profiles, the accuracy of the results were dramatically improved. This seems like a very useful result since the shear modulus case is very hard to solve for inhomogeneous interphases and consequently, there are very few simple models which can accurately predict the shear properties.

The results for the thermal expansion coefficient are exact since the 2-phase result is exact for this property. The results showed that the thermal expansion coefficient also depends on the mechanical properties, that is, the bulk and shear modulus of the interphase region.

Results for the dielectric property of an inclusion surrounded by an inhomogeneous interphase were obtained using the Maxwell-Garnett mixing rule. It was shown that the differential equations obtained are the same as that obtained using differential effective dipole approximation (DEDA) or the Tartar Formula. Therefore, the same result emerges from three different variations and is exact for a dilute suspension of spheres in a matrix. One of the assumptions of the model is that the interphase regions cannot overlap. Therefore, full volume fraction packing of inclusions is not allowed. This is also the case with the other properties. However, by utilising a reverse mapping technique similar to that used for the shear modulus, it is possible to determine the equivalent property of the homogeneous interphase. By using this homogeneous property along with the model of Vo and Shi [74], full volume fraction packing may be assumed. This is due to the fact that the Vo and Shi model adjusts the size of the interphase as the volume fraction changes. The results for a few different profiles were compared to experimental data where the parameters were adjusted to fit the data. In order to accurately predict the properties of a composite, knowledge of the behavior of the interphase is important. Alternatively, if one knows the property of the resulting composite from experimental data, then these results may be used to determine the quantitative properties of the interphase.

The final chapter produced some miscellaneous results. In it we examined the effects

on the bulk and shear modulus of composites if one of the interphase properties is held constant. For example, an integral representation for the bulk modulus was determined for the case where the bulk modulus of the interphase was constant and the shear modulus was allowed to vary and vice versa. Also, an integral representation of the shear modulus was obtained only for the case where the shear modulus is held constant and bulk modulus is allowed to vary. Also, the case of a constant Poisson's ratio was analysed. It was shown that if the Poisson's ratio of the interphase is zero and equal to that of the matrix, then the bulk modulus problem is the same as the conductivity problem. This result it seems was first discovered by Lutz and Zimmerman [42].

7.2 Original Contributions Made

It would be also worthwhile to discuss the original contributions that the research presented in this thesis has made to knowledge in the field of composite science. To categorically state the contributions made without mentioning the work of other researchers does not seem fair, so these contributions shall be discussed chapter by chapter in the context of work done by some of the other researchers in the field.

The work on the bulk modulus in chapter 2, gives an in depth description of the model used throughout the thesis. This model represents the limiting case of an n-layered inclusion which resulted in a coupled pair of first order differential equations which model the bulk modulus directly. At about the same time as these results emerged, Shen and Li [60] also derived a first order non-linear differential equation by adding layers of infinitesimal thickness to a spherical inclusion or fibre using the replacement method. It can be easily shown that the differential equations derived in chapter 2 can be used to derive the differential equation of Shen and Li. This seems reasonable to expect since the underlying structure of these models is the same. As shown by Shen and Li [60], this approach can also be used to model fibres. The differential equations derived for particles by Lombardo [40] and those derived for both particles and fibres by Shen and Li [60], also model the bulk modulus directly as opposed to solving the equilibrium equations for the displacement after a far field stress is applied, as proposed by some authors.

Much of the work done on the shear modulus in chapter 3 follows from the work done on the bulk modulus. A coupled pair of differential equations were derived which also coincide with the differential equation of Shen and Li [60] for the shear modulus as expected. A reverse mapping was utilised in order to find the bulk and shear properties of the equivalent homogeneous interphase. These properties were used in the Generalized Self Consistent Method which was originally developed by Christensen and Lo [8] and then by Theocaris [68] who incorporated a homogeneous interphase. This reverse mapping was also utilised independently by Shen and Li [61] who used a slightly different approach. The reverse mapping proposed makes improvements on the model for the shear modulus for certain interphase regions as discussed in the body of the thesis. The overall approach that was presented for the shear modulus is simple to implement in comparison to some existing models which incorporate an inhomogeneous interphase.

The work on the thermal expansion properties in chapter 4 also utilises the replacement scheme and makes use of the results on the bulk modulus. This approach to the thermal problem does not appear to have been done before and offers a way of measuring the effect that the elastic properties of an inhomogeneous interphase have on the CTE. The results are shown to be consistent with experiment and hence offer a new approach to modeling the CTE of a particle with a surrounding inhomogeneous interphase.

The dielectric constant was modeled in chapter 5. A new derivation was presented and the resulting differential equation was shown to be the same as some of the other derivations [45, 82]. It was also shown how a reverse mapping may be utilised to find the property of the equivalent homogeneous interphase. This reverse mapping is similar to that used for the shear modulus and is useful because once the equivalent homogeneous property is found, other models may be used in conjunction with the inhomogeneous interphase model. Specifically, Vo and Shi's model [74] which assumes a homogeneous interphase was utilised in conjunction with the inhomogeneous interphase model to provide new insight into the effect of the interphase on the overall dielectric properties of composites. The combining of these two models via the reverse mapping seems as though it was presented for the first time in the paper by Lombardo [38] and in this thesis.

The work in chapter 6 considers some simplifying cases for the bulk and shear problems,

for example, what effect does keeping either the bulk or shear modulus of the interphase as a constant (and allowing the other property to vary), have on the overall elastic properties of composite materials? Such questions were first considered by Ding and Weng [9] who modeled them using differential equations. However, some nice closed form solutions in terms of integrals were presented in this chapter which also model these scenarios and which are perhaps easier to implement. A result presented by Lutz and Zimmerman [42] comparing the bulk modulus and conductivity problems was also verified in this chapter from a different perspective.

Bibliography

[1] M. Abramowitz and Stegun I.A. *Handbook of Mathematical Functions*. Dover Publications, Inc., New York, 1965.

[2] Y. Benveniste. A new approach to the application of mori-tanaka's theory in composite materials. *Mechanics of Materials*, 6:147–157, 1987.

[3] L. Brand. *Differential and Difference Equations*. John Wiley & Sons , Inc., New York, 1966.

[4] D. Brune and J. Bicerano. Micromechanics of nanocomposites: comparison of tensile and compressive elastic moduli, and prediction of effects of incomplete exfoliation and imperfect alignment on modulus. *Polymer*, 43:369–387, 2002.

[5] M Chaturvedi and Y.-L. Shen. Thermal expansion of particle-filled plastic encapsulant: a micromechanical characterization. *Acta mater*, 46(12):4287–4302, 1998.

[6] T. Chen, G.J. Dvorak, and Y. Benveniste. Mori-tanaka estimates of the overall elastic moduli of certain composite materials. *Journal of Applied Mechanics*, 59:539–546, 1992.

[7] R.M. Christensen. A critical evaluation for a class of micromechanics models. *Journal of the Mechanics and Physics of Solids*, 38:379–404, 1990.

[8] R.M. Christensen and K.H. Lo. Solutions for the effective shear properties in three phase sphere and cylinder models. *Journal of the Mechanics and Physics of Solids*, 27:315–330, 1979.

[9] K. Ding and G.J. Weng. The influence of moduli slope of a linearly graded matrix on the bulk moduli of some particle- and fiber-reinforced composites. *Journal of Elasticity*, 53:1–22, 1999.

[10] L. Dong, G. Q. Gu, and K. W. Yu. First principles approach to dielectric response of graded spherical particles. *Physics Letters B*, 67:224205, 2003.

[11] J.D. Eshelby. The determination of the elastic field of an ellipsoidal inclusion and related problems. *Proceedings of the Royal Society of London*, A241:376–396, 1957.

[12] F.T. Fisher and L.C. Brinson. Viscoelastic interphases in polymer-matrix composites: theoretical models and finite-element analysis. *Composites Science and Technology*, 61:731–748, 2001.

[13] T.D. Fornes and D.R. Paul. Modeling properties of nylon 6/clay nanocomposites using composite theories. *Polymer*, 44:4993–5013, 2003.

[14] E.J. Garboczi and J.G. Berryman. Elastic moduli of a material containing composite inclusions: effective medium theory and finite element computations. *Mechanics of Materials*, 33:455–470, 2001.

[15] Z. Hashin. The elastic moduli of heterogeneous materials. *Journal of Applied Mechanics*, 29:143–150, 1962.

[16] Z. Hashin. Analysis of composite materials. *Journal of Applied Mechanics*, 50:481–505, 1983.

[17] Z. Hashin. Thermoelastic properties of particulate composites with imperfect interface. *Journal of the Mechanics and Physics of Solids*, 39:745–762, 1991.

[18] Z. Hashin. Thin interphase/imperfect interface in conduction. *Journal of Applied Physics*, 89(4):2261–2267, 2001.

[19] Z. Hashin and S. Shritkman. A variational approach to the theory of the elastic behaviour of multiphase materials. *Journal of the Mechanics and Physics of Solids*, 11:127–140, 1963.

[20] E. Herve. Thermal and thermoelastic behaviour of multiply coated inclusion-reinforced composites. *International Journal of Solids and Structures*, 39:1041–1058, 2002.

[21] E. Herve and A. Zaoui. n-layered inclusion based micromechanical modelling. *International Journal of Engineering and Science*, 31:1–10, 1993.

[22] R. HIll. Theory of mechanical properties of fibre-strengthened materials: I. elastic behaviour. *Journal of the Mechanics and Physics of Solids*, 12:199–212, 1964.

[23] L. Holliday and J. Robinson. Review: The thermal expansion of composites based on polymers. *Journal of Materials Science*, 8:301–311, 1973.

[24] S. Iijima. Helical microtubules of graphitic carbon. *Nature*, 354:56–58, 1991.

[25] I. Jasiuk and M.W. Kouider. The effect of an inhomogeneous interphase on the elastic constants of transversely isotropic composites. *Mechanics of Materials*, 15:53–63, 1993.

[26] K. Jayaraman and K.L. Reifsnider. Residual stresses in a composite with continuously varying young's modulus in the fiber/matrix interphase. *Journal of Composite Materials*, 26:770–791, 1992.

[27] K. Jayaraman, K.L. Reifsnider, and R.E. Swain. Elastic and thermal effects in the interphase: Part 1. comments on characterization methods. *Journal of Composites Technology and Research*, 15(1):3–13, 1993.

[28] K. Jayaraman, K.L. Reifsnider, and R.E. Swain. Elastic and thermal effects in the interphase: Part 1. comments on modeling studies. *Journal of Composites Technology and Research*, 15(1):14–22, 1993.

[29] P.A. Kakavas, N.K. Anifantis, and G.C. Papanicolaou. The role of imperfect adhesion on thermal expansivities of transversely isotropic composites with an inhomogeneous interphase. *Composites Part A*, 29A:1021–1026, 1998.

[30] E.H. Kerner. The elastic and thermo-elastic properties of composite media. *Proceedings of the Physical Society of London*, 69B:808–813, 1956.

[31] L.D. Landau and E.M. Lifshitz. *Theory of Elasticity*. Pergamon Press, Oxford, 1986.

[32] J.J. Lesko, K. Jayaraman, and K.L. Reifsnider. Gradient interphase regions in composite systems. *Key Engineering Materials*, 116-117:61–86, 1996.

[33] V.M. Levin. Thermal expansion coefficients of heterogeneous materials. *Mekhanika Tverdogo Tela*, 2:88–94, 1967.

[34] Y.S. Lipatov. *Polymer Reinforcement*. ChemTex Publishing, Ontario, 1995.

[35] Y.J. Liu and X.L. Chen. Continuum models of carbon nanotube-base composites using the boundary element method. *Electronic Journal of Boundary Elements*, 1(2):316–335, 2003.

[36] Y.J. Liu and X.L. Chen. Evaluations of the effective material properties of carbon nanotube-based composites using a nanoscale representative volume element. *Mechanics of Materials*, 35:69–81, 2003.

[37] N. Lombardo. Effect of an inhomogeneous interphase on the thermal expansion coefficient of a particulate composite. *Composites Science and Technology*, 65:2118–2128, 2005.

[38] N. Lombardo. A two-way particle mapping for calculation of the effective dielectric response of graded spherical composites. *Composites Science and Technology*, to appear.

[39] N. Lombardo. A two-way particle mapping for calculation of the shear modulus of a spherical inclusion composite with inhomogeneous interphase. *The ANZIAM Journal*, to appear.

[40] N. Lombardo and Y. Ding. Effect of inhomogeneous interphase on the bulk modulus of a composite containing spherical inclusions. *Proceedings of the 4th Austalasian Congress on Applied Mechanics*, pages 523–529, 2005.

[41] M.P. Lutz and R.W. Zimmerman. Effect of the interphase zone on the bulk modulus of a particulate composite. *Journal of Applied Mechanics*, 63:855–861, 1996.

[42] M.P. Lutz and R.W. Zimmerman. Effect of an inhomogeneous interphase zone on the bulk modulus and conductivity of a particulate composite. *International Journal of Solids and Structures*, 42:429–437, 2005.

[43] J.C. Maxwell-Garnett. Colours in metal glasses and in metallic films. *Philosophical Transactions of the Royal Society of London*, A 203:385–420, 1904.

[44] D.S. McLachlan, M. Blaszkiewicz, and R.E. Newnham. Electrical resistivity of composites. *Journal of the American Ceramic Society*, 73(8):2187–2203, 1990.

[45] G. W. Milton. *The Theory of Composites*. Cambridge University Press, 2002.

[46] T. Mori and K. Tanaka. Average stress in matrix and average elastic energy of materials with misfitting inclusions. *Acta Metallurgica*, 21:571–574, 1973.

[47] T. Mura. *Micromechanics of Defects in Solids*. Kluwer, Boston, 1982.

[48] G.M. Odegard, T.C. Clancy, and T.S. Gates. Modeling of the mechanical properties of nanoparticle/polymer composites. *Polymer 46*, pages 553–562, 2005.

[49] G.M. Odegard, T.S. Gates, L.M. Nicholson, and K.E. Wise. Equivalent-continuum modeling of nano-structured materials. *Composites Science and Technology*, 62:1869–1880, 2002.

[50] G.M. Odegard, T.S. Gates, K.E. Wise, C. Park, and E.J. Siochi. Constitutive modeling of nanotube-reinforced polymer composites. *Composites Science and Technology*, 63:1671–1687, 2003.

[51] M.S. Ozmusul and R.C. Picu. Elastic moduli of particulate composites with graded filler-matrix interfaces. *Polymer Composites*, 23(1):110–119, 2002.

[52] Y.P. Qiu and G.J. Weng. Elastic moduli of thickly coated particle and fiber reinforced composites. *Journal of Applied Mechanics*, 58:388–395, 1991.

[53] Y. Rao, J. Qu, and T. Marinis. A precise numerical prediction of effective dielectric constant for polymer-ceramic composite based on effective-medium theory. *IEEE Transactions on Components and Packaging Technologies*, 23(4):680–683, 2000.

[54] K.L. Reifsnider. Modelling of the interphase in polymer-matrix composite material systems. *Composites*, 25(7):461–469, 1994.

[55] W.B. Rosen and Z. Hashin. Effective thermal expansion coefficients and specific heats of composite materials. *International Journal of Engineering and Science*, 8:157–173, 1970.

[56] Z-F. Sang and Z-Y. Li. Interfacial effect on effective dielectric response of spherical granular composites. *Physics Letters A*, 331:125–131, 2004.

[57] Z-F. Sang and Z-Y. Li. Partial resonant response of composites containing coated particles with graded shells. *Physics Letters A*, 332:376–381, 2004.

[58] K.P. Sau, T.K. Chaki, and D. Khastgir. The change in conductivity of a rubber-carbon black composite subjected to different modes of pre-strain. *Composites Part A*, 29A:363–370, 1998.

[59] R.A. Schapery. Thermal expansion coefficients of composite materials based on energy principles. *Journal of Composite Materials*, 2:380–404, 1968.

[60] L. Shen and J. Li. Effective elastic moduli of composites reinforced by particle or fiber with an inhomogeneous interphase. *International Journal of Solids and Structures*, 40:1393–1409, 2003.

[61] L. Shen and J. Li. Homogenization of a fibre/sphere with an inhomogeneous interphase for the effective elastic moduli of composites. *Proceedings of the Royal Society A*, 461:1475–1504, 2005.

[62] E. Sideridis. Thermal expansion coefficients of fiber composites defined by the concept of the interphase. *Composites Science and Technology*, 51:301–317, 1994.

[63] E. Sideridis and G.C. Papanicolaou. A theoretical model for the prediction of thermal expansion behaviour of particulate composites. *Rheologica Acta*, 27:608–616, 1988.

[64] E. Sideridis, P.S. Theocaris, and G.C. Papanicolaou. The elastic modulus of particulate composites using the concept of mesophase. *Rheologica Acta*, 25:350–358, 1986.

[65] J.S. Smith, D. Bedrov, and G.D. Smith. A molecular dynamics simulation study of nanoparticle interactions in a model polymer-nanoparticle composite. *Composites Science and Technology*, 63:1599–1605, 2003.

[66] H. Tang, X. Chen, A. Tang, and Y. Luo. Studies on the electrical conductivity of carbon black filled polymers. *Journal of Applied Polymer Science*, 59(3):383–387, 1996.

[67] P.S. Theocaris. The unfolding model for the representation of the mesophase layer in composites. *Journal of Applied Polymer Science*, 30:621–645, 1985.

[68] P.S. Theocaris. The exact shear modulus of particulates based on the concept of mesophase. *Colloid and Polymer Science*, 268(12):1118–1130, 1990.

[69] P.S. Theocaris and G.D. Spathis. Glass-transition behaviour of particle composites modeled on the concept of interphase. *Journal of Applied Polymer Science*, 27:3019–3025, 1982.

[70] P.S. Theocaris and A.G. Varias. Thermal expansion properties of particulates based on the concept of mesophase. *Journal of Applied Polymer Science*, 30:2979–2995, 1985.

[71] M.G. Todd and F.G. Shi. Validation of a novel dielectric constant simulation model and the determination of its physical parameters. *Microelectronics Journal*, 33:627–632, 2002.

[72] G. Vörös and B. Pukánszky. Effect of a soft interlayer with changing properties on the stress distribution around inclusions and yielding of composites. *Composites: Part A*, 32:343–352, 2001.

[73] G. Vörös and B. Pukánszky. Prediction of the yield stress of composites containing particles with an interlayer of changing properties. *Composites: Part A*, 33:1317–1322, 2002.

[74] H.T. Vo and F.G. Shi. Towards model-based engineering of optoelectronic packaging materials: dielectric constant modeling. *Microelectronics Journal*, 33:409–415, 2002.

[75] W. Wang and I. Jasiuk. Effective elastic constants of particulate composites with inhomogeneous interphases. *Journal of Composite Materials*, 32(15):1391–1424, 1998.

[76] E-B. Wei and S-P. Tang. Dielectric responses of graded cylindrical composites. *Physics Letters A*, 328:395–399, 2004.

[77] G.J. Weng. Some elastic properties of reinforced solids, with special reference to isotropic ones containing spherical inclusions. *International Journal of Engineering and Science*, 22:845–856, 1984.

[78] G.J. Weng. Effective bulk moduli of two functionally graded composites. *Acta Mechanica*, 166:57–67, 2003.

[79] Y.M. Wu, Z.P. Huang, Y. Zhong, and J. Wang. Effective moduli of particle-filled composite with inhomogeneous interphase: Part i-bounds. *Composites Science and Technology*, 64:1345–1351, 2004.

[80] Q. Xue. Effective-medium theory for two-phase random composites with an interfacial shell. *Journal of Materials Science and Technology*, 16(4):367–369, 2000.

[81] K. W. Yu and G. Q. Gu. Effective conductivity of composites of graded spherical particles. *Physics Letters A*, 345:448–452, 2005.

[82] K.W. Yu, G.Q. Gu, and J.P. Huang. Dielectric response of spherical particles of graded materials. *Cond-Mat*, 0211532, 2003.

[83] X. Zhang, Y. Pan, Q. Zheng, and X Yi. Time dependence of piezoresistance for the conductor-filled polymer composites. *Journal of Applied Polymer Science: Part B: Polymer Physics*, 38:2739–2749, 2000.

[84] Y.H. Zhao and G.J. Weng. Effective elastic moduli of ribbon-reinforced composites. *Journal of Applied Mechanics*, 57:158–167, 1990.

[85] Y. Zhong, J. Wang, Y. Ming Wu, and Z.P. Huang. Effective moduli of particle-filled composite with inhomogeneous interphase: Part ii-mapping method and evaluation. *Composites Science and Technology*, 64:1353–1362, 2004.

Appendix A

Stress and Strain Components of a Particulate Composite when Subjected to Simple Shear

A.1 Introduction

We give here the stress and strain components of a particulate composite in each of the phases when subjected to simple shear as described in chapter 3.

In spherical polar coordinates, the strain components according to Landau and Lifshitz [31], are given by,

$$\varepsilon_{rr} = \frac{\partial u_r}{\partial r}, \qquad \varepsilon_{\theta\theta} = \frac{1}{r}\frac{\partial u_\theta}{\partial \theta} + \frac{u_r}{r}, \qquad \varepsilon_{\phi\phi} = \frac{1}{r\sin\theta}\frac{\partial u_\phi}{\partial \phi} + \frac{u_\theta}{r}\cot\theta + \frac{u_r}{r},$$
$$2\varepsilon_{\theta\phi} = \frac{1}{r}\left(\frac{\partial u_\phi}{\partial \theta} - u_\phi \cot\theta\right) + \frac{1}{r\sin\theta}\frac{\partial u_\theta}{\partial \phi}, \qquad 2\varepsilon_{r\theta} = \frac{\partial u_\theta}{\partial r} - \frac{u_\theta}{r} + \frac{1}{r}\frac{\partial u_r}{\partial \theta},$$
$$2\varepsilon_{\phi r} = \frac{1}{r\sin\theta}\frac{\partial u_r}{\partial \phi} + \frac{\partial u_\phi}{\partial r} - \frac{u_\phi}{r}$$

A.2 Strain Components

1. For the filler, $(0 \leq r \leq a)$,

$$\varepsilon_{rr} = \left[A_1 - \frac{18\nu_p}{(1-2\nu_p)}A_2 r^2\right]\sin^2\theta\cos 2\phi$$
$$\varepsilon_{\theta\theta} = \left(\left[A_1 - \frac{(7-4\nu_p)}{(1-2\nu_p)}A_2 r^2\right] + \left[-A_1 + \frac{14(1-\nu_p)}{(1-2\nu_p)}A_2 r^2\right]\sin^2\theta\right)\cos 2\phi$$
$$\varepsilon_{\phi\phi} = \left(\left[-A_1 + \frac{(7-4\nu_p)}{(1-2\nu_p)}A_2 r^2\right] + \left[\frac{(7-10\nu_p)}{(1-2\nu_p)}A_2 r^2\right]\sin^2\theta\right)\cos 2\phi$$
$$\varepsilon_{\theta\phi} = \frac{1}{2}\left[-A_1 + \frac{(7-4\nu_p)}{(1-2\nu_p)}A_2 r^2\right]\cos\theta\sin 2\phi$$
$$\varepsilon_{r\theta} = \frac{1}{2}\left[2A_1 - \frac{(14+4\nu_p)}{(1-2\nu_p)}A_2 r^2\right]\sin\theta\cos\theta\cos 2\phi$$
$$\varepsilon_{\phi r} = \frac{1}{2}\left[-2A_1 + \frac{(14+4\nu_p)}{(1-2\nu_p)}A_2 r^2\right]\sin\theta\sin 2\phi$$

2. For the interphase, $(a \le r \le b)$,

$$\varepsilon_{rr} = \left[B_1 - \frac{18\nu_i}{(1-2\nu_i)}B_2 r^2 - \frac{12b_3}{r^5} - \frac{2(5-4\nu_i)}{(1-2\nu_i)}\frac{B_4}{r^3}\right]\sin^2\theta\cos 2\phi$$
$$\varepsilon_{\theta\theta} = \left(\left[B_1 - \frac{(7-4\nu_i)}{(1-2\nu_i)}B_2 r^2 - \frac{2B_3}{r^5} + \frac{2B_4}{r^3}\right] + \left[-B_1 + \frac{14(1-\nu_i)}{(1-2\nu_i)} + \frac{7B_3}{r^5} + \frac{(1+4\nu_i)}{(1-2\nu_i)}\frac{B_4}{r^3}\right]\sin^2\theta\right)\cos 2\phi$$
$$\varepsilon_{\phi\phi} = \left(\left[-B_1 + \frac{(7-4\nu_i)}{(1-2\nu_i)}B_2 r^2 + \frac{2B_3}{r^5} - \frac{2B_4}{r^3}\right] + \left[\frac{(7-10\nu_i)}{(1-2\nu_i)}B_2 r^2 + \frac{5B_3}{r^5} + \frac{3}{(1-2\nu_i)}\frac{B_4}{r^3}\right]\sin^2\theta\right)\cos 2\phi$$
$$\varepsilon_{\theta\phi} = \frac{1}{2}\left[-B_1 + \frac{(7-4\nu_i)}{(1-2\nu_i)}B_2 r^2 + \frac{2B_3}{r^5} - \frac{2B_4}{r^3}\right]\cos\theta\sin 2\phi$$
$$\varepsilon_{r\theta} = \frac{1}{2}\left[2B_1 - \frac{(14+4\nu_i)}{(1-2\nu_i)}B_2 r^2 + \frac{16B_3}{r^5} + \frac{4(1+\nu_i)}{(1-2\nu_i)}\frac{B_4}{r^3}\right]\sin\theta\cos\theta\cos 2\phi$$
$$\varepsilon_{\phi r} = \frac{1}{2}\left[-2B_1 + \frac{(14+4\nu_i)}{(1-2\nu_i)}B_2 r^2 - \frac{16B_3}{r^5} - \frac{4(1+\nu_i)}{(1-2\nu_i)}\frac{B_4}{r^3}\right]\sin\theta\sin 2\phi$$

3. For the matrix, $(b \le r \le c)$, the ν_i's in A.2 (2) are replaced by ν_m's and B_1, B_2, B_3 and B_4 are replaced by C_1, C_2, C_3 and C_4 respectively.

4. For the equivalent homogeneous medium, $(r \ge c)$,

$$\varepsilon_{rr} = \left[D_1 - \frac{12D_3}{r^5} - \frac{2(5-4\nu)}{(1-2\nu)}\frac{D_4}{r^3}\right]\sin^2\theta\cos 2\phi$$
$$\varepsilon_{\theta\theta} = \left(\left[D_1 - \frac{2D_3}{r^5} + \frac{2D_4}{r^3}\right] + \left[-D_1 + \frac{7D_3}{r^5} + \frac{(1+4\nu)}{(1-2\nu)}\frac{D_4}{r^3}\right]\sin^2\theta\right)\cos 2\phi$$
$$\varepsilon_{\phi\phi} = \left(\left[-D_1 + \frac{2D_3}{r^5} - \frac{2D_4}{r^3}\right] + \left[\frac{5D_3}{r^5} + \frac{3}{(1-2\nu)}\frac{D_4}{r^3}\right]\sin^2\theta\right)\cos 2\phi$$
$$\varepsilon_{\theta\phi} = \frac{1}{2}\left[-D_1 + \frac{2D_3}{r^5} - \frac{2D_4}{r^3}\right]\cos\theta\sin 2\phi$$
$$\varepsilon_{r\theta} = \frac{1}{2}\left[2D_1 + \frac{16D_3}{r^5} + \frac{4(1+\nu)}{(1-2\nu)}\frac{D_4}{r^3}\right]\sin\theta\cos\theta\cos 2\phi$$
$$\varepsilon_{\phi r} = \frac{1}{2}\left[-2D_1 - \frac{16D_3}{r^5} - \frac{4(1+\nu)}{(1-2\nu)}\frac{D_4}{r^3}\right]\sin\theta\sin 2\phi$$

A.3 Stress Components

1. For the filler, $(0 \le r \le a)$,

$$\sigma_{rr} = \left[2A_1 + \frac{6\nu_p}{(1-2\nu_p)}A_2 r^2\right]\mu_p\sin^2\theta\cos 2\phi$$
$$\sigma_{\theta\theta} = \left(\left[2A_1 - \frac{2(7-4\nu_p)}{(1-2\nu_p)}A_2 r^2\right] + \left[-2A_1 + \frac{14(2+\nu_p)}{(1-2\nu_p)}A_2 r^2\right]\sin^2\theta\right)\mu_p\cos 2\phi$$
$$\sigma_{\phi\phi} = \left(\left[-2A_1 + \frac{2(7-4\nu_p)}{(1-2\nu_p)}A_2 r^2\right] + \left[\frac{(14+22\nu_p)}{(1-2\nu_p)}A_2 r^2\right]\sin^2\theta\right)\mu_p\cos 2\phi$$
$$\tau_{\theta\phi} = \left[-A_1 + \frac{(7-4\nu_p)}{(1-2\nu_p)}A_2 r^2\right]\mu_p\cos\theta\sin 2\phi$$
$$\tau_{r\theta} = \left[2A_1 - \frac{(14+4\nu_p)}{(1-2\nu_p)}A_2 r^2\right]\mu_p\sin\theta\cos\theta\cos 2\phi$$
$$\tau_{\phi r} = \left[-2A_1 + \frac{(14+4\nu_p)}{(1-2\nu_p)}A_2 r^2\right]\mu_p\sin\theta\sin 2\phi$$

2. For the interphase, $(a \le r \le b)$,

$$\sigma_{rr} = \left[2B_1 + \frac{6\nu_i}{(1-2\nu_i)}B_2 r^2 - \frac{24B_3}{r^5} + \frac{4(\nu_i-5)}{(1-2\nu_i)}\frac{B_4}{r^3}\right]\mu_i \sin^2\theta\cos 2\phi$$

$$\sigma_{\theta\theta} = \left(\left[2B_1 - \frac{2(7-4\nu_i)}{(1-2\nu_i)}B_2 r^2 - \frac{4B_3}{r^5} + \frac{4B_4}{r^3}\right] + \left[-2B_1 + \frac{14(2+\nu_i)}{(1-2\nu_i)}B_2 r^2 + \frac{14B_3}{r^5} + \frac{2B_4}{r^3}\right]\sin^2\theta\right)\mu_i\cos 2\phi$$

$$\sigma_{\phi\phi} = \left(\left[-2B_1 + \frac{2(7-4\nu_i)}{(1-2\nu_i)}B_2 r^2 + \frac{4B_3}{r^5} - \frac{4B_4}{r^3}\right] + \left[\frac{(14+22\nu_i)}{(1-2\nu_i)} + \frac{10B_3}{r^5} + \frac{6B_4}{r^3}\right]\sin^2\theta\right)\mu_i\cos 2\phi$$

$$\tau_{\theta\phi} = \left[-B_1 + \frac{(7-4\nu_i)}{(1-2\nu_i)}B_2 r^2 + \frac{2B_3}{r^5} - \frac{2B_4}{r^3}\right]\mu_i\cos\theta\sin 2\phi$$

$$\tau_{r\theta} = \left[2B_1 - \frac{(14+4\nu_i)}{(1-2\nu_i)}B_2 r^2 + \frac{16B_3}{r^5} + \frac{4(1+\nu_i)}{(1-2\nu_i)}\frac{B_4}{r^3}\right]\mu_i\sin\theta\cos\theta\cos 2\phi$$

$$\tau_{\phi r} = \left[-2B_1 + \frac{(14+4\nu_i)}{(1-2\nu_i)}B_2 r^2 - \frac{16B_3}{r^5} - \frac{4(1+\nu_i)}{(1-2\nu_i)}\frac{B_4}{r^3}\right]\mu_i\sin\theta\sin 2\phi$$

3. For the matrix, $(b \le r \le c)$, the ν_i's in A.3 (2) are replaced by ν_m's and B_1, B_2, B_3 and B_4 are replaced by C_1, C_2, C_3 and C_4 respectively.

4. For the equivalent homogeneous medium, $(r \ge c)$,

$$\sigma_{rr} = \left[2D_1 - \frac{24D_3}{r^5} + \frac{4(\nu-5)}{(1-2\nu)}\frac{D_4}{r^3}\right]\mu\sin^2\theta\cos 2\phi$$

$$\sigma_{\theta\theta} = \left(\left[2D_1 - \frac{4D_3}{r^5} + \frac{4D_4}{r^3}\right] + \left[-2D_1 + \frac{14D_3}{r^5} + \frac{2D_4}{r^3}\right]\sin^2\theta\right)\mu\cos 2\phi$$

$$\sigma_{\phi\phi} = \left(\left[-2D_1 + \frac{4D_3}{r^5} - \frac{4D_4}{r^3}\right] + \left[\frac{10D_3}{r^5} + \frac{6D_4}{r^3}\right]\sin^2\theta\right)\mu\cos 2\phi$$

$$\tau_{\theta\phi} = \left[-D_1 + \frac{2D_3}{r^5} - \frac{2D_4}{r^3}\right]\mu\cos\theta\sin 2\phi$$

$$\tau_{r\theta} = \left[2D_1 + \frac{16D_3}{r^5} + \frac{4(1+\nu)}{(1-2\nu)}\frac{D_4}{r^3}\right]\mu\sin\theta\cos\theta\cos 2\phi$$

$$\tau_{\phi r} = \left[-2D_1 - \frac{16D_3}{r^5} - \frac{4(1+\nu)}{(1-2\nu)}\frac{D_4}{r^3}\right]\mu\sin\theta\cos\theta\cos 2\phi$$

Appendix B

Derivation of the Differential Equations for the Electrical and Thermal Conductivity

B.1 Introduction

The derivation of the differential equations which model the electrical and thermal conductivity is presented here. These differential equations were stated in chapter 5 without derivation.

B.2 Analytical model

B.2.1 A Spherical Inclusion Surrounded by an Inhomogeneous Interphase

The Maxwell-Garnett approximation [43] of the dielectric constant of a composite consisting of isotropic spherical inclusions embedded in an isotropic matrix is given by,

$$\varepsilon = \varepsilon_m + \frac{c}{\frac{1}{\varepsilon_p - \varepsilon_m} + \frac{(1-c)}{3\varepsilon_m}} \tag{B.1}$$

where ε_m is the dielectric constant of the matrix, ε_p is the dielectric constant of the inclusions and c is their volume fraction.

To account for the presence of the interphase region consider Figure B.1 representing a small portion of a 3-phase composite consisting of spherical particles all of radius a, surrounded by an annular interphase region of radius b, embedded in a surrounding matrix.

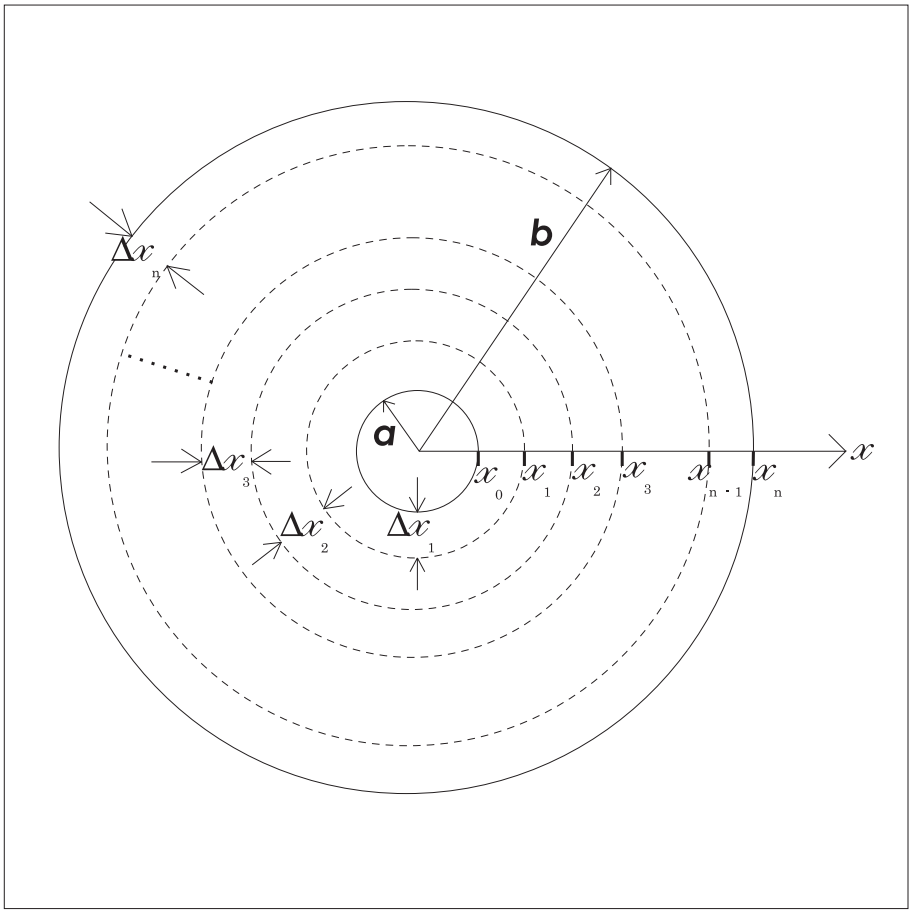

Figure B.1: Interphase consisting of n regions or layers.

We model the inclusion and interphase together as forming a new, effective spherical particle of radius b, with dielectric property denoted by ε_E. It shall be assumed throughout this work that the inclusions are well spaced apart and that the interphase regions don't overlap. Once ε_E has been found, the dielectric constant of the composite can be easily calculated using (B.1) by replacing ε_p with ε_E and letting $c = d_0 \frac{b^3}{a^3}$ where d_0 is the volume fraction of inclusions relative to all phases.

We shall now suppose that the properties of the interphase vary as continuous functions of x, where x represents the radial distance from the centre of the inclusion as shown in Figure B.1. That is, the dielectric constant of the interphase region are described by $\varepsilon(x)$, where $x \in [a, b]$. We shall also assume that $\varepsilon(x)$ is a smooth, bounded and continuous function.

Consider a partition $\mathcal{P}$ of $[a, b]$ into n subintervals defined by,

$$a = x_0 < x_1 < x_2 < \cdots < x_{i-1} < x_i < \cdots < x_{n-1} < x_n = b.$$

The lengths Δx_1, Δx_2, Δx_3, ..., Δx_n of the subintervals $[x_0, x_1]$, $[x_1, x_2]$, $[x_2, x_3]$, ..., $[x_{n-1}, x_n]$ associated with the partition $\mathcal{P}$, presently need not be the same. In each subinterval $[x_{i-1}, x_i]$, choose any point ξ_i; that is $\xi_i \in [x_{i-1}, x_i]$.

Using (B.1), the effective dielectric constant ε_1 of the inclusion and the 1st layer may be approximated by,

$$\varepsilon_1 = \varepsilon(\xi_1) + \frac{d_1}{\frac{1}{\varepsilon_0 - \varepsilon(\xi_1)} + \frac{(1-d_1)}{3\epsilon(\xi_1)}}$$

where $d_1 = (\frac{x_0}{x_1})^3$ and $\varepsilon_0 = \varepsilon_p$. Then using the replacement method originally proposed by [22] for the elastic moduli of composites, the effective dielectric constant ε_i of the inclusion up to the $i-th$ layer may be approximated by,

$$\varepsilon_i = \varepsilon(\xi_i) + \frac{d_i}{\frac{1}{\varepsilon_{i-1} - \varepsilon(\xi_i)} + \frac{(1-d_i)}{3\epsilon(\xi_i)}} \tag{B.2}$$

where $d_i = \left(\frac{x_{i-1}}{x_i}\right)^3$, $i \in \{\mathbb{N} : 1 \leq i \leq n\}$ and ε_{i-1} is an approximation to the dielectric constant of the *inner composite sphere* that is calculated from the previous step.

Our aim is to find the effective dielectric constant, ε_E, of the inclusion and whole interphase region which would be given by,

$$\varepsilon_E = \lim_{n \to \infty} \varepsilon_n$$

where ε_n is found by solving the recurrence relation (B.2).

B.2.2 The Governing Differential Equations

We may rewrite (B.2) as,

$$\varepsilon_i = \frac{A_i\varepsilon_{i-1} + B_i}{C_i\varepsilon_{i-1} + D_i} \tag{B.3}$$

where,

$$A_i = f_i d_i \quad \varepsilon(\xi_i) + d_i \qquad B_i = \varepsilon(\xi_i) - f_i d_i \varepsilon(\xi_i)^2 - d_i\varepsilon(\xi_i)$$
$$C_i = f_i d_i \qquad D_i = 1 - f_i d_i \varepsilon(\xi_i)$$

and,

$$f_i = \frac{(1-d_i)}{3d_i\varepsilon(\xi_i)}.$$

By evaluating the first few terms of the recurrence relation (B.3), a pattern can be seen as emerging which enables us to suitably estimate ε_i as,

$$\varepsilon_i = \frac{S_i(A_1\varepsilon_0 + B_1) + T_i(C_1\varepsilon_0 + D_1)}{U_i(A_1\varepsilon_0 + B_1) + V_i(C_1\varepsilon_0 + D_1)} \tag{B.4}$$

where,

$$S_i = A_i S_{i-1} + B_i U_{i-1} \tag{B.5}$$
$$U_i = C_i S_{i-1} + D_i U_{i-1} \tag{B.6}$$

which together form a pair of simultaneous first order linear difference equations with non-constant coefficients and initial conditions, $S_1 = 1$, $U_1 = 0$. Also we have, $i \in \{\mathbb{N} : 2 \leq i \leq n\}$.

We also have for T_i and V_i,

$$T_i = A_i T_{i-1} + B_i V_{i-1} \tag{B.7}$$
$$V_i = C_i T_{i-1} + D_i V_{i-1} \tag{B.8}$$

which are a pair of simultaneous equations identical to (B.5) and (B.6), but with initial conditions, $T_1 = 0$ and $V_1 = 1$. Also we have, $i \in \{\mathbb{N} : 2 \leq i \leq n\}$. It can be easily shown using mathematical induction that ε_i as represented by (B.4) along with (B.5)-(B.8), is identical to the representation given by (B.3).

We may rewrite (B.5) and (B.6) as,

$$S_{i+1} = A_{i+1}S_i + B_{i+1}U_i \tag{B.9}$$

$$U_{i+1} = C_{i+1}S_i + D_{i+1}U_i \tag{B.10}$$

where $S_1 = 1$, $U_1 = 0$ and $i \in \{\mathbb{N} : 1 \leq i \leq (n-1)\}$.
For each subinterval $[x_{i-1}, x_i]$ of the partition $\mathcal{P}$ let each Δx_i have the same width Δx and choose ξ_i to be the right hand end point, that is, we shall take $\xi_i = x_i$. Then we have,

$$(1 - d_i) = \Delta x g_i \qquad \text{where} \qquad g_i = \frac{x_i^2 + x_i x_{i-1} + x_{i-1}^2}{x_i^3}.$$

For notational convenience, A_i, B_i, C_i, and D_i may be re-written as,

$$A_i = \Delta x \alpha_i + d_i \qquad \text{where} \qquad \alpha_i = \frac{g_i}{3},$$

$$B_i = \Delta x \beta_i \qquad \text{where} \qquad \beta_i = \frac{2}{3} g_i \varepsilon(x_i),$$

$$C_i = \Delta x \gamma_i \qquad \text{where} \qquad \gamma_i = \frac{g_i}{3\varepsilon(x_i)},$$

and $D_i = 1 - \Delta x \alpha_i$.

Let $A_2, A_3, A_4, \ldots, A_n$ be discrete values of a function $A(x)$ at the discrete points x_i where $i = 2, 3, 4, \ldots, n$, i.e. $A_i = A(x_i)$. Also we have $A_{i+1} = A(x_i + \Delta x)$. Similarly for B_i, C_i, and D_i we have the functions $B(x)$, $C(x)$ and $D(x)$. Also, let S_i and U_i be values of the functions $S(x)$ and $U(x)$ at the discrete points x_i. Then, (B.9) and (B.10) may be re-written as,

$$S(x_i + \Delta x) = A(x_i + \Delta x)S(x_i) + B(x_i + \Delta x)U(x_i) \tag{B.11}$$

$$U(x_i + \Delta x) = C(x_i + \Delta x)S(x_i) + D(x_i + \Delta x)U(x_i) \tag{B.12}$$

where $S(x_1) = 1$, $U(x_1) = 0$.

With variables defined as such, it can be easily shown that in the limit as $n \to \infty$ or $\Delta x \to 0$, equations (B.11) and (B.12) convert to a pair of simultaneous differential equations given by,

$$S'(x) = -\frac{2}{x}S(x) + \frac{2}{x}\varepsilon(x)U(x) \tag{B.13}$$

$$U'(x) = \frac{1}{x\varepsilon(x)}S(x) - \frac{1}{x}U(x) \tag{B.14}$$

with conditions $S(a) = 1$, $U(a) = 0$ and $x \in [a, b]$.

Similarly, the difference equations given by (B.7) and (B.8) convert to the differential equations given by (B.13) and (B.14) after replacing S with T and U with V, but with boundary conditions given by $T(a) = 0$ and $V(a) = 1$. Therefore, only one pair of equations need to be solved with appropriate care taken when accounting for the boundary conditions.

As $n \to \infty$ we have $A_1 \to 1$, $B_1 \to 0$, $C_1 \to 0$ and $D_1 \to 1$, $S_n \to S(b)$, $U_n \to U(b)$, $T_n \to T(b)$ and $V_n \to V(b)$. Therefore, from (B.3), the effective dielectric constant of the inclusion and interphase is,

$$\varepsilon_E(b) = \frac{\varepsilon_p S(b) + T(b)}{\varepsilon_p U(b) + V(b)}. \tag{B.15}$$

The above results are useful because we are able to model the interphase inhomogeneity by smooth, bounded and continuous functions of x as opposed to using a discontinuous step like graded interface. Also, the above results are applicable to any arbitrary profile for the interphase region.

Note that we may combine S and T along with U and V since they are essentially the same function. For example, letting

$$w(x) = \varepsilon_p S(b) + T(b) \qquad \text{and} \qquad z(x) = \varepsilon_p U(b) + V(b)$$

implies that,

$$\begin{aligned} w'(x) &= -\frac{2}{x} w(x) + \frac{2}{x} \varepsilon(x) z(x) \\ z'(x) &= \frac{1}{x\varepsilon(x)} w(x) - \frac{1}{x} z(x) \end{aligned}$$

where $w(a) = \varepsilon_p$ and $z(a) = 1$.

Appendix C

A List of Maple and Mathematica Files used to Generate the Graphs

C.1 Introduction

We list here the programs that were written on the symbolic manipulation packages Maple and Mathematica which are on the compact disc accompanying this thesis. These programs were used to generate the graphs in each chapter. Note that filenames ending in *mws* are Maple Worksheets while those ending in *nb* are Mathematica Notebooks.

C.2 Programs used in each Chapter

Chapter 2

- Bulk Modulus of a particulate composite with inhomogeneous interphase.mws
- Engineered interphases for the Bulk Modulus.mws

Chapter 3

- Shear modulus of a particulate composite with homogeneous interphase.nb
- Shear Modulus of particulate composite with inhomogeneous interphase.nb

Chapter 4

- Comparison of different models for the CTE.nb
- Comparison of different inhomogeneous interphases for CTE.nb

• Effect of the Bulk Modulus of the Interphase on the CTE of a Particulate Composite.nb

Chapter 5

• Dielectric behaviour of a particulate composite (variable k)- exponential profile.nb

• Dielectric behaviour of a particulate composite (variable k)- power law profile.nb

• Dielectric behaviour of a particulate composite (variable k) - power-exponential profile.nb

• Dielectric behaviour of a particulate composite (variable P) - power-exponential profile.nb

Chapter 6

• Bulk Modulus (Linear Model-constant bulk modulus of interphase).nb

• Bulk Modulus (Linear Model-constant shear modulus of interphase).nb

• Shear Modulus (Linear Model-constant shear modulus of interphase).nb

• Bulk and Shear Modulus of a particulate composite with constant Poisson's ratio - power-exponential profile.nb